UNIVERSITY OF CALIFORNIA SAN DIEGO

Archaeomagnetism and its applications in the broader American Southwest

A dissertation submitted in partial satisfaction of the
requirements for the degree Doctor of Philosophy

in

Earth Sciences

by

Shelby A. Jones

Committee in Charge:

Professor Lisa Tauxe, Chair
Professor Catherine Constable
Professor Jeffrey Gee
Professor Thomas Levy
Professor Isabel Rivera-Collazo

2022

The dissertation of Shelby A. Jones is approved, and it is acceptable in quality and form for publication on microfilm and electronically.

University of California San Diego

2022

TABLE OF CONTENTS

LIST OF FIGURES

LIST OF TABLES

ACKNOWLEDGMENTS

Throughout my time at Scripps Institution of Oceanography, I received an immense amount of support and assistance, both personally and in my academic career. I would first like to thank my advisor, Professor Lisa Tauxe, whose expertise in the field of paleomagnetism and data management of paleomagnetic data were invaluable to the development of my methodologies and thesis. Your constant feedback pushed me to learn new skills and sharpen old ones and apply those skills to the completion of my projects. I would also like to acknowledge my unofficial second advisor, Dr. Eric Blinman, who has been a wealth of support and knowledge. Your decades of experience and willingness to share your numerous skillsets with me, not only allowed me to grow as a person but also as an archaeologist and scientist.

I would also like to thank my advisors who graciously continued to support me, even though I was no longer their student, Professors John Pryor and Chris Pluhar from Fresno State. Further, I would like to thank Dr. Marvin Rowe for the years of lunch time conversations and mentoring. I learned so much from you and I am thankful we can continue our lunch time breaks.

And a special thanks to my committee members Professors Cathy Constable, Jeff Gee, Isabel Rivera-Collazo and Tom Levy for your questions and insights over the years that made my dissertation possible and robust.

In addition, I would like to thank my family for their support and for listening to me wax poetic on my research and help me through my stressors. You are always there for me and I could not have completed this dissertation without you. And there are so many! My parents, sister, grandparents, cousins, aunts, uncles, Pedro, in-laws, chosen family, neighbors, and all the furry four-legged family. You all played a large role in my success.

And lastly, I would like to share a heartfelt thanks to my friends, both on campus and off. The completion of my dissertation is a direct result of the support and sympathetic ears you gave to me unconditionally over the years, that allowed me to discuss my research but also rest my mind. Especially my friends and lunch buddies from SIO and the international paleomagnetism community (Kate Durkin, Sarah Maher, Brendan Cych, Christeanne Santos, Anita DiChiara, Maggie Avery, Brendan Reilly, Georgie Zelenak, Kim Reed, Les Nagy, Alex Rodriquez Trejo, Annemarieke Beguin, and Geertje Ter Maat).

Chapter 2, in full, is a reprint of material as it appears in *Geochemistry, Geophysics, Geosystems*. vol. 21, doi: 10.1029/2018GC007509, 2020. Shelby A. Jones, Lisa Tauxe, Eric Blinman, Agnes Genevey. The dissertation author was the primary investigator and author of this paper. This material is based on work partially supported by National Science Foundation grants EAR1345003 and EAR1547263 to LT, the Frontiers of Innovations Scholars Program at University of California, San Diego, the Edna Bailey Sussman Research Fellowship, the Shepard Foundation Grant, and a private donation from Robert Rex.

Chapter 3, in full, is a reprint of material as it appears in *Journal of Geophysical Research - Solid Earth*. vol. 26, doi: 10.1029/2021JB022874, 2021. Shelby A. Jones, Eric Blinman, Lisa Tauxe, J. Royce Cox, Stacey Lengyel, Robert Sternberg, Jeffrey Eighmy, Daniel Wolfman, Robert Dubois. The dissertation author was the primary investigator and author of this paper. This material is based in part by National Science Foundation grants EAR1547263 and EAR1827263 to LT, a private donation from Robert Rex, and private donations to the Museum of New Mexico Foundation’s Friends of Archaeology.

Chapter 4, in full, has been submitted to the *Journal of Archaeological Sciences: Reports* for publication of the material. Shelby A. Jones, Eric Blinman, Jon C. Lohse, J. Royce Cox, Melanie Nichols, Jenni Kimbell. The dissertation author was the primary investigator and author of this paper. This material is supported in part by the Texas Department of Transportation through contract number 579XXSA202, awarded to Terracon Consultants and JCL, and supplemented by funds from the Dr. Donald E. Pierce Endowment for Archaeology and Conservation, administered by the Museum of New Mexico Foundation.

VITA

2014 Bachelor of Science with Honors, Geology
California State University, Fresno

2016 Master, Earth Sciences
University of California San Diego

2022 Doctor of Philosophy, Earth Sciences
University of California San Diego

PUBLICATIONS

Jones, S.A., E. Blinman, L. Tauxe, J.R. Cox, S. Lengyel, R. Sternberg, J. Eighmy, D. Wolfman, and R. Dubois; MagIC as a FAIR Repository for America's Directional Archaeomagnetic Legacy Data, *Journal of Geophysical Research - Solid Earth*, Volume 126, Issue 10, 23 September 2021, e2021JB022874, https://doi.org/10.1029/2021JB022874

Nesbit, K.T., W.H. Wolfe, K.K. Mullane, E.J. Chamberlain, B.A. Rasina, E. Saberski, and S.A. Jones; SCOPE: A Volunteer-led STEM Outreach Program Connecting Communities to Research, *Connected Science Learning*, Volume 3, Issue 6, November-December 2021, https://www.nsta.org/connected-science-learning/connected-science-learning-november-december-2021/scope-volunteer-led

Jones, S.A., L. Tauxe, E. Blinman and A. Genevey; Archaeointensity of the "Four Corners" Region of the American Southwest, *Geochemistry, Geophysics, Geosystems*, Volume 21, Issue 3, 12 February 2020, e2018GC007509, https://doi.org/10.1029/2018GC007509

ABSTRACT OF THE DISSERTATION

Archaeomagnetism and its applications in the broader American Southwest

by

Shelby A. Jones

Doctor of Philosophy in Earth Sciences

University of California San Diego, 2022

Professor Lisa Tauxe, Chair

In the United States Southwest in the early 1960s, an academic lineage began utilizing the techniques of paleomagnetism and geomagnetism for applications in archaeology. However, most of the research was conducted with an enterprise mindset, resulting in few published data that are often embedded in hard-to-find and hard-to-access archaeological reports, limiting the work's accessibility to geomagnetic researchers. Furthermore, when published, the results were generally averaged at the site level using statistical conventions different from today's standards, limiting the data's comparability and (re)usability. The outcome was that only small subsets of nearly six decades of archaeomagnetic measurement and research could be (re)used for geomagnetic applications, like global field modeling and archaeomagnetic dating curve development. Moreover, the development of applications of archaeomagnetism to answer questions related feature use and function stalled. This thesis undertakes an archival study to salvage and collate surviving data and metadata for archaeointensity and archaeodirectional records. The goal was accessibility, with an understanding of the limitations and quality of the dataset, where possible.

The work resulted in the compilation of 131 previously published archaeointensity values, the addition of 54 new archaeointensity values (of which 8 are considered high quality), and the digitization of measurement data for over 51,000 specimens from over 5,377 archaeodirectional sites. The compilation resulted in confirmation that the data from the various laboratories are able to be treated and used as one dataset, without any systematic biases. The archaeodirectional dataset was filtered for quality, and the highest quality 223 data with reliable chronology were included in the development of a new virtual geomagnetic pole (VGP) reference curve for the last 2000 years for the Four Corners region of the United States Southwest. Finally, I build on the work of Wulf Gose, applying the techniques of directional archaeomagnetism to understanding the use and function of enigmatic burned rock features from east Texas. The magnetic declination and inclination data, paired with the archaeological context suggest that the rocks of one feature have remained substantially in-situ since the feature’s last significant heat exposure, while the rocks of a second feature have been moved since last heating.

Chapter 1. Introduction to archaeomagnetic research and methodologies in the American Southwest

1.1 Preface and thesis summary

The following thesis chapters are representative of the work I completed as a graduate student and doctoral candidate at the Scripps Institution of Oceanography at the University of California San Diego. My research focuses on the preservation of more than six decades of historical archaeomagnetic data and contemporary applications of archaeomagnetism in the broader American Southwest. Archaeomagnetism is the study of Earth's recent magnetic field as recorded in archaeological sites, features, and artifacts. My dissertation is focused on archaeomagnetic signatures that were preserved through heating of archaeological materials, rather than magnetic characteristics preserved through detrital processes like the sedimentary infill of anthropogenically created canals or ponds.

My dissertation has three major components. First, I looked at the regional variation in the intensity (strength) of Earth's magnetic field over the last 2000 years through analyzing new pottery sherds from New Mexico and comparing those measured values with previously published data from the Four Corners region of the United States Southwest (Arizona, New Mexico, Colorado, and Utah). The second component of my thesis was to compile all the unpublished archaeodirectional measurement data collected since 1964 by an academic lineage of scientists and archaeologists working in the United States. The dataset is the first comprehensive compilation of the data from the three main contributors (Robert DuBois, Daniel Wolfman, and Jeffrey Eighmy) and represents their life's work, totaling to over 51,000 specimen data record from over 5000 archaeological features. Once compiled, the dataset was used to develop a new regional magnetic field model of variation over the last 2000 years for the Four Corners region. The third and last component builds on the aspirations of Wulf Gose (Gose 2000) to apply paleomagnetic methods to the study and interpretation of burned archaeological rock. In this study, I used archaeodirectional data from two anthropogenically heated features in east Texas, to explore feature form and function.

My dissertation consists of four chapters, this introduction and three chapters that encapsulate the results from each of the three projects mentioned above. They are titled:

1) Introduction to archaeomagnetic research and methodologies in the American Southwest
2) Archeointensity of the Four Corners Region of the American Southwest
3) MagIC as a FAIR Repository for America's Directional Archaeomagnetic Legacy Data
4) Archaeomagnetic directional studies as a revolutionary tool for understanding feature form and function: A case study of two burned rock features in a multi-component site in east Texas, USA

The latter three chapters have or will be published in peer reviewed journals. As a result, the three chapters are structured with their own introductions, methods, results, discussion and conclusion sections. This thesis introduction serves as a foundation to all three latter chapters, primarily focusing on the requisite background of archaeodirectional studies as both Chapters 3 and 4 have an archaeodirectional focus. Chapter 2 has an archaeointensity focus and a well-defined introduction and methods section. Chapters 3 and 4 both describe the sampling methods used in brevity, requiring further description here in the introductory chapter.

The chapters are connected as part of a broader theme of understanding the variation in Earth's recent magnetic field in the American Southwest and applying the data and techniques of archaeomagnetism to both geomagnetic and archaeological research questions.

1.2 Archaeomagnetic Background

Archaeomagnetism, at the confluence of archaeology and geophysics, applies many of the techniques of paleomagnetism to address questions related to the history of archaeological features. The structure of Earth's magnetic field varies with time, and anthropogenic materials, sediments, and rocks can acquire magnetic properties that reflect the prevailing conditions at the time of the magnetic acquisition. Measurement and subsequent interpretation of a material's magnetic characteristics can inform on both the material's chronology and the event(s) of its history.

Traditionally, archaeomagnetic investigations in the broader United States Southwest have focused primarily on quantifying a material's preserved remanent magnetization (usually vector direction, but also magnitude known as intensity) with applications to archaeological chronology (archaeomagnetic dating; Blinman and Cox, in press) and for inclusion in geophysical models. However, there is an increasing interest in using the variation in the magnetic properties across features (e.g. direction of remanence, firing efficiency, magnetic susceptibility) to support interpretations of feature form, use, history, and post-depositional processes. Of especial consideration is the use of archaeomagnetism to interpret otherwise enigmatic archaeological contexts and functions (e.g. burned rock features, Jones et al., in review).

1.2.1 Foundations

Magnetic remanence acquisition in the context of archaeological sites is overwhelmingly in the form of thermal remanent magnetism through human use of fire for cooking or through accidental burning of structures. The archaeological materials most often studied are those that are anthropogenically heated (hearths, burned floors, pottery, etc.) because the heating and subsequent cooling of the material generally preserves a stable and measurable remanent magnetization (e.g. Eighmy and Sternberg 1990). When heated in the presence of a magnetic field, the atomic-scale magnetic moments within the magnetic mineral crystals enter a state of instability, with no memory of their former alignment – formally defined as a state of superparamagnetic behavior (Neél 1949). Upon subsequent cooling, this superparamagnetic behavior ceases, and the atomic magnetic moments re-enter a state of stability as close to parallel as possible with the Earth's prevailing magnetic field, effectively preserving a record of the qualities of Earth's magnetic field at the time of cooling. If the temperature reached is sufficiently high, all the material's magnetic moments behave paramagnetically at temperature and all the moments re-align upon cooling, preserving a thermal remanent magnetization (TRM). This temperature is known as the Curie point and occurs at 580° and 675°C for magnetite (Dunlop and Özdemir 1997) and hematite (O'Reilly 1984), respectively. If the temperature reached does not exceed the Curie temperature of the magnetic mineral crystals in the material, then the subset of magnetic moments that entered into superparamagnetic behavior (at their magnetic unblocking temperature) and did re-align upon cooling (through their magnetic blocking temperature) preserve a partial thermal remanent magnetization (pTRM, initially described by Nagata 1943). Often, this pTRM is still detectable during laboratory measurement and is common in anthropogenically heated materials, since most heating events (e.g. cooking fires; Blinman et al. 2017) do not reach temperatures as high as the Curie temperature (a notable exception is heating in kilns; Shepard 1995).

The total net magnetization of the material is formally referred to as the natural remanent magnetization (NRM) and represents the integrated effect of the material's magnetic history. In archaeomagnetism, the NRM is commonly complex because archaeological materials often experience multiple magnetization and heating events. In these cases, the complex history may be detailed through laboratory study, but not always. Since heating can re-initiate superparamagnetic behavior, additional heating events effectively erase the magnetic moments that were previously acquired at the new temperature and below (e.g. Nagata 1961). In instances where a subsequent heating event of a higher temperature occurs, there will be no preserved magnetic signature of the past heating event. But in cases where subsequent heating event(s) occur at lower temperatures than an earlier heating, there is a potential that measurement and data analysis maybe able to differentiate the magnetic signatures of the original and overprinting remanent magnetization directions. Depending on the research question, these overprinting magnetic signatures may have incredible value or may obscure the higher-temperature magnetic remanence of importance. Detailed laboratory measurement procedures and post-measurement statistical analyses are required to understand this type of complex thermal histories, but these complex histories can result in robust perspectives on the anthropogenic feature's history and function, and sometimes the age of magnetic acquisition.

Overprinting magnetic signatures are not just limited to pTRMs. They can result from a number of different phenomena, each formally defined, and can all partially or completely overprint the primary remanent magnetization. Most common in archaeological settings are viscous remanent magnetizations (VRM) and chemical remanent magnetizations (CRM).

VRMs are almost always present and are usually acquired by the least stable subset of magnetic moments within the material (first noticed by Thellier 1938). At ambient temperature and pressures, these least stable magnetic moments can exhibit superparamagnetic behavior and have the potential to realign their magnetic moments with Earth's present-day magnetic field on the order of days to centuries. Because VRMs are acquired by the least stable magnetic moments in the material, they will influence the measured NRM but are easy to remove during the laboratory procedure and often do not affect the final interpretation.

CRMs are the by-product of the chemical alteration of the magnetic minerals within the material (first noticed by Haigh 1958 and further explored e.g. Kobayashi 1961). They can be the result of mineral weathering and converting one magnetic mineral into another but can also result from the precipitation of magnetic minerals into or on the material (for example a hematite-based cement within a porous sedimentary rock or an alteration rind). In archaeological contexts, the anthropogenic use of a material (such as a roasting or boiling stone) may predispose the material to develop a CRM that is different in the nature or pace of weathering than is seen in non-anthropogenically influenced samples.

Lastly, in addition to magnetic qualities established through thermal means (pTRMs and TRMs), magnetization of sediments can result from grains settling out of suspension. This type of magnetization is known as detrital remanent magnetization (DRM) and is usually orders of magnitude weaker than TRM signatures. The magnitude of a DRM is related to the rate grains settled out of suspension, the flow regime and turbulence those grains experienced as they settled, and the shape, size, and mineralogy of the grains (e.g. Nagata 1961). DRMs can be present in a variety of archaeological contexts, both as in-situ archaeological formations (e.g. canals or dammed ponds) and as pre-existing geologic magnetizations (e.g. heated sedimentary rocks). Canal or ponded sediments can have a DRM that is relevant to archaeological interpretations. While the DRMs preserved in sedimentary rocks (which have been collected and reorganized into built features) reflect the conditions of the rock's formation and may result in "noise" in archaeomagnetic investigations.

In most cases, the primary DRM is not the remanent magnetization essential to the archaeomagnetic research question and such DRMs are weak enough that they do not confound the interpretation of an overprinting pTRM or TRM. But in special cases, a DRM can form in environments that create non-random magnetic alignments (anisotropy). This anisotropy can form naturally, as a result of stream flow and mineralogy, and can result from human actions. Troweling, pottery construction, or polishing of floor or wall plasters can contribute to an anisotropic DRM signature, and that anisotropy can be persistent and influence subsequent overprinting magnetization. In such cases, the precision and accuracy of the interpretation can be influenced. High quality archaeointensity experiments include steps to identify, measure, calculate, and correct for anisotropy. These anisotropy corrections experiments were completed on the pottery sherds studied in Chapter 2 and a further description of the method is included in that text.

1.2.2 Earth's magnetic field

Foundational to archaeomagnetism is that the magnetic properties (e.g. the remanent magnetization(s) and mineralogy) of the studied material inform on functional history and the dynamic geometry of Earth's magnetic field. In archaeomagnetism, most research questions focus on the subtle variations of Earth's magnetic field that occur through time and space, known as paleosecular variation (PSV). Investigating PSV is a two-fold process in archaeomagnetism: 1) Foundational research that uses published magnetic records and the independent dating potential of archaeological features to build and test the reliability of models of regional PSV (e.g. DuBois 1989 and Jackson et al. 2000). And 2) using the accumulated knowledge of regional PSV as a chronology tool in archaeology to date magnetic records of unknown age (e.g. Deaver 1998), a discipline known as archaeomagnetic dating.

PSV is the result of the dynamic structure of Earth's magnetic field. Through the collection, measurement, and analysis of oriented and well-dated material, the remanent magnetization in the studied material can be used to investigate the field structure at the time of magnetic remanence acquisition, analogous to understanding the dynamic field geometry through discrete "snap shots". With enough discrete data, models of the PSV through time can be developed. In United States archaeomagnetism, the common way of viewing PSV through time is by tracing the movement of the geomagnetic north pole through time, referred to as constructing virtual geomagnetic pole (VGP) reference curves.

A VGP location is calculated using a feature's remanent magnetization and the site's latitude-longitude. The result is a location, usually within the Arctic circle, that estimates the past location of the geomagnetic north pole, as observed from the location of original firing site. The transformation from the vector characterization of the preserved magnetization to VGP position is convenient because it permits comparison of the remanent magnetizations from disparate sites, at a regional level. This is incredibly useful since Earth's magnetic field is not strictly a dipole. While, the dipole structure accounts for roughly 90-95 percent of the field's power, the small contributions of non-dipole field geometries (e.g. quadrupole, octupole, etc.) contribute significantly to regional field variability and cause VGP reference curves to be regionally specific.

1.2.3 Archaeomagnetism applications in the United States

Commonly, regional archaeomagnetic VGP reference curves are constructed for areas of up to a ~500 to 1000 km radius (750 km is preferred by this author based on the variation seen in the data across the latitudinal spread of the Four Corners region of the American Southwest, and used as the threshold for Chapters 2 and 3), as the non-dipole influences can cause too much variation in the dataset beyond this radius and the data should be treated independently. The United States tradition of archaeomagnetism began in the 1960s, and the focus has been on the development and use VGP curves for archaeomagnetic dating of the remanent magnetization directions preserved in thermal features. The VGP position calculated from of the TRMs or pTRM can be compared with the appropriate regional reference curve and can be used to infer a date range.

Presently in the United States, three regions have proposed VGP calibration curves:

1) The Four Corners region of the United States Southwest has by far the most data, and multiple generations of reference curves have been proposed (reviewed in Blinman and Cox, in press, and summarized in Chapter 3). The curves proposed for this region have and continue to be used for archaeomagnetic dating.
2) A curve encompassing the Lower Mississippi River region of the Southeastern U.S. (Arkansas focus) was proposed by Dan Wolfman (1982; 1990).

3) A mid-continent curve covering the latitudes north of the Lower Mississippi River curve (but also including much of Wolfman's Arkansas data) was proposed by Stacey Lengyel (Lengyel 2004; Lengyel et al. 1999).

Much of the rest of the U.S. does not yet have a proposed reference curve, largely due to a low density of data, including Texas, that lies between the Four Corners region and the Lower Mississippi River region. However, the PSV of the eastern seaboard from 1600 CE to present has been modeled from historical records of magnetic direction in sea captains' log books (Jackson et al. 2000). This model can be utilized in much the same way as a VGP calibration curve for applications of archaeomagnetic dating along the east coast of the United States.

Whether or not a regional reference curve exists, the contemporaneity of multiple features within a site can be evaluated by comparing the remanent magnetization(s) direction of each. If different features have non-parallel remanence directions, this can be interpreted as evidence that the features are not contemporaneous. Conversely, if different features have parallel remanence directions, those features have the potential to be contemporaneous; however, there is a chance for an erroneous conclusion. VGP variation is not unidirectional, and at times the reference curves cross over themselves. This overlap can result in a single pole position (or remanence direction) that is achieved at multiple times in the past. In these cases, and if a full TRM is present in the material, specialized laboratory measurements that can interpret the strength of Earth's past magnetic field can be used to distinguish the timing of some points of overlap.

Beyond dating and contemporaneity assessments, archaeomagnetic analyses have the potential to contribute to the understanding of the use and post-depositional processes that affect burned rock features. Wulf Gose from the University of Texas at Austin applied paleomagnetic methods usually applied to tectonic questions to archaeological burned rock features (Nickels et al. 1998; Gose 2000). The approach evaluates whether the remanent magnetization of the individual rocks within a thermal feature are coherent or dispersed (non-parallel). If the rocks have coherent remanent magnetization directions, it can be inferred that the thermal feature is intact. If the magnetization directions from the rocks are dispersed, it can be inferred that the rocks moved since their magnetic acquisition. Minor movements in the magnetization directions of in-situ rocks are expected as a result of normal post-abandonment processes. But radical realignments of the remanent magnetizations may support interpretations of human behavior at time of use.

1.3 Technical Discussion of Methodology: Archaeodirectional

1.3.1 Archaeomagnetic coordinate systems

Sampling design is dependent on the research goals, but in general, most archaeomagnetic studies rely on the preservation of measurable magnetic remanence that inform on feature history. The Office of Archaeological Studies (in Santa Fe, NM) utilizes methods of directional archaeomagnetic sampling that were adopted by their predecessors Daniel Wolfman, Jeffrey Eighmy, and Robert DuBois. The procedure is multi-step and utilizes non-magnetic fast curing plaster to fully encase specimens within 1-inch plaster cubes (DuBois used 1.7-inch plaster cubes). This method ensures that even slightly cohesive materials remain intact throughout transportation and laboratory measurement, and every measurement made is precisely aligned within the magnetometer.

Successful TRM archaeomagnetic studies require appropriate magnetic mineralogies, anthropogenic heating event(s) sufficiently hot to result in a TRM (or pTRM) magnetic alignment, recovery of a carefully aligned set of 1-inch specimen cubes, and step-wise laboratory measurement of the specimen cubes paired with analysis to determine a direction of the preserved magnetization. These remanent magnetizations, characterized through laboratory measurement, are expressed as vectors in a cartesian coordinate system (XYZ) with respect to a carefully aligned reference corner noted as a quarter circle on the plaster encasement at time of sampling. During analysis, the measured cartesian vectors of the preserved magnetizations are mathematically transformed into a polar coordinate system (angular direction and magnitude) using the cube's in-field geometry to determine the relationship between modern geographic north and the ancient geomagnetic north.

In archaeomagnetism and paleomagnetism, the magnetization direction is expressed in terms of declination and inclination. Declination is the angle from the geographic north pole to the horizontal projection of the preserved magnetization direction, calculated using the X and Y measurement (ranging from 0° to 360° clockwise). Inclination is the angle between the preserved magnetization direction and horizontal plane, calculated using the Z measurement (ranging from -90° to +90° and defined as positive when the magnetization direction is down).

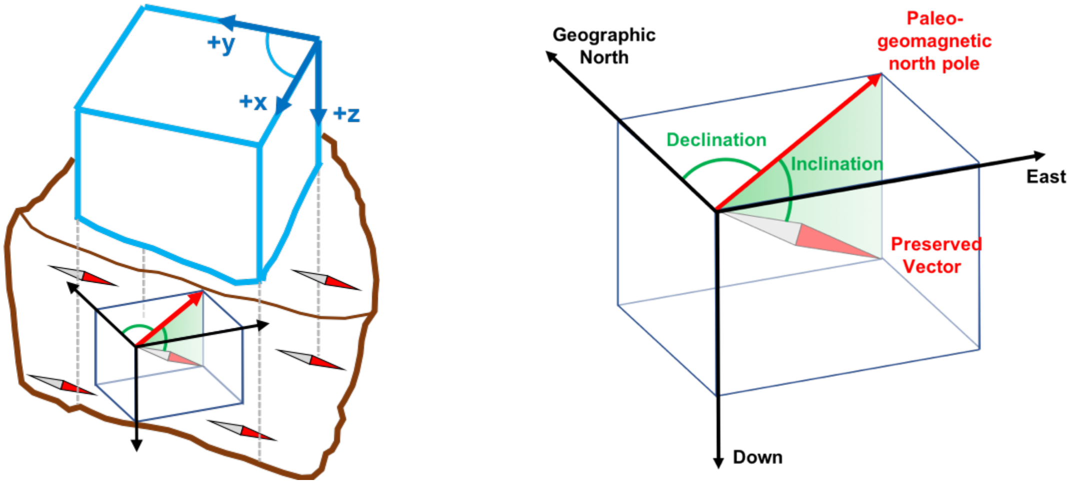

Figure 1.1: Schematic, depicting the coordinate system utilized in plaster cube sample for directional archaeomagnetism in the United States, with respect to the terminology used to describe the measured magnetization.

1.3.2 Consideration of sampling locations

Successful field sampling of archaeological surfaces relies on the intentional and careful sampling of several rocks that span the feature and any lithologic diversity. This intentionality ensures sampling reliability and research quality. The ideal candidate material does not exhibit any post-abandonment movement, is large enough to support six to twelve specimen cubes to ensure statistical robustness of the final interpretations, and has been heated to high temperatures. Prior to sampling, each sampling location is examined for signs of movement, size, and potential of heating, if the substrate is not ideal, a different substrate is selected for sampling. Traditionally, United States-based archaeomagnetists selected sampling areas based on oxidation color, striving for red oxidation rinds, due to their presumed association with higher temperature heating events. But many variables in a fire (e.g. oxygen availability and length of heating) can affect the color of oxidation/reduction rinds independently of the heat that establishes the thermal magnetic properties. Relying solely on the presence of red-hue rinds alone may eliminate the consideration of reduced materials that would otherwise be successful magnetic recorders. The Office of Archaeological Studies (OAS) Archaeomagnetism Laboratory favors an approach of estimating the heat the material experienced through assessing hardness of heated earthen materials, as mud converts to a ceramic-like material during a burn, which results in ping sound rather than a duller thud, when tapped.

Following sampling location selection, detailed notes on the location of the heated rock within the room or feature, the room or feature's location within the site, and the site's location are recorded. The sampling surface is gently brushed clean of dust to ensure the epoxy bond between the affixed plaster cubes and the specimen's surface is stable. A strategic sampling plan is developed for each sampled location, with a clear plan of where plaster cubes/supports will be placed and in what sequence. This is critical, as compass orientation measurements are taken along the +y edge of each plaster cube, and subsequent placement of plaster cubes might block access.

During field sampling, special consideration is given to the recognition and removal of nearby contaminating magnetic fields that could influence the precision and accuracy of field orientation measurements. Prior to orientation measurements, grid states, scaffolding, nails, chaining pins, phones, metal clipboards, keys, etc. are removed from the immediate vicinity of the rock. When needed and where possible, a sun-compass is used to calculate the effects local magnetic field distortion. In the presence of immoveable large contaminating magnetic fields, such as underground steel pipelines or metal fencing, this approach results in a more precise local magnetic declination than a calculation using the International Geomagnetic

Reference Field (IGRF) model. All locally calculated declinations are compared with the IGRF calculation of declination for confirmation.

1.3.3 Laboratory analysis methods

Over the decades, archaeomagnetic directional determinations were carried out in a variety of laboratories using a variety of instruments and a variety of measurement and analysis protocols. Almost exclusively, spinner magnetometers (both commercial and custom, DuBois) were used for measurement. To this day, spinner magnetometers are utilized by the OAS's Archaeomagnetism Laboratory. Usually, classical step-wise alternating field (AF) demagnetization protocols were used by the various laboratories, often with single axis degaussing system in a three-step protocol to ensure each axis of the specimen cube was demagnetized prior to measurement. Multi-step measurement protocols were employed to ensure measurement reliability. The spin protocol used by Daniel Wolfman and currently by the OAS Archaeomagnetism Laboratory measures each specimen axis twice in both the positive and negative directions (e.g. +x and -x) for a total of two measurements of each axis. Each composite measurement reported is the arithmetic mean of the four measurements. The six-step protocol ensures that +z and -z are both measured twice, which is a particular benefit in archaeomagnetic studies because often archaeomagnetic samples are heterogeneous in nature resulting from a lack of centering of the magnetic specimen within the plaster cube encasement and the possible magnetic heterogeneity of the substrate. DuBois' protocols changed over the decades, resulting in the use of several different magnetometers, using several different measurement protocols, as has Eighmy.

In United States Southwest archaeomagnetism, it is common practice to let the specimens "rest" within a zero field for at least two weeks prior to measurement, which allows the least stable VRMs to randomize, decreasing the risk of a systemic bias in the NRM measurements due to weak magnetizations that have been acquired during sample transportation and preparation.

The set of steps used in AF demagnetization of specimen cubes is project, substrate, and laboratory dependent. In most recent decades, five to seven demagnetization steps are measured between the initial NRM measurement and the last measurement, which is typically a peak demagnetization field of roughly 300 Oersteds (Oe, 30mT). Through AF demagnetization, the objective is to progressively neutralize the specimen's magnetic moments until the magnitude of the measured magnetization is less than 20% of the strength of the original NRM. However, historically DuBois did not adhere to this custom, as it was his practice to employ pilot group studies. From a set of specimen cubes from a single archaeomagnetic site, two to three specimens were selected for multi-step demagnetization. After initial NRM measurements for all specimen cubes, only the selected specimens were demagnetized and measured progressively. A "best-step" was selected based on the perceived reduction in the dispersion of the measured specimen magnetic direction, and the remaining specimen cubes were demagnetized to that level and measured once.

Since Lengyel assumed responsibility for the Eighmy laboratory, the Eighmy laboratory began individually assessing the declination and inclination of each specimen cube using primarily principal component analysis (basis in eigenvectors; Kirschvink 1980) prior to analysis of the archaeological feature (archaeomagnetic site), as a whole. Conversely, Eighmy's initial practice and the practice adopted by Wolfman (OAS) was a continuation of

DuBois' "best-step" concept of analysis, analyzing the entire set of specimen cubes from a single feature as a unit, using the measurement data from one AF step from each cube and averaging just those data together as an arithmetic mean calculated in spherical coordinates (known as a Fisher mean; Fisher 1953).

It is uncommon in both current archaeomagnetic laboratories (Wolfman's at OAS, and Eighmy's curated with Stacey Lengyel) to utilized great-circle plane analysis, which is beneficial when the remanent magnetizations of interest is a weak pTRM overprinting a strong TRM or pTRM, common in archaeomagnetism.

All United States-based archaeomagnetism laboratories historically and presently calculate the archaeomagnetic site average from the relatable cubes of the sampled archaeological feature, using a Fisher mean (1953). This mean is reported as the feature's declination and inclination, with a statistical uncertainty reported as an α_{95} (meaning there is a 95% probability that the average falls within the bounds of cone with an angular radius equivalent to the α_{95}, in degrees). This mean and α_{95} are transformed to calculate a VGP position (Equations 1.1 and 1.2) and associated uncertainty ellipse, which aids in visualization and VGP-based archaeomagnetic calendric dating.

$$\cos(\theta_p) = \cos(\theta_s)\cos(\theta_m) + \sin(\theta_s)\sin(\theta_m)\cos(D) \qquad 1.1$$

Equation 1.1: The equation used to transform the remanent magnetization direction the feature into the latitude of the VGP position at the time of magnetic acquisition in the past. Where, θ_p is the colatitude of the of the VGP pole, calculated from the colatitude of the archaeological site (θ_s), the magnetic colatitude (θ_m), and the preserved declination (D). Colatitude (θ) is relatable to latitude (λ) by $\lambda = 90 - \theta$. The magnetic colatitude is calculated from the equation $\cot(\theta_m) = ½ \tan(I)$, where I is the preserved inclination.

$$\sin(\Delta\emptyset) = \sin(\theta_m) * \frac{\sin(D)}{\sin(\theta_p)} \quad 1.2$$

Equation 1.2: The equation used to transform the remanent magnetization direction the feature into the longitude of the VGP position at the time of magnetic acquisition in the past. Where, $\Delta\Phi$ is the angular difference between the VGP position and archaeological site longitudes, calculated from the magnetic colatitude (θ_m), the preserved declination (D), the colatitude of the archaeological site (θ_s). If $\cos(\theta_m) \geq \cos(\theta_s)\cos(\theta_p)$, then $\Phi_p = \Phi_s + \Delta\Phi$. Or if $\cos(\theta_m) < \cos(\theta_s)\cos(\theta_p)$, then $\Phi_p = \Phi_s - \Delta\Phi$. Where Φ_p is the longitude of the VGP position, and Φ_s is the longitude of the archaeological site, in range 0-360°.

1.3.4 VGP-based archaeomagnetic dating

Using a graphical depiction of the VGP and uncertainty ellipse, juxtaposed against the pre-defined regional reference curve, an archaeomagnetic-derived age range can be interpreted. As uncertainty terms become larger, the VGP interpretation is less precisely known and the date range interpretations become increasingly large and less useful. Preferred uncertainty terms are less than an α_{95} of 4° (Jones et al. 2021, Fig S1). Where possible, calendric archaeomagnetic dates are interpreted based on several of the previously proposed reference curves available for the Four Corners region of the United States Southwest.

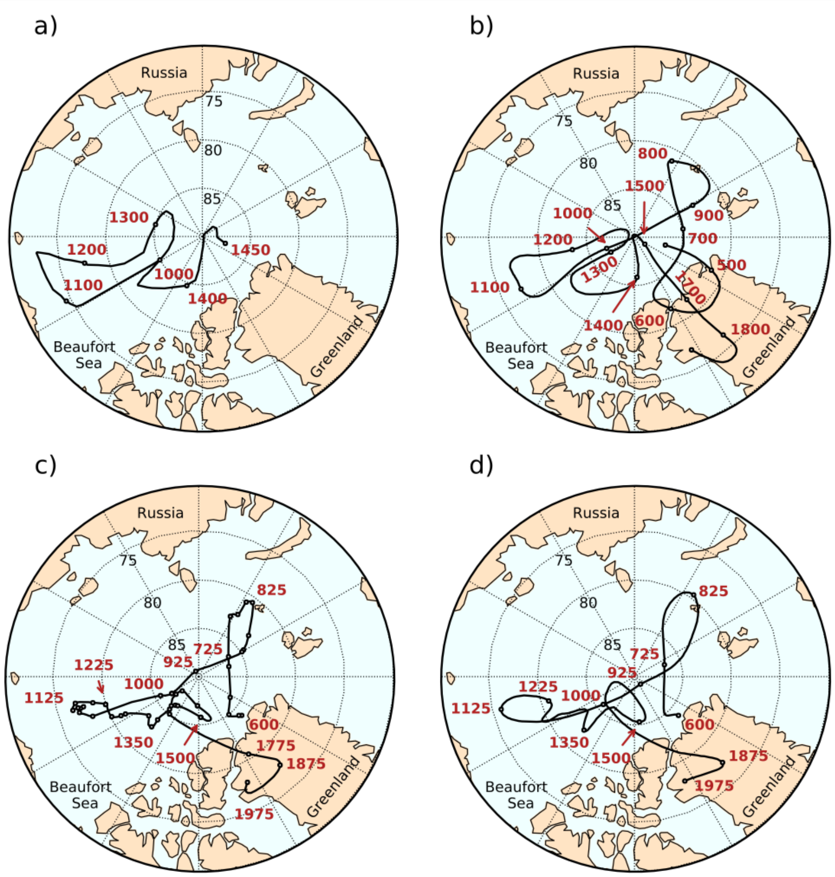

Figure 1.2: The most commonly used previously published regional virtual geomagnetic pole (VGP) reference curves for the Four Corners region, used for archaeomagnetic dating. a) Wolfman (unpub.), b) DuBois [1989], c) SWCV595 (LaBelle & Eighmy 1995), d) SWCV2000 (Lengyel & Eighmy 2002).

To the extent that reference curve paths are accurate and the archaeological feature's VGP position is the expression of the targeted remanent magnetization exclusively, the uncertainty ellipses should perfectly overlap the curve path. However, neither assumption can be made with absolute confidence. Post-depositional processes, as well as specimen mineralogy and magnetic anisotropy, can slightly or significantly affect the preserved remanent magnetization that is central to the research question. A good example is a burned wall that is slightly slumped; the slump may be imperceptible to the eye but the remanent magnetization and thus the VPG position of the burned wall could be drastically different. Additionally, depending on VGP position and uncertainty value, an ellipse can intersect the reference curve in multiple locations, each of which could support a valid date interpretation. Since only one date range is actually relevant to the archaeological event that produced the pTRM or TRM, independent information must be used by the archaeologist to determine which archaeomagnetic date range is appropriate. Archaeomagnetic date interpretations are most useful when there are multiple sources of chronology that can help focus attention on a particular date range as relevant.

Data that are independently dated can be added to the database for later inclusion in the development of future regional-reference curves, as in seen in Chapter 3.

References

Blinman, E. and J.R. Cox. (*in press*) Theory, technique, and performance: Time for renewal in southwestern archaeomagnetic dating. In S.E. Nash and E.L. Baxter (eds.), *Pushing boundaries: Proceedings of the 16th biennial southwest symposium (Chapter 8)*. University Press of Colorado. Boulder, Colorado.

Blinman, E., J.M. Heidke, and M.R. Miller (2017) Cooking Technologies. In B.J. Mills and S. Fowles (eds.), *Oxford Handbook of Southwest Archaeology (Chapter 31)*. Oxford University Press, New York.

Butler, R.F. (1992) *Paleomagnetism: Magnetic Domains to Geologic Terranes*. Blackwell Scientific Publications. Boston, Massachusetts. Available digitally: https://www.geo.arizona.edu/Paleomag/

Deaver, W.L. (1998) Chronological Issues of the LVAP. In S.M. Whittlesey, R. Ciolek-Torrello, and J.H. Altschul (eds.), *Vanishing River: Landscapes and Lives of the Lower Verde Valley, The Lower Verde Archaeological Project (Chapter 12)*. SRI Press, Tucson, Arizona. Chapter 12. 447-490.

DuBois, R. (1989) Archaeomagnetic results from southwest United States and Mesoamerica, and comparison with some other areas. *Physics of the Earth and Planetary Interiors*. 56(1-2), 18-33. https://doi.org/10.1016/0031-9201(89)90033-2

Dunlop, D.J. and Ö Özdemir (1997) *Rock Magnetism Fundamentals and Frontiers*. Cambridge University Press. Cambridge.

Eighmy, J.L. (1980) *Archaeomagnetism: A Handbook for the Archaeologist*. Cultural Resource Management Series. Heritage Conservation and Recreation Service Publication Number 58. Colorado State University. Fort Collins, Colorado.

Eighmy, J.L. and R. Sternberg (1990) Archaeomagnetic Dating. *The University of Arizona Press*. Tucson, Arizona.

Fisher, R.A. (1953) Dispersion on a sphere. *Proceedings of the Royal Society of London, Series A*. 217(1130), 295-305. https://doi.org/10.1098/rspa.1953.0064

Gose, W.A. (2000) Palaeomagnetic Studies of Burned Rocks. *Journal of Archaeological Science*. 27, 409-421. https://doi.org/10.1006/jasc.1999.0465

Haigh, G. (1958) The process of magnetization by chemical change. *The philosophical Magazine*. 3(27), 267-286. https://doi.org/10.1080/14786435808238219

Jackson, A., A.R.T. Jonkers, and M.R. Walker (2000) Four centuries of geomagnetic secular variation from historical records. *Philosophical Transactions of the Royal Society of London*. Series A: 358, 957-990. https://doi.org/10.1098/rsta.2000.0569

Jones, S.A., E. Blinman, L. Tauxe, J.R. Cox, S. Lengyel, R. Sternberg, J. Eighmy, D. Wolfman, and R. DuBois. (2021) MagIC as a FAIR repository for America's directional archaeomagnetic legacy data. *Journal of Geophysical Reviews: Solid Earth*. 126. https://doi.org/10.1029/2021JB022874

Jones, S.A., E. Blinman, J.C. Lohse, J.R. Cox, M. Nichols, and J. Kimbell (in review) Archaeomagnetic directional studies as a revolutionary tool for understanding feature form and function: A case study of two burned rock features in a multi-component site in east Texas, USA. *Journal of Archaeological Science: Reports*

Kirschvink, J.L. (1980) The least square line and plane and the analysis of paleomagnetic data. *Geophysical Journal International of the Royal Astronomical Society*. 62(3), 699-718. https://doi.org/10.1111/j.1365-246x.1980.tb02601.x

Kobayashi, K. (1961) An Experimental Demonstration of the Production of Chemical Remanent Magnetization with Cu-Co Alloy. *Journal of Geomagnetism and Geoelectricity*. 12(3), 148-164. https://doi.org/10.5636/jgg.12.148

LaBelle, J., and J.L. Eighmy (1995) *1995 Additions to the list of independently dated virtual geomagnetic poles and the south-west master curve*. Archaeometric Laboratory Technical Series No. 7. Colorado State University. Fort Collins, Colorado.

Lengyel, S.N. (2004) *Archaeomagnetic Research in the U.S. Midcontinent*. PhD dissertation. University of Arizona. Tucson, Arizona.

Lengyel, S.N., J.L. Eighmy, and L.P. Sullivan (1999) On the Potential of Archaeomagnetic Dating in the Midcontinent Region of North America: Toqua Site Results. *Southeastern archaeology*. 18, 156-171.

Lengyel, Stacey, and J.L. Eighmy (2002). A revision to the U.S. southwest archaeomagnetic master curve. *Journal of Archaeological Science*. 29(12), 1423-1433. https://doi.org/10.1006/jasc.2001.0807

Nagata, T. (1943) The Natural Remanent Magnetism of Volcanic Rocks and Its Relation to Geomagnetic Phenomena. *Bulletin of the Earthquake Research Institute*. 21(1). https://doi.org/10.15083/0000034350

Nagata, T. (1961) *Rock magnetism (revised edition)*. Maruzen. Tokyo.

Neél, L. (1949) Théorie du traînage magnétique des ferromagnétiques en grains fins avec application aux terrescuites. *Annales de Géophysique*. 5, 99-136. https://hal.archives-ouvertes.fr/hal-03070532/

Nickels, D.L., B.J. Vierra, and Wulf Gose. (1998) Fire-cracked Rock. In B.J. Vierra (ed.), *41MV120: A Stratified Late Archaic Site in Maverick County, Texas (Chapter 10)*. Published by the Center for Archaeological Research, The University of Texas at San Antonio. San Antonio, Texas.

O'Reilly, W. (1984) *Rock and Mineral Magnetism*. Blackie. Glasgow.

Shepard, A.O. (1995) *Ceramics for the Archaeologist*. Carnegie Institution of Washington. Washington, D.C.

Tauxe, L., R. Shaar, L. Jonestrask, N.L Swanson-Hysell, R. Minnett, A.A.P. Koppers, C.G. Constable, N. Jarboe, K. Gaastra, and L. Fairchild (2016) PmagPy: Software package for paleomagnetic data analysis and a bridge to the Magnetics Information Consortium (MagIC) Database. *Geochemistry, Geophysics, Geosystems*. 17(6), 2450-2463. https://doi.org/10.1002/2016GC006307

Wolfman, D. (1990) Archaeomagnetic dating in Arkansas and the border areas of adjacent states – II. In J. Eighmy and R. Sternberg (eds.), *Archaeomagnetic Dating (Chapter 14)*. University of Arizona Press. Tucson, Arizona.

Wolfman, D. (unpublished) *Archaeomagnetic Reference Curve for the American Southwest*. Unpublished figure. On file with the New Mexico Office of Archaeological Studies. Santa Fe, New Mexico.

Wolfman, Dl. (1982) Archeomagnetic dating in Arkansas and the border areas of adjacent states. In N. Trubowitz and M. Jeter (eds.), *Arkansas archeology in review* (p. 277-300). Fayetteville, Arkansas.

Chapter 2: Archeointensity of the Four Corners Region of the American Southwest

AGU100

Geochemistry, Geophysics, Geosystems

RESEARCH ARTICLE
10.1029/2018GC007509

Key Points:
- IZZI protocol paleointensity experiments were conducted on 54 new pottery sherds from New Mexico
- The new results were compared with previously published data that were filtered for highest quality
- Cooling rates were calculated from thermocouple data collected from experimental pottery firings

Supporting Information:
- Supporting Information S1

Correspondence to:
S. A. Jones,
saj012@ucsd.edu

Citation:
Jones, S. A., Tauxe, L., Blinman, E., & Genevey, A. (2020). Archeointensity of the four corners region of the American southwest. *Geochemistry, Geophysics, Geosystems*, *21*, e2018GC007509. https://doi.org/10.1029/2018GC007509

Received 2 MAR 2018
Accepted 8 JUN 2018
Accepted article online 12 FEB 2020

Archeointensity of the Four Corners Region of the American Southwest

S. A. Jones[1], L. Tauxe[1], E. Blinman[2], and A. Genevey[3]

[1]Scripps Institution of Oceanography, University of California, San Diego, San Diego, CA, USA, [2]New Mexico Department of Cultural Affairs, Office of Archeological Studies, Santa Fe, NM, USA, [3]Sorbonne Universités, UPMC Univ Paris 06, CNRS, UMR 8220, Laboratoire d'Archeologie moléculaire et Structurale (LAMS), Paris, France

Abstract New paleointensity experiments were conducted using the IZZI protocol (a variation on the Thellier-Thellier method) on 289 specimens from 54 baked pottery fragments collected from four archeological sites in the American Southwest. Anisotropy experiments were conducted to correct for anisotropy of remanence, a common problem in archeological material. Additionally, the effect of cooling rate was evaluated and the calculated paleointensity values were adjusted accordingly. Using the Thellier graphical user interface program, the specimen results were analyzed, averaged by sample (i.e., pottery fragment), filtered for the highest quality, and converted to Virtual Axial Dipole Moments (VADMs). Stylistic evidence, historical documentation, and dendrochronology analyses provide age constraints with up to decade resolution for the VADM results. We compared these new results with the highest quality previously published paleointensity values from the Four Corners region of the American Southwest—defined here as the four states of New Mexico, Arizona, Utah, and Colorado. None of the previously published data were corrected for cooling rate and only some were corrected for anisotropy, resulting in a systematic bias between data sets. To accommodate this difference, an estimated cooling rate correction was applied to all the previously published data. No correction can be made for anisotropy as this is specimen specific. Our estimated cooling rate correction and the empirical correction applied to the new data both require an estimation of the historical cooling rate of the pottery. Experimental pottery firings using one ancient technique and outfitted with thermocouples were conducted to determine the historical cooling rate.

1. Introduction

Understanding the variation in Earth's magnetic field strength before historical records relies on worldwide measurements derived from paleointensity experiments on “accidental” recorders of the field strength such as rocks or archeological artifacts. Burned and baked archeological materials are generally regarded as good recorders of paleointensity because these materials are frequently heated to and cooled from high temperatures, which resets the magnetization of the magnetic grains (e.g., Thellier & Thellier, 1959). Furthermore, over millennia humans have settled in all regions of the world producing burned and baked artifacts, and as such the global distribution of paleointensity records is potentially large and spatially diverse. However, the spatial distribution of paleointensity data in the global database is not uniform, with the majority of values coming from the Northern Hemisphere, primarily from Europe (Figure 1). While other areas have been studied, their contribution to the global database has been more limited. This lack of global coverage affects the precision of global field models (e.g., Constable et al., 2016).

One studied, but underrepresented, region of the world with a great deal of potential for improving our understanding of the variation in Earth's magnetic field strength is the American Southwest. The Native American cultures of the American Southwest, specifically those from the Four Corners region (defined here as the four states of New Mexico, Arizona, Utah, and Colorado) produced vast amounts of pottery. This pottery, mostly found today as fragments (i.e., sherds) in archeological sites, span millennia and is uniquely suited to not only contribute to the effort of improving the spatial distribution of paleointensity records but also to inform on fundamental questions related to the acquisition of magnetic remanence in pottery. Specifically, we have the opportunity to build on the understanding of the effects cooling rate has on paleointensity (e.g., Genevey et al., 2008, 2016; Morales et al., 2011).

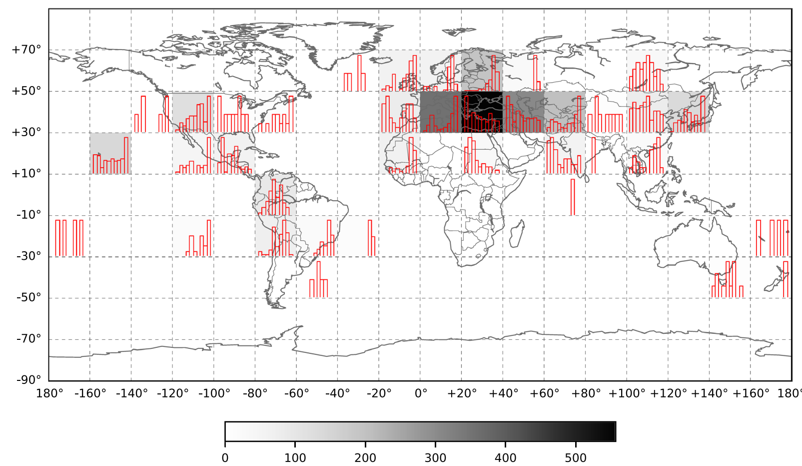

Figure 1. Spatial and temporal distribution of paleointensity data from the 2500 years: The data are available in the GeoMAGIA database (Brown et al., 2015). The shading of each grid depicts the number of paleointensity results available in the gridded region. The bin of the overlaid histogram represent 250 years, with 2500 years before present on the left and the year 2000 CE on the right. Map adapted from Figure S1 in Mitra et al. (2013). GeoMAGIA data downloaded on 9 January 2018.

Previous paleointensity experiments, primarily conducted during the 1960s, 1970s, and 1980s (Bucha et al., 1970; Champion, 1980; Coe, 1967; Games & Davey, 1985; Hsue, 1978; Lee, 1975; Parker, 1976; Sternberg, 1982, 1989; Sternberg & Butler, 1978; Strangway et al., 1968) on pottery sherds and volcanics in the American Southwest yielded results with a large degree of scatter (Figure 2). Here, we reanalyze the previously published data for the highest quality (Figure 2) and conduct new paleointensity experiments on additional pottery sherds collected from the same region (Figure 3).

2. Archeological Context and Chronology

The pottery selected for this study were excavated from four precisely dated archeological sites in the Santa Fe region of the greater Four Corners area (Table 1). All of the pottery studied are of Native American earthenwares shaped using the coiling technique (Text S1 in the supporting information) and produced in either the prehistoric or historic periods (before or after 1600 CE), specifically the fourteenth, seventeenth, eighteenth, and nineteenth centuries CE. The selected fragments have either a shape and/or a decor allowing the identification of their function and the attachment to a culture. In particular, only noncooking vessel forms were included to minimize the risk of secondary thermal magnetic components, and the bowl and storage jar sherds that were included were also screened for any evidence of postfiring exposure to heat (creosote accumulations or oxidation reduction patterns consistent with discard into a fire). For photos of each pottery fragment used in this study, refer to Text S7.

Pottery vessels from these traditions are fragile and have generally limited use lives (e.g., Kohler & Blinman, 1987:7-8). Cooking jars have the shortest use lives (often ~1 year) and constitute about 70% of sherds in refuse (Wilson, 2013:170). Serving and storage vessels (the vessels that yielded the sherds used in this study) generally have longer use lives, but their proportion in refuse (about 30%) argues for regular breakage. Heirloom vessels (those still in use by households 20 years after manufacture) may exist in the serving and storage category, but the sherds in this study are consistent with the decorative styles expected for the dating of their components, and we have no reason to believe that heirloom vessels have contributed sherds to the study. Also, archeological firing features (e.g., kiln pits) associated with the pottery traditions are small (Guthe, 1925; Post & Lakatos, 1995), consistent with the production of five or fewer vessels at any one firing, so large-scale stockpiling of vessels prior to distribution and use is unlikely. Of possibly more concern, experimental firings demonstrated that some of the clay types used in the Four Corners pottery traditions

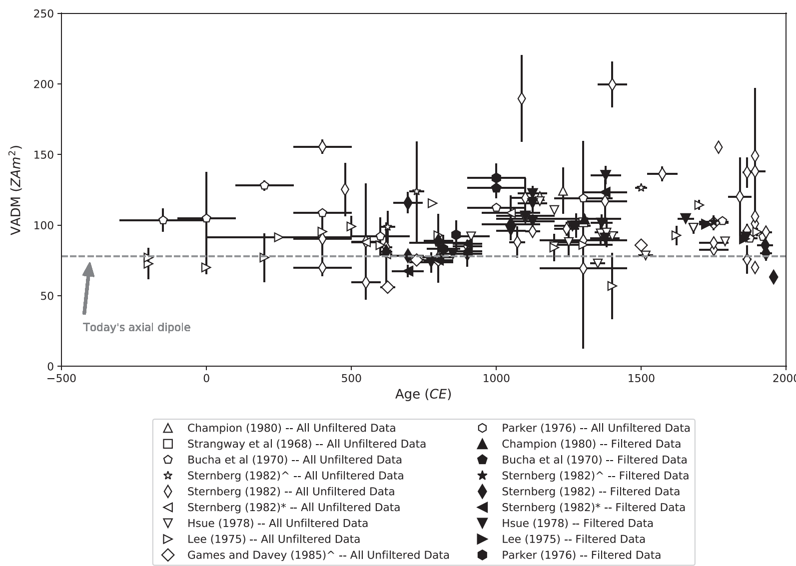

Figure 2. Previously published data: There are 131 unique previously published paleointensity values over the last 2500 years in the Four Corners region of the American Southwest (New Mexico, Arizona, Utah, Colorado). These data were originally analyzed using several different methodologies. To standardize the analysis process, all available specimen data were reanalyzed and all data were filtered for the highest quality using the approach outlined in section 5. The 36 highest-quality (filtered) samples are marked with solid black symbols, while the remaining data are marked with white symbols. The data from Sternberg and Butler (1978) are not included in this figure because all nine samples were further analyzed and updated sample results were published in Sternberg (1982)∗. The updated Sternberg and Butler (1978) data published in Sternberg (1982)∗ are denoted by left pointing triangles. The sample data from Sternberg (1989) are not included either because they are identical to the data published in Sternberg (1982), and we chose to cite the original publication. The Games and Davey (1985)^ data, denoted by large diamonds, are sister specimens of samples published in Sternberg (1982)^, denoted by stars. Sample averages from Coe (1967) are not included because none of the samples from the Four Corner region were successful recorders of paleointensity.

were fired at lower temperatures (as much as 150–200 °C lower) than other clay types (Hensler & Blinman, 2002: 377–378), but any sherds from low-fired vessels would not have passed our strictest selection criteria.

2.1. LA 4968: Spanish Colonial Site, Near Pojoaque, NM

LA 4968 was the residence of Vicente Valdez and his family from approximately 1830 to 1868 CE. Included in the highest-quality results is a single Powhoge Polychrome jar sherd (EU01-03, Powhoge is one type of the Tewa Polychrome ware). It was recovered from the upper fill of a granary within the site (Moore, 2018, see related manuscript). Although the granary provenience is relatively late in the occupation, the derivation of the sherd from the fill suggests that the vessel was broken and discarded while the granary was still in use. A conservative interpretation is that the jar could have been manufactured within the range of shortly before the site occupation to shortly before abandonment, translating into a date range of 1825–1860 CE.

2.2. LA 98: Pueblo San Marcos, Near Santa Fe, NM

Pueblo San Marcos is a large multicomponent pueblo with both Native American and Spanish Colonial occupations that span the fourteenth through seventeenth centuries CE (Ramenofsky et al., 2009). Excavations of the mission church and convento complex were undertaken by David Hurst Thomas of the American Museum of Natural History between 1999 and 2001 (Thomas, 2003). Although the excavated mission structures may have been constructed as late as the 1660s, pottery from the excavations included sherds of all time periods that had been incorporated into the adobe construction materials. However, those bowl rims from the excavated collections that were classified as Glaze F were locally produced in the latter half of the

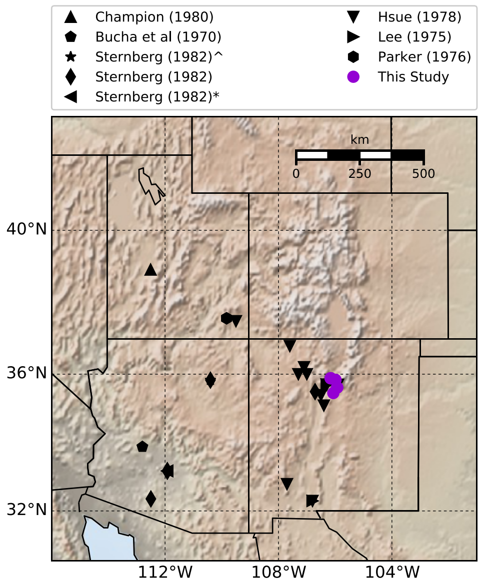

Figure 3. Location map of highest quality data: The sampling location of the 36 highest-quality previously published data are marked with solid black symbols, while those of the eight samples resulting from this study are marked with purple circles. The four states (from the bottom right corner clockwise) New Mexico, Arizona, Utah, and Colorado comprise the Four Corners region of the American Southwest. From the intersection of the four states, in the center of the map, to their farthest corner is about 750 km.

seventeenth century, postdating the initial Spanish presence at the site (Blinman, 2003:70-71). One Glaze F bowl rim sherd (EU02-04) contributed to the highest-quality intensity data. The runny quality of the glaze and the effective abandonment of the mission at the time of the Pueblo Revolt yields a date range assignment of 1640–1680 CE.

2.3. LA 12: Arroyo Hondo Pueblo, Near Santa Fe, NM

Arroyo Hondo Pueblo is a large two-component village that was excavated by the School of American Research (now the School of Advanced Research) between 1970 and 1974 (Creamer, 1993). Tree ring samples provide the precise chronology for the components, and Component I was constructed between 1315 and 1330 CE (Creamer, 1993: 134–138). Only a single tree ring cutting date suggests remodeling after 1330 CE, and it is likely that abandonment occurred before 1340 CE. A single sherd from a Galisteo black-on-white bowl from this component produced the highest-quality results (EU03-09). It originated from Ceramic Horizon Group I, defined as a stratigraphically early cultural deposit within this component (Lang, 1993: 167). A conservative interpretation is that the vessel could have been brought to the site by the initial occupants but was broken and discarded during the active period of growth of the pueblo. The intensity data from this sherd are included in this report with a date range of 1310–1330 CE.

Component II tree ring dates are abundant in the 1370–1390 CE period, with an isolated construction episode at 1410 CE (Creamer, 1993:134-138). Highest-quality pottery samples EU05-02 (Galisteo black-on-white bowl) and EU05-09 (Pindi black-on-white bowl) are associated with Ceramic Horizon Group XIII, affiliated with the late occupation within Component II (Lang, 1993:176-177). A conservative interpretation is that the vessels could have been made between the height of pueblo growth and the abandonment of the pueblo. The two sherds within this group are assigned a date span of 1390–1420 CE.

2.4. LA 65005: Pedro Sanchez Rancho, Near Los Alamos, NM

Land grant records indicate that the LA65005 site was occupied between 1742 and 1763 CE as a Spanish Colonial rancho, with the possibility of some minor continued nonresidential use of the location into the last decades of the eighteenth century (Moore, 2001: 177–181). The pottery was obtained from excavations in a trash accumulation in what had been a shallow arroyo, and it is likely that the sherds date narrowly to the actual residential use of the site by the Pedro Sanchez family. High-quality results are associated with two Tewa Polished red bowl sherds (EU06-04 and EU06-08) and a Tewa Polished black jar sherd (EU06-06). For this study, the conservative date range for the samples is set at 1740–1770 CE.

2.5. Chronology of Previously Published Data

The chronology of the previously published data was not updated in this study, although some of the dates have been updated since their initial publication (Bowles et al., 2002). If a chronology was updated by Bowles et al. (2002), the updated value was used for this study. Several different chronology techniques were employed to determine the ages of the previously published samples. A summary can be found in Table 2.

3. Methods

3.1. Paleointensity Experiments

Specimens for paleointensity experiments were created from pottery sherds (i.e., samples) by gluing a single pea-sized fragment (oblate or prolate fragments of roughly 5–7 mm in diameter) into a 12 mm diameter borosilicate vial using potassium silicate and microfiber silica filter paper. To assess the viability of each pottery sherd as a paleointensity recorder, preliminary experiments were conducted on two specimens per sherd. If either or both of these two specimens were found favorable to intensity determination an additional 7 to 19 specimens were created for use in secondary experiments.

Table 1
Archeological Context

Potsherd	Age (CE)	Dating method	Sherd style	Location	Lat.	Long.	Catalog information
EU01-01	1825–1860	PS, HD	Tewa Polychrome	LA 4968	35.8	254.0	LA 4968-270-1
EU01-02	1825–1860	PS, HD	Tewa Polychrome	LA 4968	35.8	254.0	LA 4968-247-1
EU01-03	1825–1860	PS, HD	Tewa Polychrome	LA 4968	35.8	254.0	LA 4968-293-7
EU01-04	1825–1860	PS, HD	Tewa Polychrome	LA 4968	35.8	254.0	LA 4968-268-1
EU01-05	1825–1860	PS, HD	Tewa Polychrome	LA 4968	35.8	254.0	LA 4968-404-3
EU01-06	1825–1860	PS, HD	Tewa Polychrome	LA 4968	35.8	254.0	LA 4968-285-1
EU01-07	1825–1860	PS, HD	Tewa Polychrome	LA 4968	35.8	254.0	LA 4968-352-1
EU02-01	1625–1680	PS, HD	Glaze Polychrome F	LA 98	35.5	253.9	AMNH 2001, Cat 99.12.4901, Lot 1, Count 1
EU02-02	1640–1680	PS, HD	Glaze Polychrome F	LA 98	35.5	253.9	AMNH 1999, Cat 99.12.1664, Lot 2, Count 1
EU02-03	1640–1680	PS, HD	Glaze Polychrome F	LA 98	35.5	253.9	AMNH 1999, Cat 99.12.1446, Lot 2, Count 1
EU02-04	1640–1680	PS, HD	Glaze-on-yellow F	LA 98	35.5	253.9	AMNH 2001, Cat 99.12.4727, Lot 2, Count 1
EU02-05	1625–1680	PS, HD	Glaze red F	LA 98	35.5	253.9	AMNH 1999, Cat 99.12.671, Lot 6, Count 1
EU02-06	1640–1680	PS, HD	Glaze-on-red F	LA 98	35.5	253.9	AMNH 1999, Cat 99.12.969, Lot 10, Count 1
EU02-07	1625–1680	PS, HD	Glaze red F	LA 98	35.5	253.9	AMNH 1999, Cat 99.12.608, Lot 29, Count 1
EU03-01	1310–1330	PS, D, S	Santa Fe B/W	LA 12	35.6	254.1	Group 1, Box 107, Bag 23E, 12-18-49-8
EU03-02	1310–1330	PS, D, S	Santa Fe B/W	LA 12	35.6	254.1	Group 1, Box 107, Bag 23E, 12-18-49-8
EU03-03	1310–1330	PS, D, S	Santa Fe B/W	LA 12	35.6	254.1	Group 1, Box 107, Bag 23E, 12-18-49-8
EU03-04	1310–1330	PS, D, S	Santa Fe B/W	LA 12	35.6	254.1	Group 1, Box 107, Bag 23E, 12-18-49-8
EU03-05	1310–1330	PS, D, S	Santa Fe B/W	LA 12	35.6	254.1	Group 1, Box 107, Bag 23A, 12-18-49-8
EU03-06	1310–1330	PS, D, S	Poge B/W	LA 12	35.6	254.1	Group 1, Box 107, Bag 23G, 12-18-49-8
EU03-07	1310–1330	PS, D, S	Poge B/W	LA 12	35.6	254.1	Group 1, Box 107, Bag 23G, 12-18-49-8
EU03-08	1310–1330	PS, D, S	Wiyo B/W	LA 12	35.6	254.1	Group 1, Box 107, Bag 21G, 12-18-49-6
EU03-09	1310–1330	PS, D, S	Galisteo B/W	LA 12	35.6	254.1	Group 1, Box 107, Bag 21B, 12-18-49-6
EU03-10	1310–1330	PS, D, S	Santa Fe B/W	LA 12	35.6	254.1	Group 1, Box 107, Bag 21F, 12-18-49-6
EU03-11	1310–1330	PS, D, S	Santa Fe B/W	LA 12	35.6	254.1	Group 1, Box 107, Bag 21F, 12-18-49-6
EU03-12	1310–1330	PS, D, S	Poge B/W	LA 12	35.6	254.1	Group 1, Box 107, Bag 21E, 12-18-49-6
EU04-01	1315–1390	PS, D, S	Poge B/W	LA 12	35.6	254.1	Group 2, Comp II, Ceramic X, Box 80, Bag 32-G, 12-11-3-9
EU04-02	1315–1390	PS, D, S	Santa Fe B/W	LA 12	35.6	254.1	Group 2, Comp II, Ceramic X, Box 80, Bag 30-A, 12-11-3-7
EU04-03	1315–1390	PS, D, S	Santa Fe B/W	LA 12	35.6	254.1	Group 2, Comp II, Ceramic X, Box 80, Bag 30-A, 12-11-3-7
EU04-04	1315–1390	PS, D, S	Santa Fe B/W	LA 12	35.6	254.1	Group 2, Comp II, Ceramic X, Box 80, Bag 29-C, 12-11-3-6
EU04-05	1315–1390	PS, D, S	Santa Fe B/W	LA 12	35.6	254.1	Group 2, Comp II, Ceramic X, Box 80, Bag 29-C, 12-11-3-6
EU04-06	1315–1390	PS, D, S	Santa Fe B/W	LA 12	35.6	254.1	Group 2, Comp II, Ceramic X, Box 80, Bag 29-C, 12-11-3-6
EU04-07	1315–1390	PS, D, S	Pindi B/W	LA 12	35.6	254.1	Group 2, Comp II, Ceramic X, Box 80, Bag 29-E,12-11-3-6
EU04-08	1315–1390	PS, D, S	Pindi B/W	LA 12	35.6	254.1	Group 2, Comp II, Ceramic X, Box 80, Bag 29-E, 12-11-3-6
EU04-09	1315–1390	PS, D, S	Santa Fe B/W	LA 12	35.6	254.1	Group 2, Comp II, Ceramic X, Box 80, Bag 28-D, 12-11-3-5
EU04-10	1315–1390	PS, D, S	Pindi B/W	LA 12	35.6	254.1	Group 2, Comp II, Ceramic X, Box 80, Bag 28-G, 12-11-3-5
EU05-01	1315–1420	PS, D, S	Galisteo B/W	LA 12	35.6	254.1	Group III, Comp II, Group XIII, Box 74, Bag 7B, 12-9-8-IV (Phase 1)
EU05-02	1390–1420	PS, D, S	Galisteo B/W	LA 12	35.6	254.1	Group III, Comp II, Group XIII, Box 74, Bag 7B, 12-9-8-IV (Phase 1)
EU05-03	1315–1420	PS, D, S	Galisteo B/W	LA 12	35.6	254.1	Group III, Comp II, Group XIII, Box 78, Bag 44F, 12-10-4-2N
EU05-04	1315–1420	PS, D, S	Galisteo B/W	LA 12	35.6	254.1	Group III, Comp II, Group XIII, Box 78, Bag 44F, 12-10-4-2N
EU05-05	1315–1420	PS, D, S	Santa Fe B/W	LA 12	35.6	254.1	Group III, Comp II, Group XIII, Box 78, Bag 44E, 12-10-4-2N
EU05-06	1315–1420	PS, D, S	Santa Fe B/W	LA 12	35.6	254.1	Group III, Comp II, Group XIII, Box 78, Bag 42E, 12-10-4-IIIS
EU05-07	1315–1420	PS, D, S	Galisteo B/W	LA 12	35.6	254.1	Group III, Comp II, Group XIII, Box 78, Bag 40A, 12-10-4-3N
EU05-08	1315–1420	PS, D, S	Galisteo B/W	LA 12	35.6	254.1	Group III, Comp II, Group XIII, Box 77, Bag 62, 12-10-3 (10,12,13)
EU05-09	1390–1420	PS, D, S	Wiyo or Pindi	LA 12	35.6	254.1	Group III, Comp II, Group XIII, Box 77, 12-10-3-II
EU06-01	1740–1770	PS, HD	Polished Red	LA 65005	35.9	253.8	Cat No: 35489, Loc: LoA 203 443 B-1, FS 33, #1
EU06-02	1740–1770	PS, HD	Tewa Polychrome	LA 65005	35.9	253.8	Cat No: 35489, Loc: LoA 203 443 B-1, FS 51, #2

Table 1 *Continued*

Potsherd	Age (CE)	Dating method	Sherd style	Location	Lat.	Long.	Catalog information
EU06-03	1740–1770	PS, HD	Polished Red	LA 65005	35.9	253.8	Cat No: 35489, Loc: LoA 203 443 B-1, FS 51, #3
EU06-04	1740–1770	PS, HD	Polished Red	LA 65005	35.9	253.8	Cat No: 35489, L-oc: LoA 203 443 B-1, FS 51, #4
EU06-05	1740–1770	PS, HD	Polished Red	LA 65005	35.9	253.8	Cat No: 35489, Loc: LoA 203 443 B-1, FS 50, #5
EU06-06	1740–1770	PS, HD	Polished Black	LA 65005	35.9	253.8	Cat No: 35489, Loc: LoA 203 443 B-1, FS 37, #6
EU06-07	1740–1770	PS, HD	Tewa Polychrome	LA 65005	35.9	253.8	Cat No: 35489, Loc: LoA 203 443 B-1, FS 37, #7
EU06-08	1740–1770	PS, HD	Polished Red	LA 65005	35.9	253.8	Cat No: 35489, Loc: LoA 203 443 B-1, FS 22, #8
EU06-09	1740–1770	PS, HD	Polished Black	LA 65005	35.9	253.8	Cat No: 35489, Loc: LoA 203 443 B-1, FS 49, #9

Note. C=^{14}C, S = stratigraphy; PS = ceramic (pottery) typology evolution; T = thermoluminescence; M = modern; AM = archeomagnetic; HD = historic documents and material culture; D = dendrochronology; A = other archeological and historical methods. (Borrowed from ; Bowles et al., 2002) Location refers to the archeological site identifier. In the state of New Mexico LA stands for Laboratory of Archaeology, and the number is the numeric site identifier that distinguishes archeological sites from each other. The catalog information is critical to understanding the archeologic context, from which the pottery sherds were excavated. Additional information and photos of the sherd styles are available at this site (http://ceramics.nmarchaeology.org).

Each specimen within the secondary experiments was subject to 18 progressively higher heating steps (100, 150, 200, 250, 300, 325, 350, 375, 400, 425, 450, 475, 500, 525, 550, 575, 585, and 600 °C) cooling in both a zero field and in a laboratory-controlled field of 40 μT. Cooling steps alternated between zero field and infield steps according to the IZZI protocol of Yu et al. (2004). Additionally, seven lower temperature infield steps (so-called "pTRM checks" of, e.g., Thellier & Thellier, 1959) were repeated to check for chemical alteration of the magnetic minerals during experimentation. The IZZI experimental data were analyzed using the Thellier GUI program (Shaar & Tauxe, 2013), part of the PmagPy software package of Tauxe et al. (2016).

The specimens included in the secondary experiments that passed the strict selection criteria (Table 3) were subjected to anisotropy and cooling rate experiments. Using the protocol of Shaar et al. (2016), anisotropy of thermal remanent magnetization (ATRM) tensors were calculated for each specimen that passed the strict specimen selection criteria. Eight heating steps were conducted at the highest temperature reached during the IZZI protocol experiment. The first and last heating steps were conducted in a zero field to test for

Table 2
Summary of Previously Published Papers

Citation	Studied material	Experiment	pTRM checks	Aniso. corr.	Cooling rate correction	Dating method
Strangway et al. (1968)	Lava	van Zijl version of Königsberger	No	No	No	Not listed
Bucha et al (1970)	Ceramics and baked clay	Thellier	No	No	No	C, AM, PS, D, S, or M
Lee (1975)	Ceramics and baked clay	Thellier	No	No	No	A, C, or AM
Parker (1976)	Ceramics and baked clay	Thellier	No	No	No	D
Hsue (1978)	Ceramics and baked clay	Thellier	No	No	No	A, C, or AM
Champion (1980)	Lava	Thellier	Yes	No	No	C, or D & AM
Games and Davey (1985)	Ceramics	Shaw ARM	No	Incl.	Incl.	A, PS, D, HD, or M
Sternberg (1982)	Ceramics	Thellier	Yes	Yes	No	A, PS, D, HD, or M

Note. The data from Sternberg and Butler (1978) are included in Sternberg (1982). All the data from Sternberg (1982) are summarized by Sternberg (1989). As such, the Sternberg and Butler (1978) and Sternberg (1989) publications are not listed below. C = ^{14}C; S = stratigraphy; PS = ceramic (pottery) typology evolution; M = modern; AM = archeomagnetic; HD = historic documents and material culture; D = dendrochronology; A = other archeological and historical methods. (Table after Bowles et al., 2002).

Table 3
Selection Criteria

Criteria group	Statistic	Threshold
Specimen paleointensity	FRAC	≥0.79
	β	≤0.100
	SCAT	on
	gmax	≤0.6
	|k'|	≤0.164
	DANG	≤5
	MAD	≤5
	N_{ptrm}	≥2
	$N_{measurements}$	≥3
Anisotropy criteria	Alteration check	≤5%
	Use *F* test	on
Cooling rate criteria	Alteration check	≤5%
Sample paleointensity	$N_{specimens}$	≥3
	Age σ	≤ ±150
	σ (μT and/or %)	≤ ±6 μT and/or 5%

Note. All the new data from this study were subject to strict selection criteria to determine the highest-quality sample averages. Additionally, the sample paleointensity thresholds were applied to the previously published data. Criteria described in Paterson et al. (2014) and Shaar and Tauxe (2013).

alteration throughout the experiment. The middle six steps were completed in a field of 40 μT in the following orientations order ($+x, +y, +z, -x, -y, -z$). Additional alteration checks were conducted by comparing the pairs $+x, -x$ and $+y, -y$ and $+z, -z$. If any of the four alteration checks differed by 5%, the ATRM results were rejected by the Thellier GUI program. ATRM tensors and anisotropy corrections were calculated within the Thellier GUI, which uses the equations compiled in Veitch et al. (1984). Anisotropy experiments were considered necessary due to the coiling technique used in the production of these pottery (see Text S1 in the supporting information).

During experimentation, specimens were cooled from the set temperature to room temperature in less than 1 hr. Archeological evidence suggests that the techniques used to create the majority of the archeological pottery in the region involved cooling the pottery from at least 700 °C to the ambient temperature, usually overnight (Blinman & Swink, 1997; Swink, 2004). In order to account for the difference in the preserved magnetization due to cooling rate as noted by, for example, Fox and Aitken (1980), a cooling rate correction was carried out using the protocol outlined in Shaar et al. (2016) (similar to that described in Chauvin et al., 2000 and Genevey & Gallet, 2002). Three heating steps were completed in a field of 40 μT on the specimens that passed the strict selection criteria. A fast cooling step at a rate of 43.6 °C/min, a slow cooling step at a rate of 1.3 °C/min, followed by a second fast cooling step to check for alteration. Cooling rate corrections were rejected if the alteration between the two fast cooling steps was greater than 5%. Using the functions within Thellier GUI, a cooling rate correction was calculated assuming a historic cooling rate of 6.21×10^{11} K/Ma (1.308 °C/min). This cooling rate was selected based on estimation of the historic cooling rate as described in section 3.2. After applying anisotropy and cooling rate corrections, sample averages were calculated for each pottery sherd using the selection criteria (Table 3).

The notion of "site" in archeomagnetism overlaps with, but can be different than, the geomagnetic notion of "site." In both disciplines, a site is linked to a specific geographic location (latitude and longitude). However, an archeological site can have one or many discrete temporal occupations or components that range in age, potentially over several centuries. It is recognized that despite derivation from a single component and even provenience within a site, the ceramic fragments reported here may have different dates of magnetic acquisition. To guarantee that statistically reliable averaging is completed on a collection of specimens that cooled in a single unique firing event, only specimens from a single pottery fragment are averaged together

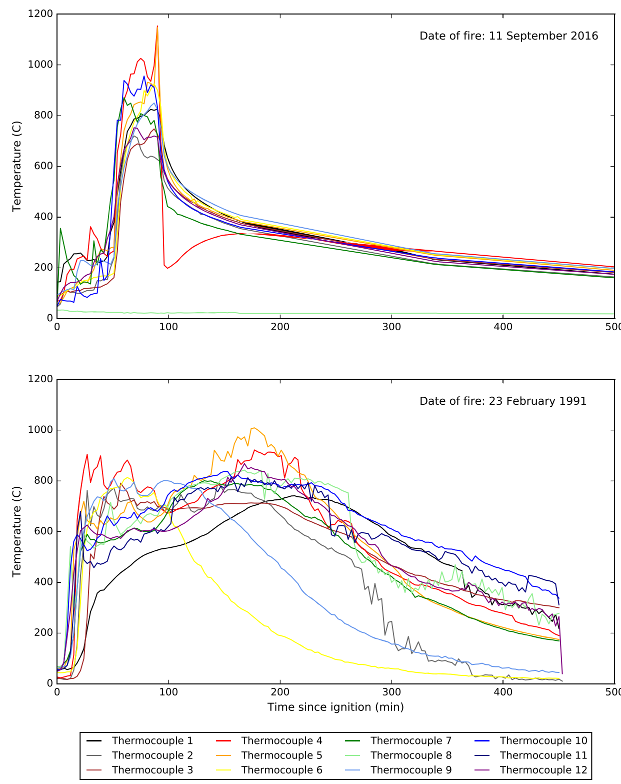

Figure 4. Thermocouple results of two experimental pottery firings: (top) 11 September 2016 and (bottom) 23 February 1991. Using the ancient firing technology original to the Ancestral Pueblo people, two experimental pottery firings were conducted outfitted with thermocouples located inside the air void under upside-down pottery pieces. The variation in the cooling curves of the thermocouple results from the heterogeneity in temperatures within a natural kiln pit. The cooling rate of each thermocouple was calculated between 500 and 200 °C using the method of Shaar et al. (2016), also see Text S3.

in this study. This definition is consistent with the MagIC database definition of a site—a single cooling event. Hence, in this study the "site" identifier is the same as the "sample."

3.2. Determination of Cooling Rate

One of the most challenging quantities to estimate in a paleointensity experiment is the historical cooling rate. In most cases, the historical cooling rate is assumed based on theoretical models or industrial or ethnographic observations of pottery production. But these estimates may not be relevant for specific ancient pottery production traditions across different locales and ranges of raw materials. Without an independent means of corroboration, assumptions can lead to the adoption of inaccurate cooling rate corrections. An empirical approach to determining the historic cooling rate for each material in each locale would be ideal, but is not possible or undertaken in many situations.

Fortunately, much effort has been focused on the ancient pottery technologies of the Ancestral Pueblo people who occupied the Four Corners region. Hundreds of experimental pottery firings exploring the ancient firing techniques have been conducted by an artist-archeologist pair (Clint Swink and EB) and others. Their experimentation has yielded a historically replicable pottery firing regime (Blinman & Swink, 1997, also see

Table 4
Experimentally Calculated Cooling Rates

Date	Thermocouple	Rate (°C/min)	Time (hr)	Note
23 Feb 1991	1	2.217	2.256	
	2	*7.253*	*0.689*	*Not in average, above vessels*
	3	1.178	4.245	
	4	1.691	2.958	
	5	2.169	2.306	
	6	*3.927*	*1.273*	*Not in average, below vessels*
	7	2.131	2.346	
	8	1.057	4.732	
	9	*3.672*	*1.362*	*Not in average, below vessels*
	10	1.979	2.527	
	11	0.958	5.221	
	12	1.277	3.917	
11 Sep 2016	1	1.070	4.674	
	2	1.043	4.792	
	3	1.014	4.929	
	4	*159.770*	*0.031*	*Not in average, broken vessel*
	5	0.951	5.260	
	6	0.964	5.185	
	7	0.889	5.625	
	8			*Ambient temperature*
	9	1.010	4.949	
	10	0.917	5.454	
	11			*Failed thermocouple*
	12	1.029	4.861	
	Average	1.308 ± 0.485	4.235 ± 1.197	

Note. Cooling rates calculated between 500 and 200 °C using the method of Shaar et al. (2016) from 24 thermocouples placed within two experimental pottery firings, also see Text S3 in the SI.

Text S2) and has provided us with dozens of thermocouple records. Two of these thermocouple records (23 February 1991 and 11 September 2016; see Figure 4) are representative of the ancient cooling rates. These records were designed to document the heat rise in the firings, but they are useful in calculating a historical cooling rate because the thermocouples remained connected to the pyrometer for most of the overnight cooling period.

Temperature readings for the 1991 and 2016 firings were collected by placing the sensing tips of thermocouples at various positions within the pit kiln, including inside upside-down vessels, below vessels between the pottery support pieces, above vessels, and between vessels. The inside-vessel thermocouple positions record temperature variation radiated from the inner surfaces of the pieces and is the most valid record of the temperature history of the vessels, especially during heating. The temperature of each thermocouple was recorded every 3 min with an analog Honeywell 12-input strip chart pyrometer. After digitizing the analog records, cooling rates for each thermocouple were calculated using the method of Shaar et al. (2016) (also see Text S3 for individual thermocouple records). Six of the 24 individual records were not included in the average because their positions were not relevant to the cooling of the vessels, including one thermocouple that was used to record ambient air temperature during the 2016 firing (Table 4). Eighteen thermocouple records were used to calculate an average cooling rate of 1.308 °C/min or 6.21×10^{11} K/Ma (a cooling time of 4.235 hr). This average cooling rate was used as the estimated historical cooling rate required for the cooling rate correction calculation in Thellier GUI. This cooling rate is appropriate for this specific ancient pottery technology (Mesa Verde region firing model, which archeological evidence suggests is the longest-cooling ancient method in the American Southwest), but it may not be appropriate for other ancient Southwestern pottery technologies.

Table 5
Specimen Results Table

Potsherd	Sp.	N	T_{min}–T_{max} °C	Frac ≥0.79	β ≤0.1	gmax ≤0.6	DANG ≤5	MAD ≤5	|k'| ≤0.164	N_{ptrm} ≥2	Uncorr. B (μT)	Corr. B (μT)
EU01-03	B	17	000–575	0.93	0.03	0.15	0.78	1.29	0.11	5	71.1	67.7
	C	15	100–550	0.84	0.02	0.14	2.14	2.86	0.00	5	63.3	58.2
	D	15	000–525	0.80	0.02	0.12	2.67	4.13	−0.15	4	62.1	59.2
	E	16	000–550	0.88	0.01	0.12	2.42	4.94	0.00	5	52.6	50.1
	F	15	100–550	0.80	0.01	0.13	2.81	4.07	0.07	5	64.6	59.1
	G	18	000–585	0.98	0.02	0.13	1.97	3.92	0.14	6	61.8	58.9
EU02-04	B	15	100–550	0.92	0.02	0.18	1.70	4.70	0.14	5	60.4	56.1
	C	15	150–575	0.93	0.01	0.15	1.65	4.87	0.10	5	61.4	57.1
	D	18	000–585	0.96	0.01	0.16	1.21	3.83	0.06	6	61.1	57.2
	G	15	200–585	0.93	0.02	0.19	0.87	3.80	0.14	6	63.4	58.1
EU03-09	A	15	000–525	0.92	0.04	0.13	4.19	2.84	0.13	4	47.4	43.9
	B	14	000–500	0.82	0.04	0.17	1.35	3.89	−0.07	4	42.9	44.6
	C	17	000–575	0.99	0.04	0.12	3.12	4.23	0.00	5	50.2	45.9
	D	16	000–550	0.91	0.04	0.12	4.75	4.31	0.00	5	45.9	41.6
	F	16	100–575	0.97	0.04	0.11	2.65	3.87	0.00	5	49.0	44.9
	G	17	000–575	0.97	0.04	0.11	2.43	4.43	0.00	5	49.8	45.7
EU05-02	A	17	000–575	0.97	0.01	0.20	0.74	3.01	0.06	5	59.9	57.5
	B	17	000–575	0.97	0.02	0.18	0.98	4.72	0.16	5	60.4	56.9
	F	17	000–575	0.97	0.02	0.14	2.31	3.28	0.16	5	59.3	58.1
EU05-04	I	14	100–525	0.81	0.02	0.17	3.28	4.05	0.12	5	51.7	53.8
	J	15	000–525	0.81	0.02	0.16	2.65	4.34	0.10	5	47.6	41.1
	K	15	000–525	0.85	0.03	0.19	1.12	2.79	0.00	5	64.7	58.0
	L	15	000–525	0.79	0.02	0.16	1.86	3.39	0.11	5	55.5	51.8
	M	15	000–525	0.85	0.03	0.18	1.90	2.87	0.00	5	58.9	64.0
	N	15	000–525	0.83	0.03	0.14	4.17	4.11	0.16	5	57.2	62.5
	O	15	000–525	0.83	0.03	0.14	3.74	4.32	0.14	5	62.1	62.4
	P	15	000–525	0.86	0.03	0.19	1.65	2.85	0.12	5	47.4	54.1
	Q	15	000–525	0.86	0.03	0.21	1.89	3.20	0.12	5	59.4	49.1
	S	15	000–525	0.84	0.03	0.16	2.23	4.30	0.14	5	63.6	66.8
EU05-09	A	15	000 - 525	0.80	0.03	0.13	1.66	1.95	0.00	4	68.8	63.4
	B	15	000–525	0.81	0.02	0.13	1.50	3.38	−0.05	4	69.8	63.8
	C	15	100–550	0.89	0.03	0.12	1.78	3.45	0.00	5	67.0	61.2
	D	16	000–550	0.91	0.03	0.13	1.08	1.90	0.11	5	69.9	63.4
	E	16	000–550	0.91	0.03	0.12	1.52	3.41	0.00	5	68.1	62.5
	F	15	000–525	0.81	0.02	0.13	2.05	3.76	−0.06	4	65.6	59.9
	G	16	000–550	0.91	0.03	0.11	1.91	3.38	0.00	5	69.5	63.6
EU06-04	A	16	100–575	0.87	0.02	0.12	1.50	4.90	0.12	5	54.1	51.0
	B	14	150–550	0.83	0.01	0.11	3.39	4.95	0.05	5	52.2	54.6
	C	14	200–575	0.84	0.02	0.12	0.55	2.80	−0.10	5	55.9	56.3
	D	18	000–585	0.97	0.03	0.12	0.32	1.47	0.06	6	60.5	56.8
	E	16	100–575	0.91	0.02	0.12	2.47	3.12	−0.07	5	56.6	56.2
	F	16	150–585	0.87	0.02	0.11	1.49	3.53	0.15	6	66.0	61.6
	G	16	100–575	0.92	0.01	0.11	1.00	3.58	−0.03	5	50.7	56.5
EU06-06	F	13	250–575	0.82	0.02	0.26	0.26	1.67	0.14	5	50.0	47.1
	J	15	100–550	0.84	0.04	0.20	2.55	4.46	0.00	6	55.5	52.1
	S	15	150–575	0.92	0.03	0.23	0.51	1.80	0.13	6	49.1	48.6

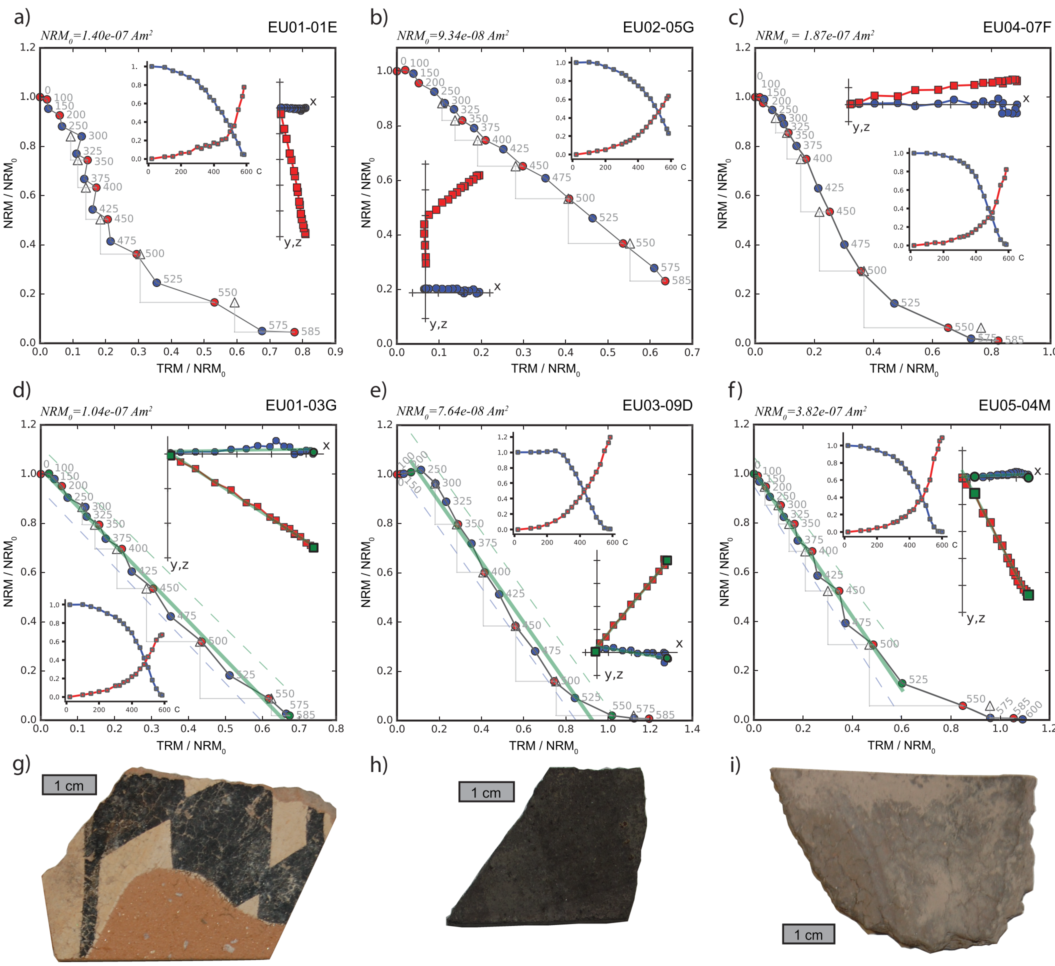

Figure 5. Representative Arai plots and Zijderveld diagrams for specimens from this study: The overall success rate for specimens and samples satisfying the strict selection criteria (Table 3) is 30% and 40%, respectively. Sample EU01-01E (a) failed the selection criteria because it is too curved. Sample EU02-05G (b) shows a specimen that failed because the maximum angular deviation (MAD) of the directional vector was too large. And Sample EU04-07F (c) failed the selection criteria for being too curved and having a low FRAC. Samples EU01-03G, EU03-09G, and EU05-04 M (d–f) show representative specimens that satisfied the selection criteria and their associated pottery sherd (g–i).

4. Results

4.1. Paleointensity Experiments

A total of 289 specimens were collected from 54 pottery sherds from four archeological sites. Of these, 108 specimens were part of the preliminary experiments and the remaining 181 specimens from 20 samples (four archeological sites) were part of the secondary experiments. In the secondary experiments, 58 specimens (success rate of 30%) and eight samples (success rate of 40%) passed the strict acceptance criteria (Table 3). Figures 5a–5c show three examples of specimens that failed the acceptance criteria. Figures 5d–5i show three examples of specimens that passed the acceptance criteria and the associated pottery sherd from which the

Table 5 *Continued*

Potsherd	Sp.	N	T_{min}–T_{max} °C	Frac ≥0.79	β ≤0.1	gmax ≤0.6	DANG ≤5	MAD ≤5	|k'| ≤0.164	N_{ptrm} ≥2	Uncorr. B (μT)	Corr. B (μT)
EU06-08	B	13	250–575	0.80	0.02	0.16	1.08	2.23	0.07	5	64.9	64.8
	C	14	200–575	0.81	0.02	0.13	1.75	4.30	−0.12	5	63.4	60.2
	D	15	200–585	0.82	0.03	0.12	2.75	3.77	−0.06	6	64.1	60.7
	E	18	000–585	0.92	0.04	0.17	1.98	4.67	0.00	6	71.1	66.3
	F	15	200–585	0.82	0.02	0.16	0.96	2.41	−0.12	6	57.7	54.7
	G	15	200–585	0.84	0.03	0.15	2.45	2.84	−0.15	6	69.5	65.9
	I	14	150–550	0.90	0.02	0.13	1.58	1.94	−0.13	6	63.8	64.9
	J	19	000–600	1.00	0.04	0.15	0.99	2.89	0.00	7	74.2	70.7
	K	18	000–585	0.99	0.03	0.17	0.93	2.80	−0.06	7	60.6	66.9
	M	15	200–585	0.86	0.02	0.13	1.35	1.97	−0.16	7	66.3	62.8
	O	18	100–600	0.98	0.02	0.11	1.51	2.27	−0.03	7	63.4	64.8
	S	16	100–575	0.97	0.02	0.13	1.90	3.27	−0.15	6	71.5	70.5

Note. This contains only the 58 specimens that passed the strict criteria. All specimen and measurement data are available at this site (http://earthref.org/MagIC/doi/10.1002/2018GC007509). Sp. = Specimen; T_{min} = minimum temperature step used to determine the paleointensity; T_{max} = maximum temperature step used to determine the paleointensity; Uncorr. = uncorrected; Corr. = corrected; *B* = intensity.

specimen was derived. Data from all specimens will be available in the MagIC database upon publication at this site (http://earthref.org/MagIC/doi/10.1002/2018GC007509).

Anisotropy experiments conducted on specimens during the secondary experiments yielded anisotropy corrections typically in the range of 1% to 4%, but several specimens have corrections between 6% and 10%, with one correction of nearly 16%. The range of these anisotropy corrections underline the importance of evaluating each pottery specimen individually. Using a cooling rate of 1.308 °C/min or 6.21×10^{11} K/Ma, cooling rate corrections of varying percent were applied to the samples that passed the strict acceptance criteria. The applied cooling rate corrections range from −4.85% to −9.41% with an average of −6.73%. The resulting highest-quality specimen and sample paleointensity results, corrected for anisotropy and cooling rate, are reported in Tables 5 and 6, respectively.

TRM is usually assumed to be linearly related to the applied field, but this is not strictly true and nonlinearity can become significant for higher field intensities (Selkin et al., 2007). In order to test the significance for our samples, a nonlinear TRM experiment, using the method of Selkin et al. (2007) was conducted

Table 6
Sample Results Table

Potsherd	Location	State	Lat.	Long.	Age CE	*n*	Corrected $B \pm \sigma$ (μT)	Corrected VADM ±σ (ZAm^2)
EU01-03	LA 4968	NM	35.8	254.0	1825–1860	6	58.40 ± 5.55	106.00 ± 10.10
EU02-04	LA 98	NM	35.5	253.9	1640–1680	4	56.50 ± 0.83	103.00 ± 1.50
EU03-09	LA 12	NM	35.6	254.1	1310–1330	6	43.70 ± 1.57	79.60 ± 2.86
EU05-02	LA 12	NM	35.6	254.1	1390–1420	3	56.80 ± 0.53	103.00 ± 0.97
EU05-04	*LA 12*	*NM*	*35.6*	*254.1*	*1315–1420*	*10*	*55.70± 7.79*	*101.0± 14.20*
EU05-09	LA 12	NM	35.6	254.1	1390–1420	7	61.60 ± 1.42	112.00 ± 2.59
EU06-04	LA 65005	NM	35.9	253.8	1740–1770	7	55.60 ± 3.11	101.00 ± 5.64
EU06-06	LA 65005	NM	35.9	253.8	1740–1770	3	48.70 ± 2.60	88.40 ± 4.72
EU06-08	LA 65005	NM	35.9	253.8	1740–1770	12	63.90 ± 4.42	116.00 ± 8.02

Note. This contains the samples that passed the strict selection criteria. Note that although several specimens from EU05-04 pass the strict selection criteria, the standard deviation of the sample average exceeds the threshold of the selection criteria and as such is not included in Figure 7. The data are included in italics for reference.

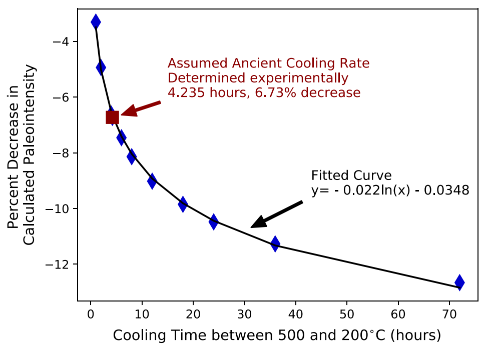

Figure 6. Empirical effect of cooling rate on paleointensity: The application of 10 assumed historical cooling rates on the calculated paleoinitensity of the successful pottery sherds from this study shows that the selection of a historical cooling rate has a profound affect. Note the doubling in the percent decrease between an assumed cooling time of 1 hr (3.31%) and 4 hr (6.61%). This is critical in the Four Corners region because almost all pottery traditions cool within 1 and about 4 hr.

at 75 μT. The results demonstrated that the nonlinear TRM effect was insignificant. See Text S4 in the supporting information.

Although rock magnetic experiments were not conducted on these specimens, analysis of the magnetic remanence versus temperature as a proportion of the original NRM (Figure 5) permits a general understanding of the remanence carriers. With the exception of specimen EU02-05G (Figure 5b), all specimens were demagnetized to below 10% of their original remanence by 600 °C. The demagnetization was generally steady as the temperature increased progressively. These behaviors suggest that the magnetic remanence carrier is a combination of magnetite and titanomagnetite.

4.2. Empirical Effect of Cooling Rate on Successful Samples

Ten different assumed ancient cooling times (1, 2, 4, 6, 8, 12, 18, 24, 36, and 72 hr) were applied to the set of our samples that passed the strict selection criteria. The resulting cooling rate corrected paleointensity values were compared to the noncooling rate-corrected paleointensity values to calculate percent decrease for each sample. The percent decrease for each sample was then averaged and a natural logarithmic curve was fit to the data (Figure 6). In agreement with similar previous experiments (e.g., Genevey et al., 2008; Hartmann et al., 2010), one critical observation is that the assumed ancient cooling rate used to calculate the cooling rate correction has a profound effect on paleointensity values reported. A change from 1 to 4 hr doubles the percent decrease from 3.31% to 6.61%. The slower the cooling rate, the less profound of an impact a small change in cooling rate has on the paleointensity values, as is expected with logarithmic functions. A cooling rate consistent with the ancient methods of 1.308 °C/min or 4.235 hr, results in an averaged 6.73% decrease.

4.3. Success Rate and Archeological Context

The 58 new specimens from the eight samples presented here that successfully passed our strict selection criteria represent 30% and 40% of those measured, respectively. This success rate is low but not inconsistent with other paleointensity experiments. In an attempt to understand what may contribute to failure of the experiment, we adopted an archeological approach rather than a rock magnetic approach, which has had limited success in the past (e.g., Mitra et al., 2013).

Archeologists commonly group ceramics based on physical and design characteristics visible to the naked eye or using a binocular microscope. In the American Southwest, the commonly utilized types can be accessed at this site (http://ceramics.nmarchaeology.org). Each ceramic type is defined by attributes common to a single time, production tradition, use, and the basic properties of the clays and temper. Thus, considering the paleointensity success of pottery sherds from a typology perspective may be useful in terms of preselection because past humans consciously chose source(s) material to achieve a specific result, so a relationship between the source(s) material and the successful preservation of paleointensity is a possibility.

Table 7 lists our results by ceramic type. Of the 11 pottery types sampled in this study, some performed better than others. For example, of the six Galisteo black-on-white sherds measured, two passed our strict criteria (33% success rate). In contrast, the extremely common and long-lived Santa Fe black-on-white type was very unsuccessful; none of the 15 samples tested passed our criteria. The Tewa Polychrome type was also limitedly successful, while the Polished (Tewa) Red type was quite successful (40%). The remaining seven types studied here have sample sizes too small to make any robust claim. Further experimentation on different types is ongoing to determine if any statistically reliable trends exist. A trend could be the result of several factors including (1) the clay and temper used to make the pottery and (2) the firing and subsequent cooling conditions the pot experienced.

5. Comparison With Previously Published Data

Experiments conducted on material from the Four Corners region primarily during the 1960s, the 1970s and the 1980s produced 131 paleointensity estimates spanning the last 2500 years. While most of these sample averages have been input into the GeoMAGIA database (Brown et al., 2015) and the metadata loaded into

Table 7
Percentage of Sherds That Satisfied the Strict Selection Criteria, Organized by Ceramic Tradition

Pottery tradition	Sherds	Successful sherds	Success rate
Galisteo black-on-white	6	2	33%
Santa Fe black-on-white	15	0	0%
Poge black-on-white	4	0	0%
Wiyo black-on-white	1	1	100%
Pindi black-on-white	3	0	0%
Glaze polychrome	3	0	0%
Glaze-on-yellow	1	1	100%
Glaze-on-red F	3	0	0%
Tewa polychrome	9	1	11%
Polished (Tewa) red	5	2	40%
Polished (Tewa Kapo) black	2	1	50%

Note. Considering ceramic typology as a preselection criteria may prove to be a useful perspective. In this study, 11 pottery types were randomly sampled. Some pottery types, for example, the Galisteo black-on-white and the polished (Tewa) red, successfully preserved the paleointensity. Others, for example, the Santa Fe black and white, did not preserve paleointensity well. A full description of the pottery types including photos is available at this site (http://ceramics.nmarchaeology.org).

MagIC database (http://earthref.org/MagIC), or both, some previously published data are not included in either database (Table 8). The two databases are actively being updated.

The previously published sample averages were calculated prior to the development of strict selection criteria, although each individual author attempted to filter data for the highest quality. In an attempt to reconcile the different approaches to filtering data, we recalculated all sample averages from the published specimen data, when available. These updated sample averages were subjected to the same three sample paleointensity selection criteria as used in the present study (Table 3).

- The number of specimens included in the sample average must be greater than or equal to three.
- There must be an estimate of age uncertainty, and uncertainty must be less than or equal to 150 years (range of 300 years).
- The standard deviation (σ) of the calculated paleointensity value must be less than or equal to 6 μT and/or 5% of the intensity value.

Additionally, the affect of anisotropy and cooling rate corrections were considered. Failing to correct for the anisotropy of remanence tends to increase the scatter of specimen level results, but does not create

Table 8
Publications Included in the GeoMAGIA and MagIC Databases

Publication	GeoMAGIA	MagIC
Strangway et al. (1968)	X	X
Bucha et al. (1970)	X	X
Lee (1975)	X	X
Parker (1976)		
Hsue (1978)	X	X
Sternberg and Butler (1978)[a]		
Champion (1980)	X	X
Sternberg (1982)[a]		
Games and Davey (1985)	X	X
Sternberg (1989)	X	X

[a]Data included in Sternberg (1989).

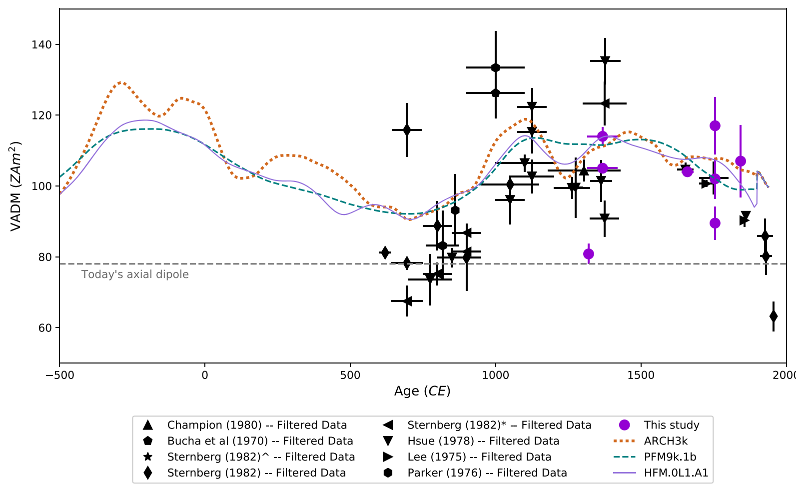

Figure 7. Highest-quality paleointensity sample averages for the Four Corners region: The solid black symbols represent the 36 highest-quality previously published sample averages after cooling rate correction. The solid purple circles indicate the eight highest-quality sample averages from this study after ATRM and cooling rate corrections. The dispersion evident in the data sets is likely due to the lack of precise cooling rate and ATRM corrections in the previously published data and uncertainty in the age of each pottery sherd. The combined data affirm the global decrease in magnetic field strength over the last several hundred years, indicate the presence of at least one maximum between 1100 CE and 1400 CE, and suggest the presence of second minimum at 700 CE and 900 CE. Note that the general trends in the data set are also predicted by the global model predictions for the region (ARCH3k of Korte et al., 2009, PFM9k.1b of Nilsson et al., 2014, and HFM.0l1.A1 of Constable et al., 2016). The global models overestimate the trends, because the data presented here are filtered for highest quality and cooling rate corrected. The models are based on the entire unfiltered, uncorrected previously published data in Figure 2.

a systematic bias in the averaged intensity. Failure to account for cooling rate, on the other hand, does lead to a bias, as samples cooled more slowly in their original firing will have, most often, a higher magnetization than those acquired in a quickly cooled laboratory setting. This difference leads to a high bias in uncorrected results.

At the time of measurement and analysis of the previously published data, cooling rate correction experiments were not customary (Table 2) and only Sternberg (1982) conducted anisotropy experiments. The result is a systematic difference between the previously published data set and the data present here. While this difference cannot be rectified without conducting cooling rate and anisotropy experiments on the original specimens, the effect of cooling rate can be estimated using the results from the newly measured specimens. We applied a 6.73% decrease to each specimen in the entire previously published data set (except for data obtained from lava flows, which were left unchanged) and then recalculated the sample averages. This 6.73% decrease is derived from the empirical analysis described in section 4.2. After the correction, the two data sets (previously published and the new samples presented here) are more closely aligned with each other and to the modern value of the virtual axial dipole moment (Figure 7). The previously published data corrected for cooling rate and filtered for highest quality are available in Table 9.

6. Discussion

6.1. Scatter in the Thermocouple Determination of Cooling Rate

The variation seen in the precise temperature records of the two experimental firings (1991 and 2016) of this Four Corners pottery tradition is illustrative of the real-world challenges of deriving cooling rates for past pottery technologies. Decreased variability of kiln temperatures and cooling rates between the 1991 and the 2016 experimental firings represent improvements in firing technique on the part of Clint Swink and EB. These improvements had the incidental effect of lowering the variability and mean cooling rate

10.1029/2018GC007509

Table 9
Previously Published Sample Result Table Contains the sample averages, corrected for the effects cooling rate, that passed the strict selection criteria used in this study

Citation	Sample ID	Material	Location	State	Lat.	Long.	Age CE ±σ	n	Uncorrected $B \pm \sigma$ (μT)	Corrected $B \pm \sigma$ (μT)	Corrected VADM ± σ (ZAm^2)
Champion (1980)	IcSU	Lava	Ice Spring Field Black Rock Desert	UT	38.93	247.49	1304.0 ± 125[a]	3	59.63 ± 1.75	N/A	104.33 ± 3.07[b]
Bucha et al. (1970)	50	Ceramic	Snaketown	AZ	33.90	247.20	1300.0 ± 100.0	5	71.11 ± 5.59	66.3 ± 5.21	123.36 ± 9.70
Sternberg (1982)	PA001	Ceramic	Hickiwan Village	AZ	32.36	247.59	1956.5 ± 0.5	3	35.73 ± 2.38	33.3 ± 2.22	63.20 ± 4.20
	SN001[c]	Ceramic	Snaketown outlier	AZ	33.19	248.08	1375.0 ± 75.0[a]	3	70.43 ± 3.54	65.7 ± 3.3	123.28 ± 6.19
	SN004[c]	Ceramic	Snaketown	AZ	33.19	248.08	900.0 ± 50.0[a]	3	49.57 ± 1.46	46.2 ± 1.36	86.75 ± 2.55
	SN005[c]	Ceramic	Snaketown	AZ	33.19	248.08	900.0 ± 50.0[a]	3	46.53 ± 4.13	43.4 ± 3.85	81.45 ± 7.23
	SN006[c]	Ceramic	Snaketown	AZ	33.19	248.08	800.0 ± 50.0[a]	3	42.97 ± 1.82	40.1 ± 1.70	75.20 ± 3.18
	SN007[c]	Ceramic	Snaketown	AZ	33.19	248.08	695.0 ± 55.0[a]	3	38.53 ± 2.48	35.9 ± 2.31	67.44 ± 4.34
	SN011	Ceramic	Snaketown	AZ	33.19	248.08	1050.0 ± 100.0[a]	3	57.37 ± 0.29	53.5 ± 0.27	100.41 ± 0.51
	SN013	Ceramic	Snaketown	AZ	33.19	248.08	620.0 ± 20.0[a]	3	46.37 ± 0.25	43.2 ± 0.24	81.15 ± 0.44
	SN014	Ceramic	Snaketown	AZ	33.19	248.08	695.0 ± 50.0[a]	3	66.17 ± 4.32	61.7 ± 4.03	115.81 ± 7.56
	SN015	Ceramic	Snaketown	AZ	33.19	248.08	695.0 ± 55.0[a]	3	44.70 ± 1.08	41.7 ± 1.01	78.24 ± 1.89
	SN016	Ceramic	Snaketown	AZ	33.19	248.08	800.0 ± 50.0[a]	3	50.70 ± 3.97	47.3 ± 3.70	88.74 ± 6.94
	SN018	Ceramic	Snaketown	AZ	33.19	248.08	900.0 ± 50.0[a]	3	45.57 ± 5.35	42.5 ± 4.99	79.75 ± 9.37
	WA002[d]	Ceramic	Walpi	AZ	35.83	249.60	1750.0 ± 50.0	4	60.40 ± 2.74	56.3 ± 2.55	102.30 ± 4.63
	WA015	Ceramic	Walpi	AZ	35.83	249.60	1927.5 ± 27.5	3	50.67 ± 2.95	47.3 ± 2.75	85.81 ± 5.00
	ZI001	Ceramic	Zia Pueblo	NM	35.50	253.29	1930.0 ± 20.0	3	47.13 ± 3.12	44.0 ± 2.91	80.15 ± 5.30
Hsue (1978)	1	Baked Clay	Cuba	NM	36.0	252.7	1100.0 ± 100.0	4	62.98 ± 1.45	58.7 ± 1.35	106.44 ± 2.45
	3	Baked Clay	Berrendal Creek	NM	32.8	252.3	1050.0 ± 50.0	3	54.60 ± 3.92	50.9 ± 3.65	96.04 ± 6.89
	6	Baked Clay	Cochiti	NM	35.7	253.7	1262.5 ± 62.5	4	58.63 ± 1.82	54.7 ± 1.70	99.45 ± 3.09
	8	Ceramic	Santa Fe River	NM	35.7	254.1	1363.0 ± 37.5	3	59.80 ± 3.48	55.8 ± 3.24	101.44 ± 5.90
	12	Ceramic	Lindrith	NM	36.2	252.9	1275.0 ± 25.0	4	59.03 ± 5.06	55.1 ± 4.72	99.45 ± 8.54
	17	Baked Clay	Fort Fillmore	NM	32.3	253.2	1861.0 ± 2.0	3	51.73 ± 0.21	48.3 ± 0.19	91.57 ± 0.37
	18	Ceramic	Tijeros Canyon	NM	35.1	253.6	1375.0 ± 50.0	6	53.13 ± 3.01	49.6 ± 2.81	90.80 ± 5.15
	19	Baked Clay	Cochiti	NM	35.7	253.7	1653.0 ± 28.0	3	61.67 ± 1.14	57.5 ± 1.06	104.61 ± 1.93
	20	Ceramic	Cochiti	NM	35.7	253.7	1125.0 ± 50.0	4	72.13 ± 3.10	67.3 ± 2.89	122.35 ± 5.25
	21	Ceramic	Waldo Galister Dam	NM	35.4	253.5	1377.0 ± 52.0	3	79.43 ± 3.84	74.1 ± 3.58	135.25 ± 6.53
	22	Baked Clay	Navajo Reservoir	NM	36.8	252.4	850.0 ± 50.0	4	47.65 ± 1.61	44.4 ± 1.50	79.76 ± 2.70
	31	Ceramic	Aneth	UT	37.5	250.5	775.0 ± 75.0	4	44.30 ± 4.36	41.3 ± 4.07	73.53 ± 7.24
	34	Baked Clay	Cuba	NM	36.0	253.0	1125.0 ± 75.0	5	60.76 ± 2.82	56.7 ± 2.63	102.69 ± 4.77
	35	Baked Clay	Cochiti	NM	35.7	253.7	1125.0 ± 50.0	4	67.95 ± 3.56	63.4 ± 3.32	115.27 ± 6.03
Lee (1975)	158	Baked Clay	Cochiti	NM	35.7	253.7	1725.0 ± 50.0	3	55.3 ± 0.54	55.51 ± 0.54	100.65 ± 0.98
	184	Baked Clay	Fort Filmore	NM	32.3	253.2	1856.0 ± 5.0	3	47.6 ± 9.33	47.72 ± 0.94	90.28 ± 1.77

10.1029/2018GC007509

Table 9 *Continued*

Citation	Sample ID	Material	Location	State	Lat.	Long.	Age CE $\pm\sigma$	n	Uncorrected $B \pm \sigma$ (μ]T)	Corrected $B \pm \sigma$ (μ[T)	Corrected VADM $\pm$ σ (ZAm^2)
Parker (1976)	PA001	Ceramic	Utah Hwy 95 Proj.	UT	37.58	250.17	817.5 ± 57.5	4	47.5 ± 5.63	44.3 ± 5.25	79.00 ± 9.36
	PA002	Ceramic	Utah Hwy 95 Proj.	UT	37.58	250.17	861.0 ± 11.0	5	53.2 ± 5.83	49.6 ± 5.44	88.49 ± 9.70
	PA003	Ceramic	Utah Hwy 95 Proj.	UT	37.58	250.17	1000.0 ± 100.0	4	76.2 ± 5.89	7.11 ± 5.49	133.38 ± 10.31

Note. This contains the sample averages, corrected for the effects cooling rate, that passed the strict selection criteria used in this study.
[a]Age from Bowles et al. (2002), updated from original citation . [b]VADM does not include an estimated cooling rate correction. [c]Sample also published in Sternberg and Butler (1978) but corrected for anisotropy in Sternberg (1982). [d]Sister sample of a sample published in Games and Davey (1985).

from 1.628 ± 0.515 °C/min to 0.987 ± 0.061 °C/min, respectively. Since every firing is unique and affected by external factors that cannot be individually quantified in the archeological record, such as the weather (e.g., temperature and wind speed) and the geometry of the kiln pit (e.g., round vs. rectangular, depth) and the person(s) conducting the firing, we assert the overall average of 1.308 ± 0.485 °C/min is a more accurate characterization for this pottery tradition as a whole. When the geographic frame of archeological pottery samples is expanded from the Four Corners area to the greater American Southwest, the variability in clays and their firing performance (Hensler and Blinman 2002:377-380) suggests that independent cooling rate corrections need to be explored for the major ancient technologies.

6.2. Archeointensity Secular Variation in the Four Corners Region

The cooling rate-corrected previously published data and the fully corrected data from this investigation represent the highest-quality data available in the Four Corners area. These span from about 600 CE to the present, although coverage is discontinuous. Two temporal gaps exist from 900 CE to 1000 CE and from 1400 CE to 1600 CE, which pose a challenge in modeling the field regional, showing the need for further experimentation to populate these ranges with data. The general global decrease in field strength over the last several hundred years to its current minimum can also be observed in the Four Corners. A second minimum, nearly equivalent to today's field strength, is observed at 700 CE to 900 CE. At least one maximum is observed between 1100 CE and 1400 CE. During some temporal intervals, for example, between 700 CE to 900 CE, the data show limited scatter. In other time intervals, for example, 1100 CE to 1400 CE, there is much greater dispersion within the data set. This scatter could be caused by the following:

- The lack of an anisotropy correction (data from Bucha et al., 1970; Hsue, 1978; Lee, 1975; Strangway et al., 1968, and Parker, 1976).
- Anisotropy corrections using an out-of-favor technique (data from ; Sternberg, 1982), that yielded corrections of 1% to 45%.
- Inaccuracies in the cooling rate correction estimate of 6.73%.
- Inaccuracies in chronology (see a full description in Bowles et al., 2002).

Similarly, there is a scatter in the intensity results obtained from the three pottery fragments collected at LA 65005: Pedro Sanchez Rancho, which may be caused by a number of different phenomena.

- The chronology could be inaccurate: Even though inaccurate chronology could explain the variation seen during other time periods in the Four Corners region, it is likely not the reason for the scatter seen in the LA 65005 sherds. As described in section 2.4 the occupation of Pedro Sanchez Rancho was short and supported with historic documentation. Furthermore, even a less precise chronology based solely on the pottery typology (Tewa Polychrome, and Polished red) does not explain the variation.
- Challenges with the anisotropy correction: The IZZI experimental data do not support this hypothesis because the anisotropy corrections were small (<10%) and were successful in decreasing the scatter seen within specimens of the same pottery fragment.
- Variation in the historic cooling rate that would affect the cooling rate correction result: The magnitude of scatter seen in the preserved field intensity in these three pottery sherds is too large to be attributed to just the effect of cooling rate (Figure 6).
- Rapidly changing field: While a rapidly changing field has been shown to yield highly scattered intensities within a short time period (Shaar et al., 2016 and Ben-Yosef et al., 2017) similar to that seen in the pottery results from LA 65005, there are too few data available to make a fully justified argument.

7. Archeological Considerations That May Affect Archeointensity Success Rate in Pottery

7.1. The Clay and Temper Used to Make the Pottery

Ancient Southwestern pottery is constructed from natural clays, added tempers (angular sand sized grains that help limit shrinkage during formation), and applied slips and paints. These materials were chosen and mixed together by the ancient potters to achieve the desired plasticity, shrinkage, and finished appearance. Potters prepared different clay-temper combinations for different functions (heat resistant cooking pots versus strong serving vessels). As such, many different raw materials were often combined in varying proportions to achieve the desired function. These raw materials were usually obtained within only a few kilometers of the potter's residence (Arnold, 1985: 32–57). Unfortunately for the paleomagnetist, this means that there can be high geographic variability in the rock magnetic properties of sherds, and variability is increased during periods when potters are moving across the landscape in response to climate change (Blinman, 2008).

On the positive side, pottery was used everyday and its fragility resulted in a piece's failure and disposal after only a few months to years of use, ensuring a large supply of potential recorders of Earth's magnetic field intensity. Furthermore, the process of learning and developing production technologies was conservative, so once production technologies were worked out for a particular suite of regional resources, pottery production traditions tended to be stable.

The high availability of sherds with the potential for precise temporal resolution are positive aspects of pottery in geomagnetic studies. However, this usability is constrained by the variability in the historic resources and the work needed to identify which production traditions are best suited for paleomagnetic study. Also, the ancient farming communities responsible for the production of the pottery were susceptible to even small-scale climate change, which can upset pottery production traditions and result in time periods (such as the tenth century CE) when pottery are limited.

7.2. The Firing and Subsequent Cooling Conditions the Pot Experienced

In addition to the various types of materials used in pottery formation, the firing conditions may greatly affect the paleointensity success rate of a sample. For example, the style of firing technique presented in the thermocouple data of this paper is only one technique used by the ancient peoples of the Four Corners region. This technique reaches temperatures exceeding 800 °C and has the slowest cooling rate because the pottery is left buried overnight to cool ambiently. Other techniques reach lower temperatures and cool much faster. For example, a piece of pottery fired within a structure of cottonwood bark, wood, and/or dung on the ground surface may only reach temperatures of 600 °C and may cool in under 1 hr (Guthe, 1925: Tables X and XI).

The selection criteria presented in this paper require pottery that has been heated to above 500 °C because otherwise a linear trend in the Arai plot of the large temperature range (as required by the FRAC criterion) is nearly impossible to achieve. As such, pottery traditions fired at lower temperatures are more likely to be unsuccessful paleointensity recorders. Furthermore, the ancient peoples developed firing techniques that produced oxic, anoxic, or a combination of oxic and anoxic conditions. The differences in oxidation conditions likely affected the mineralogy of the magnetic grains preserved in the pottery and the remanence. By utilizing ceramic typology and technology as a preselection criteria, pottery types known to be fired in lower temperature conditions or unfavorable oxygen conditions can be eliminated prior to paleomagnetic experimentation.

8. Conclusions

In this study, we present new data for 289 specimens from 54 samples. Of these, eight samples passed the strictest selection criteria and were deemed reliable archeointensity values. These new data are the first intensity data published from the Four Corners region since the 1980s. The new data do not fill any temporal gaps in the archeointensity record but they do align well with the highest-quality previously published data, after the application of an estimated cooling rate correction to the legacy data. The combined data set of new and existing intensity values record a minimum 700 CE and a maximum or two between 1100 and 1400 CE. These are generally consistent with global model predictions for the region, although the number of inflection points, the amplitude, and the resolution of the models do not fully agree with each other or the data, as expected because the models are based on slightly different input data.

As outlined in previous archeointensity studies (e.g., Chauvin et al., 2000; Genevey et al., 2008, 2016; Hartmann et al., 2010), we also show that uncertainties in the estimation of the historical cooling rate can greatly affect the calculated paleointensity. It becomes imperative that detailed consideration of the historical cooling rate estimate is conducted and where possible, we recommend that independent cooling rate experimental firing be conducted on all firing techniques or at least the slowest cooling technique within a cultural region. Close collaboration with archeologists will further this aim. And lastly, it may be useful to regard ceramic typology as a viable method of preselection of pottery sherds for paleointensity.

Acknowledgments
This work was partially funded by NSF Grants EAR1345003 and EAR1547263 to L. T., the Frontiers of Innovations Scholars Program at University of California, San Diego, the Edna Bailey Sussman Research Fellowship, the Shepard Foundation Grant, and a private donation from Robert Rex. We are very grateful to the Office of Archaeological Studies, the School for Advanced Research, and the Museum of Indian Arts and Culture for providing access to the pottery sherds used in this study and for allowing destructive analysis. Special thanks to the field archeologists whose careful excavations and interpretations established the geochronology of each pottery sherd. The data presented in this paper can be accessed in the MagIC database (http://earthref.org/MagIC/doi/10.1002/2018GC007509) upon publication. The Jupyter Python notebooks used to filter and analyze the data in this study can be viewed in Texts S5 and S6 in the supporting information, and at this link (https://earthref.org/ERDA). We wish to acknowledge the reviewers (Greig Paterson and two anonymous) and the Associate Editor for their helpful comments, which improved the manuscript.

References

Arnold, D. E. (1985). *Ceramic theory and cultural process*. New York: Cambridge University Press.

Ben-Yosef, E., Millman, M., Shaar, R., Tauxe, L., & Lipschits, O. (2017). Six centuries of geomagnetic intensity variations recorded by royal Judean stamped jar handles. *PNAS*, 6. https://doi.org/10.1073/pnas.1615797114

Blinman, E. (2003). Preliminary results of pottery analysis. In D. H. Thomas (Ed.), *Excavations at Mission San Marcos New Mexico, 2001* (pp. 60–97). New York: American Museum of Natural History.

Blinman, E. (2008). 2000 years of cultural adaptation to climate change in the southwestern United States, *Royal colloquium: Past climate change: Human survival strategies, Ambio: A Journal of the Human Environment, Special Report* (Vol. 14). Royal Swedish Academy of Sciences. https://doi.org/10.1579/0044-7447-37.sp14.489

Blinman, E., & Swink, C. (1997). Technology and organization of Anazasi Trench kilns. In B. Rice (Ed.), *The prehistory and history of ceramic kilns, Ceramics and Civilization* (Vol. 7, pp. 85–102). Westerville, Ohio: The American Ceramic Society.

Bowles, J., Gee, J., Hildebrand, J., & Tauxe, L. (2002). Archaeomagnetic intensity results from California and Ecuador: Evaluation of regional data. *Earth and Planetary Science Letters*, *203*, 967–981. https://doi.org/10.1016/S0012-821X(02)00927-5

Brown, M. C., Donadini, F., Korte, M., Nilsson, A., Korhonen, K., Lodge, A., et al. (2015). GEOMAGIA50.v3: 1. General structure and modifications to the archeological and volcanic database. *Earth, Planets and Space*, *67*(1), 1–31. https://doi.org/10.1186/s40623-015-0232-0

Bucha, V., Taylor, R. E., Berger, R., & Haury, E. W. (1970). Geomagnetic intensity: Changes during the past 3000 years in the western hemisphere. *Science*, *168*(3927), 111–114.

Champion, D. E. (1980). Holocene geomagnetic secular variation in the western United States: Implications for the global geomagnetic field (PhD), California Institute of Technology.

Chauvin, A., Garcia, Y., Lanos, P., & Laubenheimer, F. (2000). Paleointensity of the geomagnetic field recovered on archaeomagnetic sites from France. *Physics of the Earth and Planetary Interiors*, *120*(1), 111–136. https://doi.org/10.1016/S0031-9201(00)00148-5

Coe, R. S. (1967). Paleo-intensities of the Earth's magnetic field determined from Tertiary and Quaternary rocks. *Journal of Geophysical Research*, *72*(12), 3247–3262. https://doi.org/10.1029/JZ072i012p03247

Constable, C. G., Korte, M., & Panovska, S. (2016). Persistent high paleosecular variation activity in Southern Hemisphere for at least 10,000 years. *Earth and Planetary Science Letters*, *453*, 78–86.

Creamer, W. (1993). *The architecture of Arroyo Hondo Pueblo, New Mexico*, Arroyo Hondo Archaeological Series (Vol. 7). Santa Fe: School of American Research Press.

Fox, J. M. W., & Aitken, M. J. (1980). Cooling-rate dependence of thermoremanent magnetization. *Nature*, *283*, 462–463.

Games, K. P., & Davey, P. J. (1985). Archaeomagnetic determinations for Britain and South-west USA from 600 AD to 1700 AD and their implications for medieval pottery studies. *Medieval ceramics*, *9*, 43–50.

Genevey, A., & Gallet, Y. (2002). Intensity of the geomagnetic field in western Europe over the past 2000 years: New data from ancient French pottery. *Journal of Geophysical Research*, *107*(B11), 2285. https://doi.org/10.1029/2001JB000701

Genevey, A., Gallet, Y., Constable, C. G., Korte, M., & Hulot, G. (2008). Archeoint: An upgraded compilation of geomagnetic field intensity data for the past ten millennia and its application to the recovery of the past dipole moment. *Geochemistry, Geophysics, Geosystems*, *9*, Q04038. https://doi.org/10.1029/2007GC001881

Genevey, A., Gallet, Y., Jesset, S., Thebault, E., Bouillon, J., & Lefevre, A. (2016). New archeointensity data from French early medieval pottery production (6th - 10th century AD). Tracing 1500 years of geomagnetic field intensity variations in Western Europe. *Physics of the Earth and Planetary Interiors*, *257*, 205–219.

Guthe, C. E. (1925). *Pueblo pottery making: A study at the village of San Ildefonso*. New Haven: Phillips Academy by Yale University Press.

Hartmann, G. A., Genevey, A., Gallet, Y., Trindade, RicardoIF, Etchevarne, C., Le Goff, Maxime, & Afonso, M. C. (2010). Archeointensity in Northeast Brazil over the past five centuries. *Earth and Planetary Science Letters*, *296*(3-4), 340–352. https://doi.org/10.1016/j.epsl.2010.05.016

Hensler, K. N., & Blinman, E. (2002). Experimental ceramic technology: Or, the road to ruin(s) is paved with crack(ed) pots. In S. H. Schlanger (Ed.), *Traditions, transitions, and technologies: Themes in southwestern archaeology. Proceedings of the 2000 southwest symposium* (pp. 366–385). Boulder: University Press of Colorado.

Hsue, T. S. (1978). Archeomagnetic intensity data for the Southwestern United States 700-1900 A.D. (Masters), University of Oklahoma.

Kohler, T. A., & Blinman, E. (1987). Solving mixture problems in archaeology: Analysis of ceramic materials for dating and demographic reconstruction. *Journal of Anthropological Archaeology*, *6*, 1–28.

Korte, M., Donadini, F., & Constable, C. G. (2009). Geomagnetic field for 0-3 ka: 2. A new series of time-varying global models. *Geochemistry, Geophysics, Geosystems*, *10*, Q06008. https://doi.org/10.1029/2008GC002297

Lang, R. W. (1993). Analysis and seriation of stratigraphic ceramic samples from Arroyo Hondo Pueblo. In J. A. Habicht-Mauche (Ed.), *The pottery from Arroyo Hondo Pueblo, New Mexico: Tribalization and trade in the northern Rio Grande*, Arroyo Hondo Archaeological Series (Vol. 8, pp. 167–181). Santa Fe: School of American Research Press.

Lee, S. S. (1975). Secular variation of the intensity of the geomagnetic field during the past 3,000 years in North, Central, and South America (PhD), University of Oklahoma.

Mitra, R., Tauxe, L., & Keech McIntosh, S. (2013). Two thousand years of archeointensity from West Africa. *Earth and Planetary Science Letters*, *364*, 123–133. https://doi.org/10.1016/j.epsl.2012.12.027

Moore, J. L. (2001). *Prehistoric and historic occupation of Los Alamos and Guaje Canyons: Data recovery at three sites near the pueblo of San Ildefonso*, Archaeology Notes 244. Santa Fe: Office of Archaeological Studies, Museum of New Mexico.

Moore, J. L. (2018). La 4968, the Vicente Valdez site. In J. L. Moore (Ed.), *Land use, settlement, and community in the southern Tewa basin, vol. 2: Historic sites and site components—The US 84/285 Santa Fe to Pojoaque corridor project [book one]* (pp. 109–264), Archaeology Notes 404. Santa Fe, NM: Office of Archaeological Studies, Museum of New Mexico.

Morales, J., Goguitchaichvili, A., Aguilar-Reyes, B., Pineda-Duran, M., Camps, P., Carvallo, C., & Calvo-Rathert, M. (2011). Are ceramics and bricks reliable absolute geomagnetic intensity carriers? *Physics of the Earth and Planetary Interiors*, *187*, 310–321.

Nilsson, A., Holme, R., Korte, M., Suttie, N., & Hill, M. (2014). Reconstructing Holocene geomagnetic field variation: New methods, models and implications. *Geophysical Journal International*, *198*, 229–248. https://doi.org/10.1093/gji/ggu120

Parker, R. A. (1976). Archeomagnetic secular variation (Masters), University of Utah.

Paterson, G. A., Tauxe, L., Biggin, A. J., Shaar, R., & Jonestrask, L. C. (2014). On improving the selection of Thellier-type paleointensity data. *Geochemistry, Geophysics, Geosystems*, *15*, 1180–1192. https://doi.org/10.1002/2013GC005135

Post, S. S., & Lakatos, S. A. (1995). Santa Fe black-on-white pottery firing features of the Northern Rio Grande Valley, New Mexico. In M. S. Duran & D. T. Kirk (Eds.), *Of pots and rocks: Papers in honor of A. Helene Warren, Papers of the Archaeological Society of New Mexico* (Vol. 21, pp. 141–154). Albuquerque.

Ramenofsky, A. F., Neiman, F., & Pierce, C. D. (2009). Measuring time, population, and residential mobility from the surface at San Marcos Pueblo, North Central New Mexico. *American Antiquity*, *74*, 505–530.

Selkin, P. A., Gee, J., & Tauxe, L. (2007). Nonlinear thermoremanence acquisition and implications for paleointensity data. *Earth and Planetary Science Letters*, *256*, 81–89.

Shaar, R., & Tauxe, L. (2013). Thellier GUI: An integrated tool for analyzing paleointensity data from Thellier-type experiments. *Geochemistry, Geophysics, Geosystems*, *14*, 677–692. https://doi.org/10.1002/ggge.20062

Shaar, R., Tauxe, L., Ron, H., Ebert, Y., Zuckerman, S., Finkelstein, I., & Agnon, A. (2016). Large geomagnetic field anomalies revealed in Bronze to Iron Age archeomagnetic data from Tel Megiddo and Tel Hazor , Israel. *Earth and Planetary Science Letters*, *442*, 173–185. https://doi.org/10.1016/j.epsl.2016.02.038

Sternberg, R. (1982). Archaeomagnetic secular variation of direction and paleointensity in the American Southwest (PhD), Tucson.

Sternberg, R. S. (1989). Archaeomagnetic paleointensity in the American Southwest during the past 2000 years. *Physics of the Earth and Planetary Interiors*, *56*(1-2), 1–17. https://doi.org/10.1016/0031-9201(89)90032-0

Sternberg, R. S., & Butler, R. F. (1978). An archaeomagnetic paleointensity study of some Hohokam potsherds from Snaketown, Arizona. *Geophysical Research Letters*, *5*(2), 101–104.

Strangway, D. W., Mcmahon, B. E., & Larson, E. E. (1968). Magnetic paleointensity studies on a recent basalt from Flagstaff , Arizona. *Journal of Geophysical Research*, *73*(22), 7031–7037.

Swink, C. (2004). *Messages from the high desert: The art, archaeology and renaissance of Mesa Verde pottery*. Bayfield, CO: Redtail Press.

Tauxe, L., Shaar, R., Jonestrask, L., Minnett, R., Koppers, AAP, Constable, CG, et al. (2016). PmagPy: Software package for paleomagnetic data analysis and a bridge to the Magnetics Information Consortium (MagIC) database. *Geochemistry, Geophysics, Geosystems*, *17*, 2450–2463. https://doi.org/10.1002/2016GC006307

Thellier, E., & Thellier, O. (1959). Sur l'intensité du champ magnétique terrestre dans le passé historique et géologique. *Annals of Geophysics*, *15*, 285–378.

Thomas, D. H. (2003). *Excavations at mission San Narcos, New Mexico, 2001*. New York: American Museum of Natural History.

Veitch, R. J., Hedley, I. G., & Wagner, J. J. (1984). An investigation of the intensity of the geomagnetic field during Roman times using magnetically anisotropic bricks and tiles. *Archives des Sciences (Geneva)*, *37*(3), 359–373.

Wilson, D. C. (2013). The gradual development of ssystems of pottery production and distribution across northern Rio Grande landscapes. In B. J. Vierra (Ed.), *From mountaintop to valley bottom: Understanding past land use in the northern Rio Grande Valley, New Mexico* (pp. 161–197). Salt Lake City: University of Utah Press.

Yu, Y., Tauxe, L., & Genevey, A. (2004). Toward an optimal geomagnetic field intensity determination technique. *Geochemistry, Geophysics, Geosystems*, *5*, Q02H07. https://doi.org/10.1029/2003GC000630

Supporting Information for

“Archaeointensity of the Four Corners Region of the American Southwest”

S.A. Jones-Cervantes,[1] L. Tauxe,[1] E. Blinman,[2] A. Genevey, [3]

[1]Scripps Institution of Oceanography, University of California, San Diego, La Jolla, CA 92093

[2]New Mexico Department of Cultural Affairs, Office of Archaeological Studies, Santa Fe, NM, 87507

[3]Sorbonne Universités, UPMC Univ Paris 06, CNRS, UMR 8220, Laboratoire d’archéologie moléculaire et structurale (LAMS), 75005 Paris, France

Additional Supporting Information (Files uploaded separately)

1. S1 - Pottery Forming Techniques
2. S2 - Firing Technology Model
3. S3 - Cooling Rates
4. S4 - Nonlinear TRM
5. S5 - Paleointensity Jupyter Notebook as pdf, usable ipynb file available at https://earthref.org/ERDA
6. S6- Thermocouple Jupyter Notebook as pdf, usable ipynb file available at https://earthref.org/ERDA
7. S7- Photos of the pottery sherds used for this study

Supplemental 1 - Southwestern Pottery Forming Techniques

Within the Southwestern United States, two pottery forming techniques were used to make the majority of vessels, both based on building up coils of clay to form the body of the vessel. The minority technique, used in southern Arizona, finished vessels by thinning and shaping with a paddle-and-anvil technique. The majority technique, used in the Four Corners region and elsewhere, was to scrape and press with a tool to weld the coil junctures, shape the vessel from the inside, and slightly stretch and thin the vessel wall. In many cases (primarily decorated wares), vessel surfaces were then rubbed and pressed with a stone as the vessel dried, smoothing, compacting, and eventually polishing the surface. All of these manipulations have the potential to affect the anisotropy of the magnetic minerals.

PLATE 13

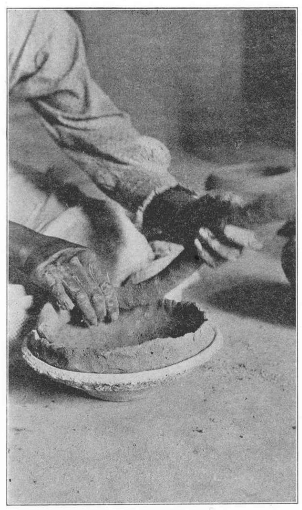

a

Applying the first roll of clay to the base. The roll is held in the left hand, and is flattened and pinched into place in the inside of the rim by the fingers of the right hand.

b

A bowl-base to which four rolls of clay have been added; the potter is making a new roll. Note the junctions of the roll on the interior of the vessel.

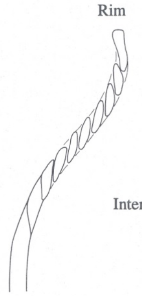

It is likely (although uninvestigated) that the coarseness and heterogeneity of pottery pastes, coupled with the small coil size of the ancient traditions, lessens the susceptibility of the pottery sherds to anisotropy complications.

The schematic diagram on the left portrays "interior coil application" technique, while the sherd on the right demonstrates the effects of interior coil application on the orientation of the fabric within the vessel wall. The sherd on the right was also polished on both interior and exterior surfaces, but the impact of polishing on the reorientation of clay minerals is confined to actual surface of the sherd.

REFERENCES CITED:

Guthe, Carl E. 1925 *Pueblo Pottery Making: A Study at the Village of San Ildefonso*. Published for the Phillips Academy by Yale University Press, New Haven.

Supplemental 2 - Mesa Verde Region Pottery Firing Model

This model is based on studies of pottery and archaeological kilns from the Four Corners region of the Southwestern United States. Validation of the model derives through experimental firings and comparisons of replicated vessels and kiln stratigraphy with archaeological examples (Blinman and Swink 1997; Swink 2004). The model is appropriate for relatively refractory shale-derived clays that require reduction conditions to bring the sintering threshold of the clay within the range of open-fire combustion. Ancient kilns are placed on the landscape to take advantage of wind-aided fuel combustion, potentially reaching temperatures of 850-950° C. The firing atmosphere begins as reducing and finishes as slightly oxidizing in order to achieve white or gray background surfaces for mineral or organic paints.

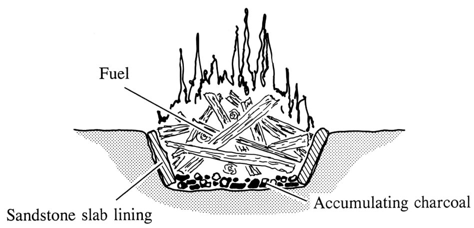

Stage 1: A shallow pit or trench, circa 1 meter across and 40 cm in depth, is excavated into the ground in an area with exposure to breezes. The pit can be lined (for ease of reuse) or unlined. A fire with wood fuel is ignited within the pit. The fuel pieces must be substantial enough in size and number to form a charcoal bed across the base of the pit, 2-5 cm thick.

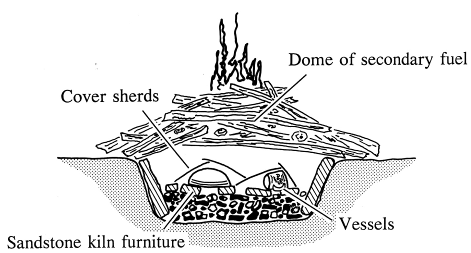

Stage 2: Sandstone slab pieces are placed on the charcoal bed, spaced to allow air flow between the pieces. Unfired vessels are placed on the slabs in a single layer, spaced to allow air flow both under and between the vessels. Cover sherds may be used to protect the upper surfaces of the vessels from direct radiant heat during the initial firing. A self-supporting dome of wood fuel is built spanning the pit. Fuel size and quantity is designed to produce a thick layer of charcoal and is ignited slowly to avoid radiant heat shock. Tremendous heat is radiated outward, but the vessels heat slowly until the dome of fuel collapses. The collapsed fuel forms a coarse charcoal layer over the vessels. Small charcoal would limit air flow and slow combustion (heating rate), so coarse charcoal is necessary. The charcoal is light weight, posing no breakage risk to the vessels.

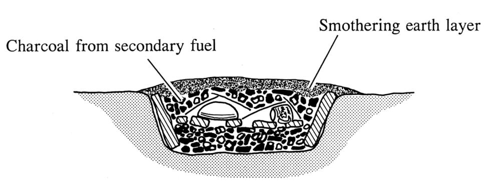

Stage 3: Maximum temperatures are reached as air flows through the coarse charcoal bed that now surrounds the vessels. Without a breeze, temperatures peak around 750° C, adequate to fire the pots but not sufficient for strong vessels or to mature iron mineral paint. With a >20 km per hour breeze, temperatures can exceed 900° C, producing strong vessels and black iron-painted designs. As charcoal size decreases and the charcoal bed thins, the temperature drops. As the temperature decreases, soil is then spread over the pit to cut off the air supply for combustion, holding vessel surfaces under "neutral" oxidation conditions. Vessels cool slowly and can be removed safely in about 18 hours.

REFERENCES CITED:

Blinman, E., and C. Swink, 1997. Technology and Organization of Anasazi Trench Kilns. In *The Prehistory and History of Ceramic Kilns*, P. Rice, ed., pp. 85-102. Ceramics and Civilization Vol. 7. The American Ceramic Society, Westerville, Ohio.

Swink, C. 2004. *Messages from the High Desert: The Art, Archaeology and Renaissance of Mesa Verde Pottery*. Redtail Press, Bayfield, Colorado.

Supplemental 3 – Cooling rate temperature profiles from thermocouples

Cooling rate temperature profiles for 22 thermocouple records, derived during two experimental firings. The methodology used during the firing is historically replicable and is described in Supplementary 1. The cooling trend between 500 and 200°C is modeled with a linear regression, consistent with the protocol of *Shaar et al. [2016]*. For each thermocouple temperature profile, the slope of linear regression is included in Table 2.

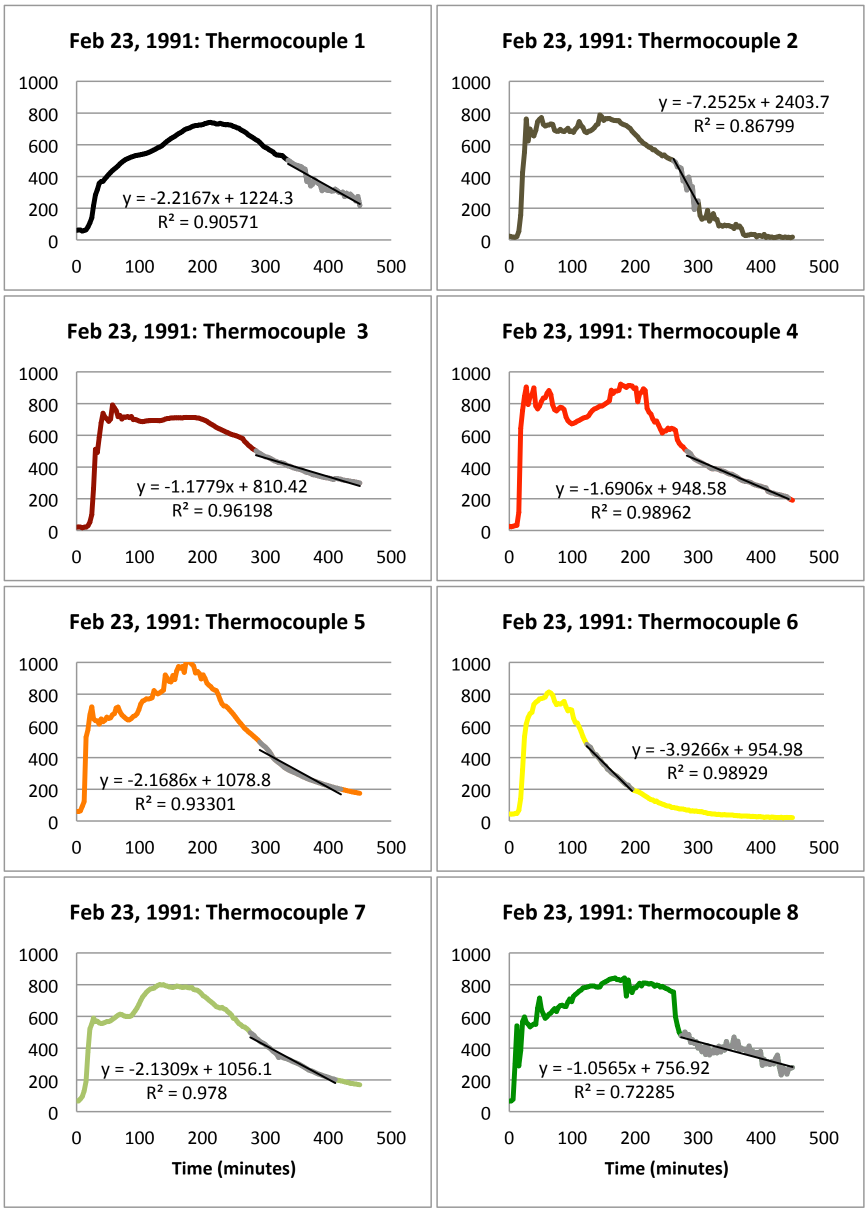
Feb 23, 1991: Thermocouple 1
y = -2.2167x + 1224.3
R² = 0.90571
Feb 23, 1991: Thermocouple 2
y = -7.2525x + 2403.7
R² = 0.86799
Feb 23, 1991: Thermocouple 3
y = -1.1779x + 810.42
R² = 0.96198
Feb 23, 1991: Thermocouple 4
y = -1.6906x + 948.58
R² = 0.98962
Feb 23, 1991: Thermocouple 5
y = -2.1686x + 1078.8
R² = 0.93301
Feb 23, 1991: Thermocouple 6
y = -3.9266x + 954.98
R² = 0.98929
Feb 23, 1991: Thermocouple 7
y = -2.1309x + 1056.1
R² = 0.978
Feb 23, 1991: Thermocouple 8
y = -1.0565x + 756.92
R² = 0.72285
0 200 400 600 800 1000
0 100 200 300 400 500
Time (minutes)

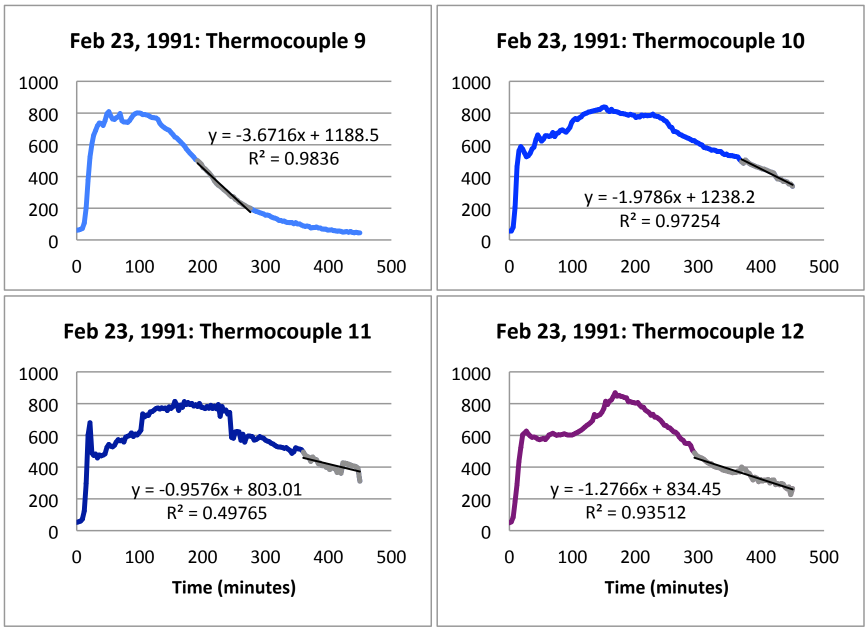
Feb 23, 1991: Thermocouple 9
y = -3.6716x + 1188.5
R² = 0.9836
Feb 23, 1991: Thermocouple 10
y = -1.9786x + 1238.2
R² = 0.97254
Feb 23, 1991: Thermocouple 11
y = -0.9576x + 803.01
R² = 0.49765
Time (minutes)
Feb 23, 1991: Thermocouple 12
y = -1.2766x + 834.45
R² = 0.93512
Time (minutes)

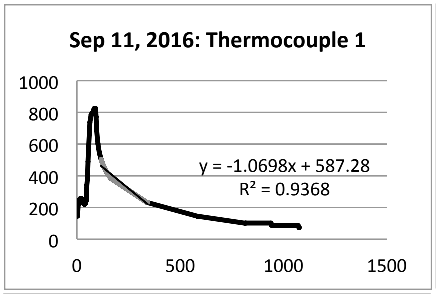
Sep 11, 2016: Thermocouple 1
1000
800
600
400
200
0
0
500
1000
1500
y = -1.0698x + 587.28
R² = 0.9368

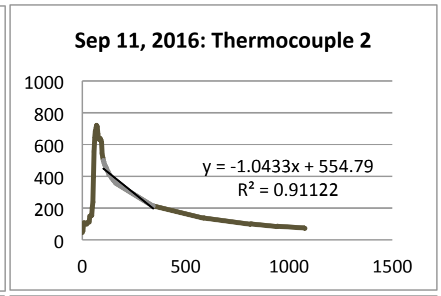
Sep 11, 2016: Thermocouple 2
1000
800
600
400
200
0
0
500
1000
1500
y = -1.0433x + 554.79
R² = 0.91122

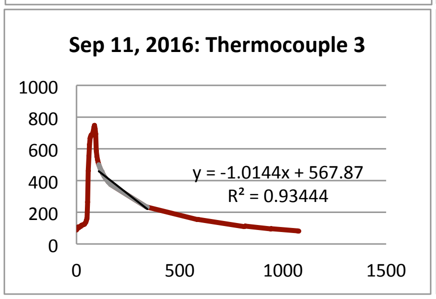
Sep 11, 2016: Thermocouple 3
1000
800
600
400
200
0
0
500
1000
1500
y = -1.0144x + 567.87
R² = 0.93444

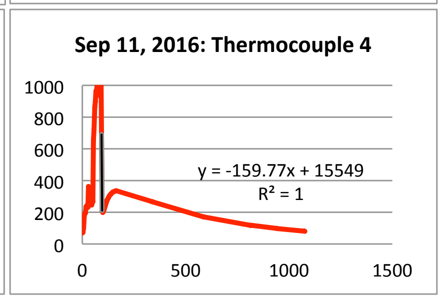
Sep 11, 2016: Thermocouple 4
1000
800
600
400
200
0
0
500
1000
1500
y = -159.77x + 15549
R² = 1

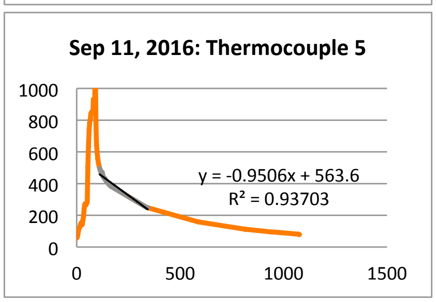
Sep 11, 2016: Thermocouple 5
1000
800
600
400
200
0
0
500
1000
1500
y = -0.9506x + 563.6
R² = 0.93703

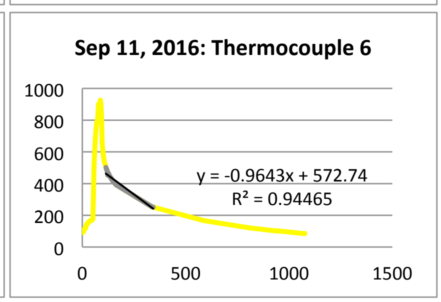
Sep 11, 2016: Thermocouple 6
1000
800
600
400
200
0
0
500
1000
1500
y = -0.9643x + 572.74
R² = 0.94465

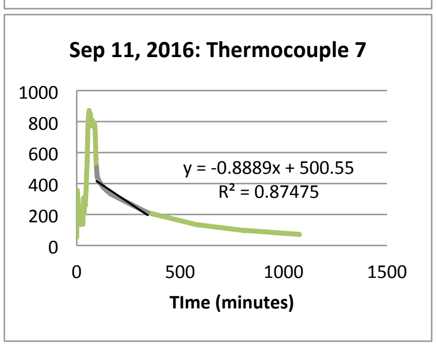
Sep 11, 2016: Thermocouple 7
1000
800
600
400
200
0
0
500
1000
1500
y = -0.8889x + 500.55
R² = 0.87475
TIme (minutes)

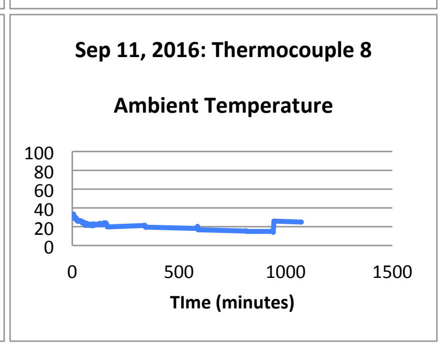
Sep 11, 2016: Thermocouple 8
Ambient Temperature
100
80
60
40
20
0
0
500
1000
1500
TIme (minutes)

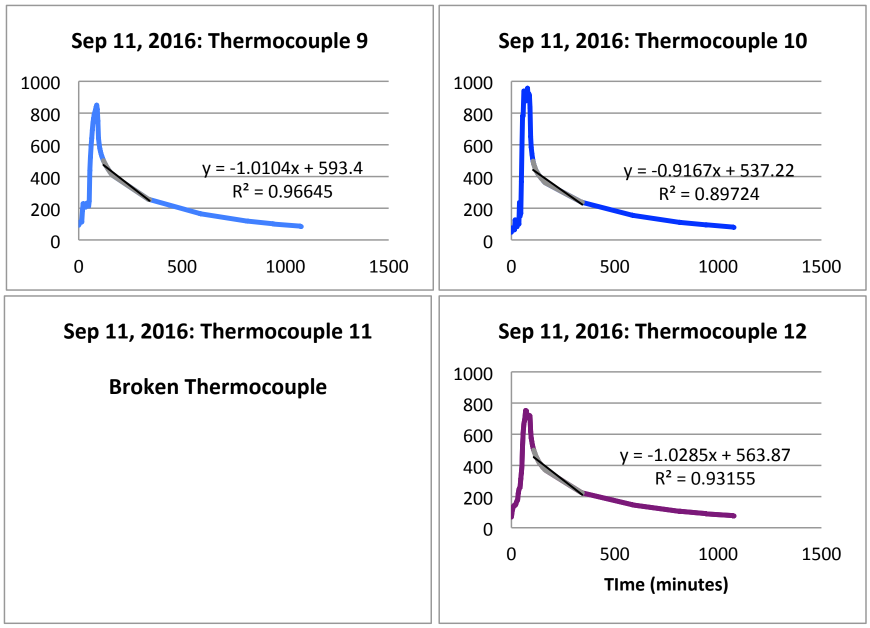
Sep 11, 2016: Thermocouple 9
y = -1.0104x + 593.4
R² = 0.96645
Sep 11, 2016: Thermocouple 10
y = -0.9167x + 537.22
R² = 0.89724
Sep 11, 2016: Thermocouple 11
Broken Thermocouple
Sep 11, 2016: Thermocouple 12
y = -1.0285x + 563.87
R² = 0.93155
0
200
400
600
800
1000
0
500
1000
1500
TIme (minutes)

Supplemental 4 – Nonlinear TRM

In order to verify that the acquisition of TRM was linearly related to the applied field, a nonlinear TRM experiment was conducted. The applied field used in the IZZI experiments was 40 µT and 70 µT for the nonlinear TRM experiment. In a case where a TRM is acquired linearly, then the ratio between the magnetization acquired at the highest temperature step of 70 µT / 40 µT should be close to 1.875. This is what is observed, showing that the samples indeed acquire magnetization linearly. The ratios of the magnetizations are on average 1.875 ± 5.96% and at maximum 1.875 + 13.74%.

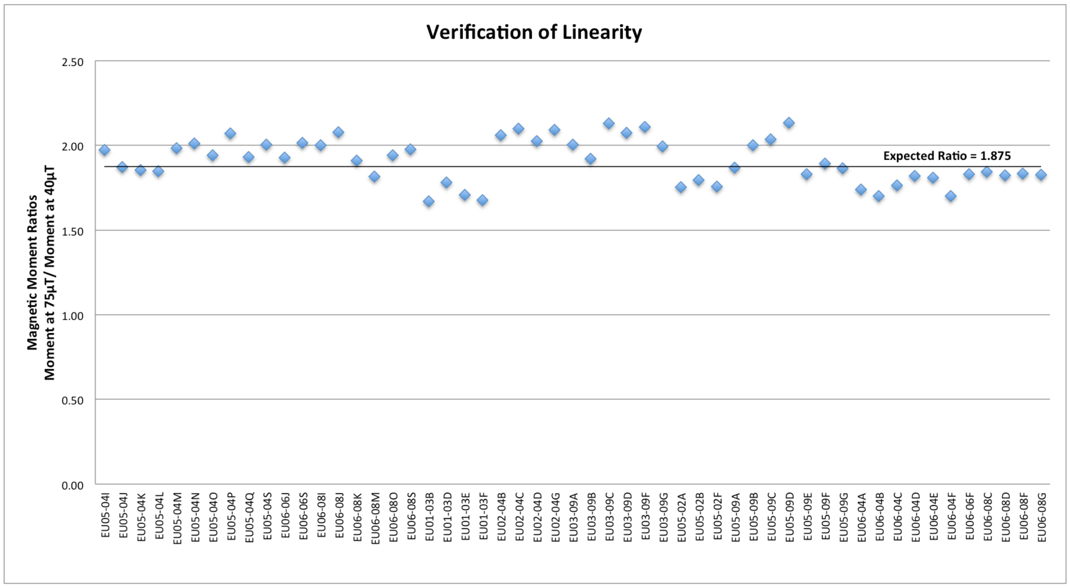

Supplemental 7 – Photos of the pottery sherds used for study
Process of producing specimens

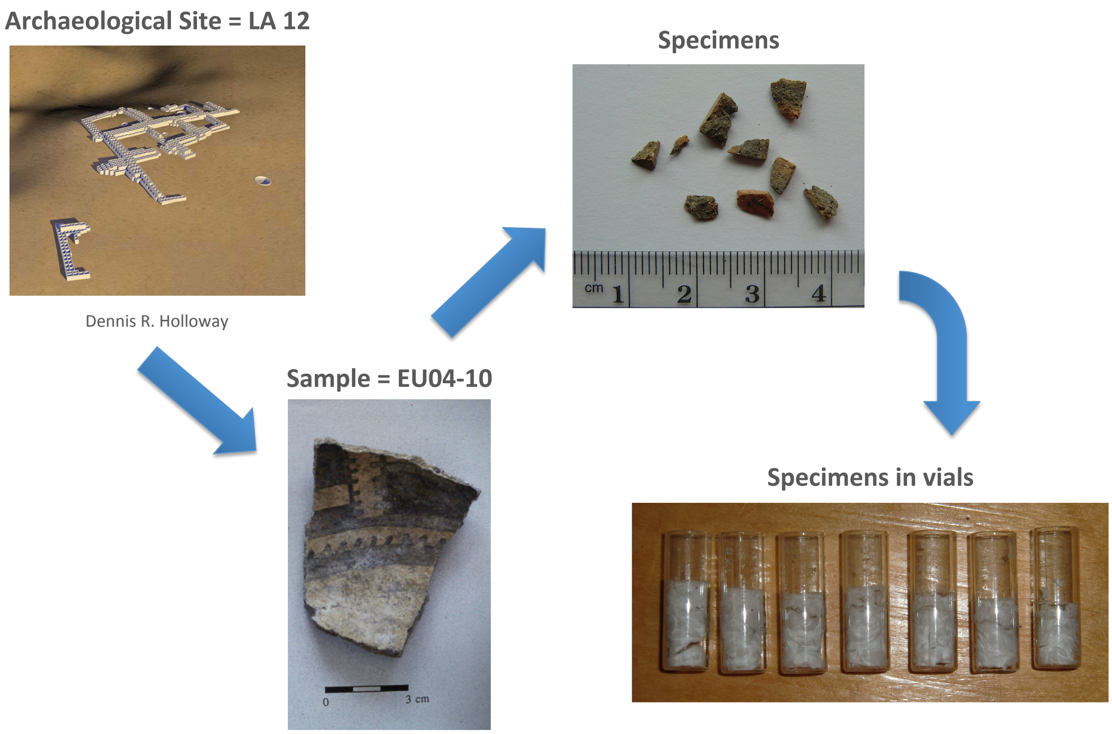

Supplemental 7 – Photos of the pottery sherds used for study
LA4968 – Spanish Colonial Site, Vincente Valdez residence (pre-sampling)

EU01-01

EU01-02

EU01-03

EU01-04

Supplemental 7 – Photos of the pottery sherds used for study
LA4968 – Spanish Colonial Site, Vincente Valdez residence (pre-sampling)

EU01-05

EU01-06

EU01-07

Supplemental 7 – Photos of the pottery sherds used for study
LA98 – Mission San Marcos (pre-sampling)

EU02-01

EU02-02

EU02-03

EU02-04

Supplemental 7 – Photos of the pottery sherds used for study
LA98 – Mission San Marcos (pre-sampling)

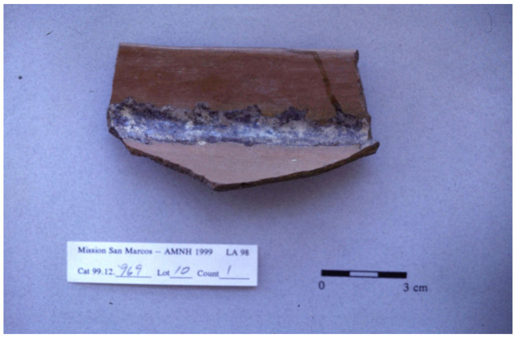

EU02-06

EU02-07

Supplemental 7 – Photos of the pottery sherds used for study
LA12 – Lower Arroyo Hondo (pre-sampling)

EU03-02

EU03-04 EU03-03 EU03-01

EU03-05

EU03-06

EU03-07

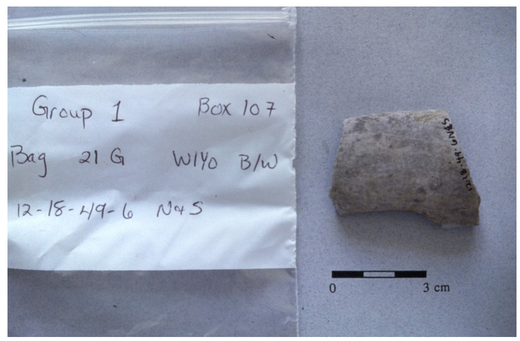

EU03-08

Supplemental 7 – Photos of the pottery sherds used for study
LA12 – Lower Arroyo Hondo (pre-sampling)

EU03-09

EU03-10

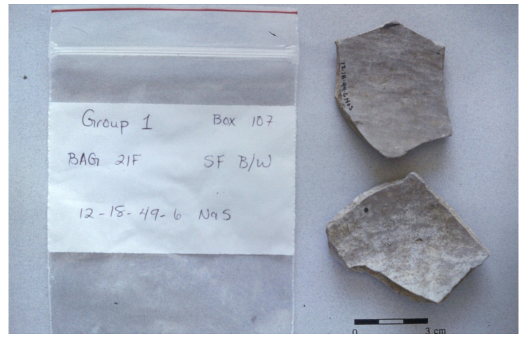

EU03-11

EU03-12

Supplemental 7 – Photos of the pottery sherds used for study
LA12 – Lower Arroyo Hondo (pre-sampling)

EU04-01

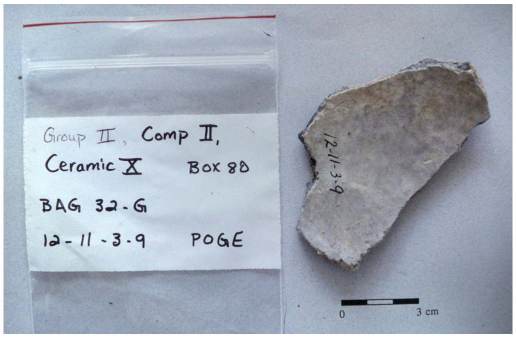

EU04-02

EU04-03

EU04-06

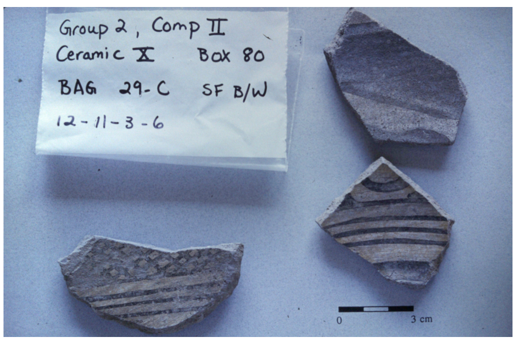

EU04-04 EU04-05

EU04-07

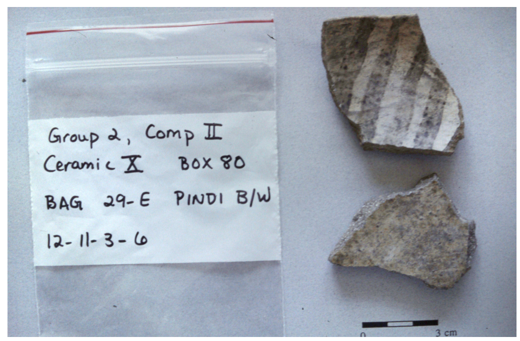

EU04-08

Supplemental 7 – Photos of the pottery sherds used for study
LA12 – Lower Arroyo Hondo (pre-sampling)

EU04-09

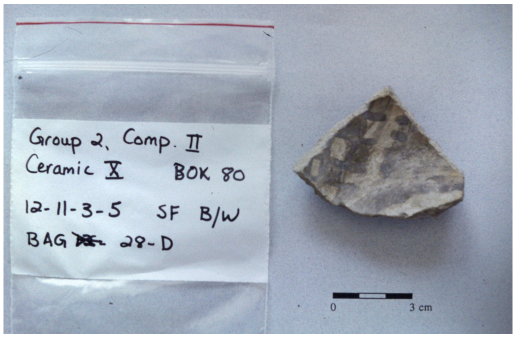

EU04-10

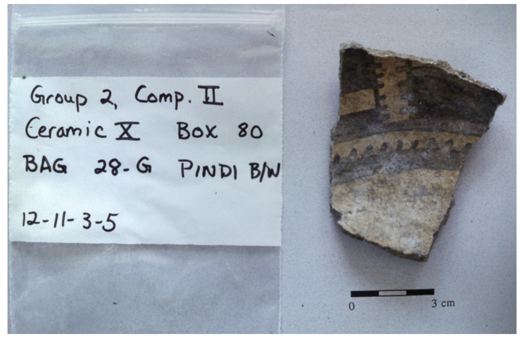

Supplemental 7 – Photos of the pottery sherds used for study
LA12 – Lower Arroyo Hondo (pre-sampling)

EU05-02

EU05-01

EU05-03

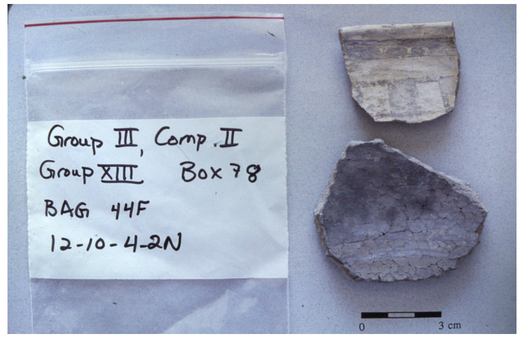

EU05-04

EU05-05

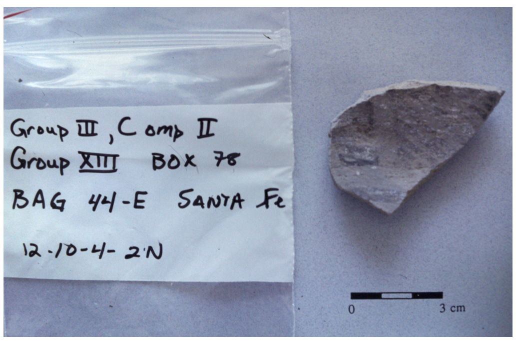

EU05-06

Supplemental 7 – Photos of the pottery sherds used for study
LA12 – Lower Arroyo Hondo (pre-sampling)

EU05-07

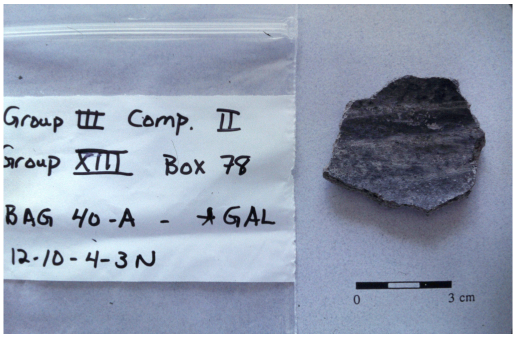

EU05-08

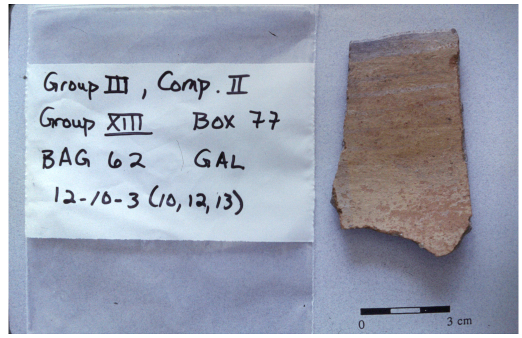

EU05-09

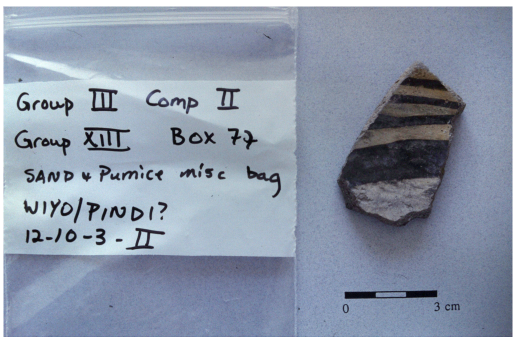

Supplemental 7 – Photos of the pottery sherds used for study
LA65005 – Pedro Sanchez Rancho (post-sampling)

EU06-01

EU06-02

EU06-03

EU06-04

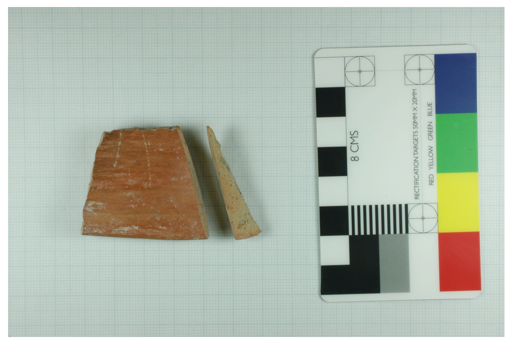

Supplemental 7 – Photos of the pottery sherds used for study
LA65005 – Pedro Sanchez Rancho (post-sampling)

EU06-05

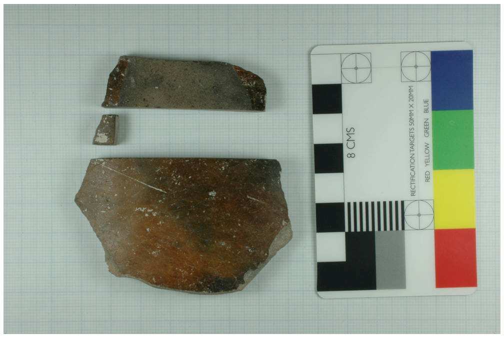

EU06-06

EU06-07

EU06-08

Supplemental 7 – Photos of the pottery sherds used for study
LA65005 – Pedro Sanchez Rancho (post-sampling)

EU06-09

Acknowledgements

Chapter 2, in full, is a reprint of material as it appears in *Geochemistry, Geophysics, Geosystems*. Jones, Shelby A.; Tauxe, Lisa; Blinman, Eric; Genevey, Agnes, 2020. The dissertation author was the primary investigator and author of this paper.

Chapter 3: MagIC as a FAIR Repository for America's Directional Archaeomagnetic Legacy Data

JGR Solid Earth

RESEARCH ARTICLE
10.1029/2021JB022874

MagIC as a FAIR Repository for America's Directional Archaeomagnetic Legacy Data

Shelby A. Jones[1,2], Eric Blinman[2], Lisa Tauxe[1], J. Royce Cox[2], Stacey Lengyel[3], Robert Sternberg[4], Jeffrey Eighmy[5], Daniel Wolfman, and Robert DuBois

[1]Scripps Institution of Oceanography, University of California, San Diego, La Jolla, CA, USA, [2]New Mexico Department of Cultural Affairs, Office of Archaeological Studies, Santa Fe, NM, USA, [3]East Tennessee State University, Johnson City, TN, USA, [4]Franklin and Marshall College, Lancaster, PA, USA, [5]Unaffiliated

†Posthumously.

Key Points:

- We digitized 6 decades of legacy archaeodirectional measurements from three archives (>51k specimens), adding them to a FAIR repository, MagIC
- The site-level results (reanalyzed using modern statistical conventions) are consistent between the archives
- The majority of the data have site provenance in North America and are dated to less than 2,000 years old

Supporting Information:

Supporting Information may be found in the online version of this article.

Correspondence to:

S. A. Jones,
saj012@ucsd.edu

Citation:

Jones, S. A., Blinman, E., Tauxe, L., Cox, J. R., Lengyel, S., Sternberg, R., et al. (2021). MagIC as a FAIR repository for America's directional archaeomagnetic legacy data. *Journal of Geophysical Research: Solid Earth*, *126*, e2021JB022874. https://doi.org/10.1029/2021JB022874

Received 5 AUG 2021
Accepted 23 SEP 2021

Author Contributions:

Conceptualization: Shelby A. Jones, Eric Blinman, Lisa Tauxe
Data curation: Shelby A. Jones, Eric Blinman, Lisa Tauxe
Formal analysis: Shelby A. Jones, Lisa Tauxe
Funding acquisition: Lisa Tauxe
Investigation: Shelby A. Jones, Eric Blinman, Lisa Tauxe, J. Royce Cox, Stacey Lengyel, Robert Sternberg, Jeffrey Eighmy, Daniel Wolfman, Robert DuBois
Methodology: Shelby A. Jones, Lisa Tauxe
Project Administration: Lisa Tauxe
Resources: Shelby A. Jones, Eric Blinman, J. Royce Cox, Stacey Lengyel,

Abstract Beginning in 1964, an academic lineage of Robert DuBois and his students, Daniel Wolfman and Jeffrey Eighmy, developed dedicated United States-based archaeomagnetic research programs. Collectively, they analyzed over 5,377 archaeomagnetic sites, primarily from North America, dated to less than 2,000 years old. Yet despite their decades of effort, few journal publications resulted. Most of their published results are embedded in archeological reports, often without technical data, which limits the data's accessibility. Furthermore, when published, the results are generally averaged at the site level using statistical conventions different from today's standards, limiting the data's comparability and (re)usability. In 2015, we undertook a salvage archival study to digitize the surviving data and metadata from the scientists' individual estates and emeritus collections. We digitized measurement data from more than 51,000 specimens, reinterpreted them using modern conventions, and uploaded them to the FAIR-adhering magnetic data repository, earthref.org/MagIC. The reinterpreted site-level results from the three laboratories are mutually consistent, permitting the individual data sets to be combined and analyzed as single regional entities. Through incorporation into the MagIC repository, these legacy data are now accessible for incorporation into archaeomagnetic and global magnetic field modeling efforts, critical to understanding Earth's magnetic field variation through time. In the Four Corners region of the United States Southwest, this digitized archive advances the development of a new regional paleosecular variation curve used in archaeomagnetic dating. This project highlights both the value and complexities of managing legacy data; the many lessons learned to set a precedent for future paleomagnetic data recovery efforts.

Plain Language Summary Archaeomagnetism is the study of Earth's past magnetic field through researching the magnetic signatures retained in well-dated archeological materials. The most commonly studied materials are those that have experienced high temperatures due to human-made fires. Due to humans' global occupation, there is a potential for globally distributed archaeomagnetic sampling, which is essential for high-resolution global magnetic field models. However, there is considerable variation in the documentation and accessibility of data from certain regions, including North America. In 2015, a salvage archival project was initiated to recover the life's work of three North American archaeomagnetists. The effort resulted in the digitization and formatting of the data within DuBois' and Wolfman's estates, and Eighmy's archive. In total, measurement data from more than 51,000 specimens, from 5,377 archeological features, were processed and uploaded to a centralized online data repository, MagIC. This repository ensures that the data, representing 130 person-years of work, are now findable and accessible, permitting the data to be re-used in future modeling projects. One such application for these data is the development of a new regional model for the Four Corners region of the United States Southwest that traces the location of the magnetic north pole through time.

1. Introduction

Archaeomagnetism applies many of the techniques of paleomagnetism to samples of anthropogenic origin. The materials most often studied are those heated by past peoples (hearths, burned floors, pottery, etc.) because the heating and subsequent cooling of the material generally preserve a stable and measurable magnetization. These heated anthropogenic materials hold tremendous potential for contributing to the understanding of variations in Earth's magnetic field over the last several thousand years because

Jeffrey Eighmy, Daniel Wolfman, Robert DuBois
Software: Shelby A. Jones, Lisa Tauxe
Supervision: Eric Blinman, Lisa Tauxe
Validation: Shelby A. Jones, Eric Blinman, Lisa Tauxe
Visualization: Shelby A. Jones, Lisa Tauxe
Writing – original draft: Shelby A. Jones, Eric Blinman
Writing – review & editing: Shelby A. Jones, Eric Blinman, Lisa Tauxe, Robert Sternberg, Jeffrey Eighmy

anthropogenic materials often have more precise chronologies than natural rocks or sediments and are spatially and temporally diverse. This is especially true as past humans had a nearly global distribution (excluding oceans) and their dependence on fire for warmth and cooking has resulted in an abundance of sites for investigation. Additionally, past cultures moved about the landscape at a relatively slow rate, which means most regions have the potential to preserve a nearly continuous record of absolute field variations.

Unfortunately, there is considerable variation in the abundance, documentation, and accessibility of archaeomagnetic records across the world. Published archaeomagnetic records are primarily clustered in the Northern Hemisphere, specifically Europe. While other areas are being or have been studied, their current contributions to the global databases are more limited (Figure 1). This lack of uniform coverage limits the resolution of global and regional field models.

One such under-published area in the global databases is the United States Southwest. Fortunately, this is not for lack of archaeomagnetic study (Figure 2). Over nearly six decades, starting in the early 1960s, an academic lineage of scientists and archaeologists dedicated their careers to the development of a highly robust directional archaeomagnetic record covering the greater Four Corners region of the United States Southwest (defined here as the four states of New Mexico, Arizona, Utah, and Colorado) and elsewhere. But these records were developed for archeological dating purposes and an archeological audience, and in comparison to other global regions, these laboratories' data have seen limited peer-reviewed publication. Only about 10% of the site-level data are available in open source paleomagnetic archives, such as GeoMAGIA (Brown et al., 2015) and MagIC (Tauxe et al., 2016). The remaining 90% of the data are generally either unpublished or sparsely published in hard-to-access archeological reports. Moreover, when the data were published, the averaged site-level results were typically reported and not the specimen or measurement data, limiting their potential for reproducibility and reinterpretation.

Fortunately, the original directional measurement data for over 5,000 archeomagnetic sites (defined here as a single heated feature in an archeological site, such as a single hearth) are still available in personal collections. In this study, we digitized and reanalyzed the directional measurement data from the previously under-published sites within the Robert DuBois, Daniel Wolfman, and Jeffrey Eighmy-Stacey Lengyel collections. In the process, we submitted the measurement data, along with our new interpretations, and, where possible, independent chronology estimates to the MagIC database. This is the first step toward the long-term goal of making these invaluable data FAIR principles compliant, that is, they are Findable, Accessible, Interoperable, and Reusable (Wilkinson et al., 2016).

Bringing these legacy data sets into FAIR compliance is useful for geomagnetism and also for archeology. One of the original motivations for collecting the data was to develop regional virtual geomagnetic pole (VGP) reference curves of paleosecular variation, in support of directional archaeomagnetic dating. These three investigators operated under the well-documented assumption that Earth's magnetic field varies through time and the result of this variation is a traceable magnetic north pole path through time (defined as a VGP curve) that can be used as a relative, and in some cases as an absolute, dating technique. With this goal in mind, over decades these investigators collected independently dated archaeodirectional samples, measured specimens, then used those data to develop VGP curves using their own subsets of the complete data set and a variety of curve construction techniques (e.g., DuBois, 1989; Hagstrum & Blinman, 2010; Kawai et al., 1965; LaBelle & Eighmy, 1995; Lengyel & Eighmy, 2002). This resulted in the development of different VGP curves for the Four Corners region of the United States Southwest with significant discrepancies between them (Figure 3). This has led to incongruent archaeomagnetically derived age ranges (Blinman & Cox, 2018).

Recognizing these discrepancies, two of the longest-term goals of this data recovery project are:

1. Develop a new VGP reference curve for the Four Corners region using modern statistical techniques and data from all contributors, and
2. To support a web-based platform that is accessible to archaeologists desiring to update previously published archaeomagnetically derived chronologies.

But these goals require data to be FAIR principle compliant, making this data rescue project critical to the success of these aims.

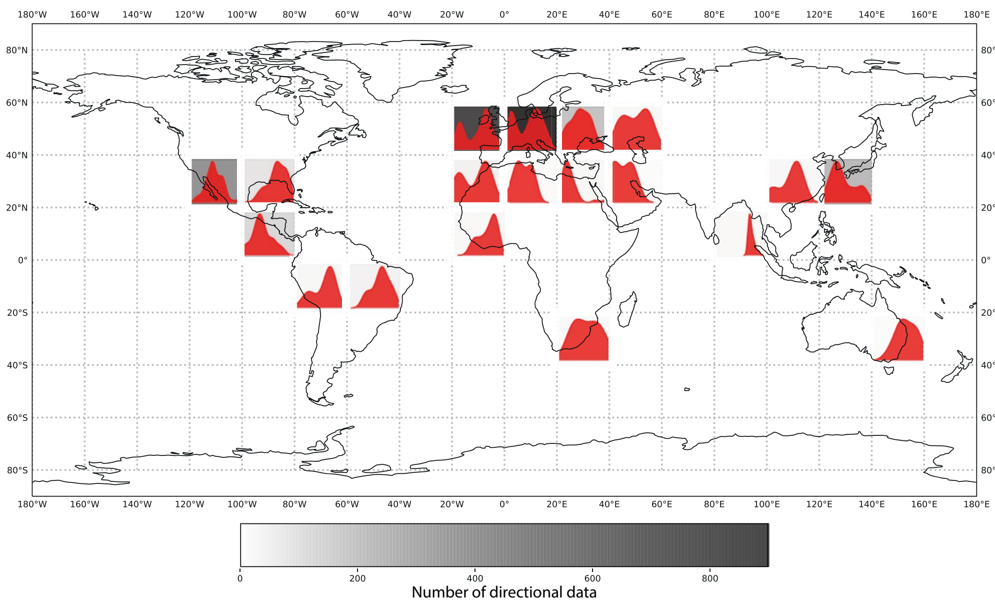

Figure 1. Spatial and temporal distribution of archaeomagnetic directional data from the last 2,000 years, by provenance. The shading of each latitude-longitude defined grid depicts the number of archaeomagnetic directional results available in the gridded region (volcanic data excluded). The overlaid red histograms represent the temporal distribution of the results, with 2,000 years before present on the left and the year 2000 CE on the right. GeoMAGIA data were downloaded on January 19, 2021 (Brown et al., 2015).

2. A Brief History of Archeomagnetism in the United States

As early as the 1950s, scientists from Europe and Japan began developing archaeomagnetic theory, methods, and applications (e.g., Aitken, 1961; Burlatskaya & Petrova, 1961; Cook & Belshé, 1958; Thellier & Thellier, 1951; Watanabe, 1959) but they were not embraced by North American scientists until the early 1960s. In 1964, geophysicist Robert DuBois began his life-long pursuit of sampling and measuring archaeomagnetic materials. Within a few years, he had amassed a large enough data set of archaeomagnetic data with associated dates, that he began publishing the first VGP models of paleosecular variation for the Four Corners region (e.g., DuBois, 1989; DuBois, 2008; DuBois & Watanabe, 1965; Watanabe & DuBois, 1965; Weaver, 1967). He used the resulting VGP maps to date archeological sites in the region. Most noteworthy was DuBois' partnership with Emil Haury, who used DuBois' archaeomagnetically derived dates to confirm his hypothesis about the early irrigation development at the Snaketown site (a pre-Spanish, Hohokam culture site 30 miles or 48 km southeast of Phoenix, Arizona) (Eighmy, 2000:107; Haury, 1976:331–333). This partnership led to the development of the foundational cultural chronology that is still used in the southern Arizona region (Deaver, 1998:464–490; Schiffer, 1982:327–329). For further details refer to the Supporting Information S1.

Through the decades, Sternberg, students of DuBois, and others used pottery from the Four Corners region to investigate the archaeointensity record through time. These data were evaluated in Jones et al. (2020).

3. Brief Description of Terminology Used in This Paper

The purpose of this data recovery project is to make this large mass of archeologically derived data available for use by the paleomagnetism community through incorporation into the MagIC database. As such, this study's data files are formatted to be consistent with the nomenclature used in the MagIC database (adopted

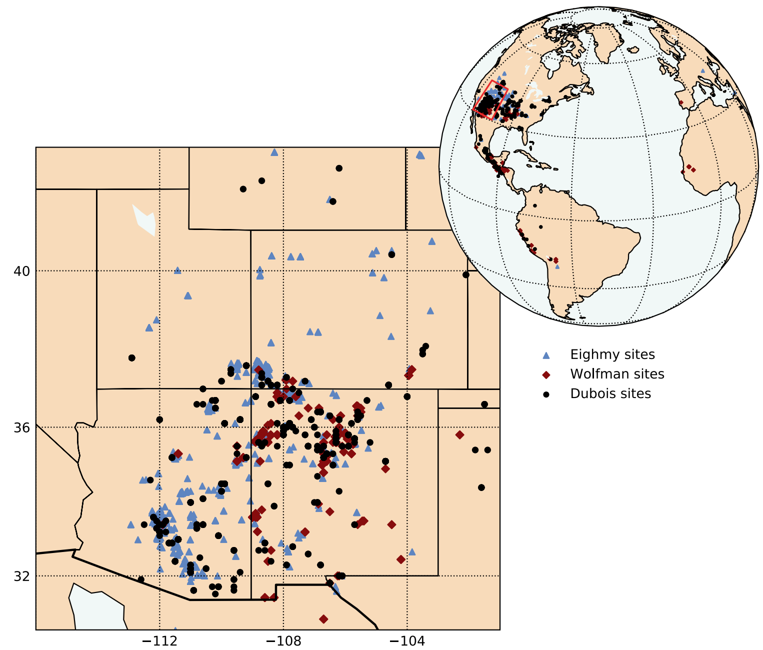

Figure 2. Location map of sites sampled for archaeomagnetic direction, by contributor. The red quadrangle on the globe represents the bounds of the inset. The inset map depicts the sampling locations within the four United States states (from the bottom right corner clockwise) New Mexico, Arizona, Utah, and Colorado. This region has the highest sampling density in our data set and comprises the Four Corners region of the United States Southwest. From the intersection of the four states, in the center of the map, to their farthest corner is about 750 km.

from the paleomagnetism community), which differs significantly from the definitions traditionally used by archaeologists (Table 1).

The MagIC database understands a site as a feature with uniform magnetic properties and a single age (Tauxe et al., 2016). An example of a paleomagnetic site would be a single lava flow or sedimentary layer. This nomenclature most closely aligns with the archeologist's definition of a feature (e.g., hearths), which records a single heating event. The use of the MagIC definition of site eliminates the potential age ambiguity associated with the archeological definition of a site, due to generational reuse and reoccupation.

Applying the MagIC definition of site to an archeological context (e.g., a hearth), promotes an archeological "site" to MagIC's definition of a location. In this study, the archeological site names (MagIC locations) are frequently recorded with alternative names, because United States' archeological sites are designated by an official alpha-numeric identifier and a common name. For example, the archeological site in New Mexico known as Lower Arroyo Hondo or Arroyo Hondo is also known as LA12. During this data recovery effort, standardized alphanumeric location identifiers were preferred but not always accessible, and were not independently added by these authors. If multiple identifiers were recognized in the metadata of the legacy records, then all are recorded in the MagIC compatible files.

The MagIC definition of a sample is material collected from a MagIC site. As an analogy with a lava flow, a paleomagnetic sample would be the multi-centimeter-long drilled cylinder. Back in the laboratory, the core (sample) can be subdivided into MagIC specimens, all with the same orientation and can be individually measured. Archeological features (MagIC sites) can be heated surfaces rather than heated masses, and

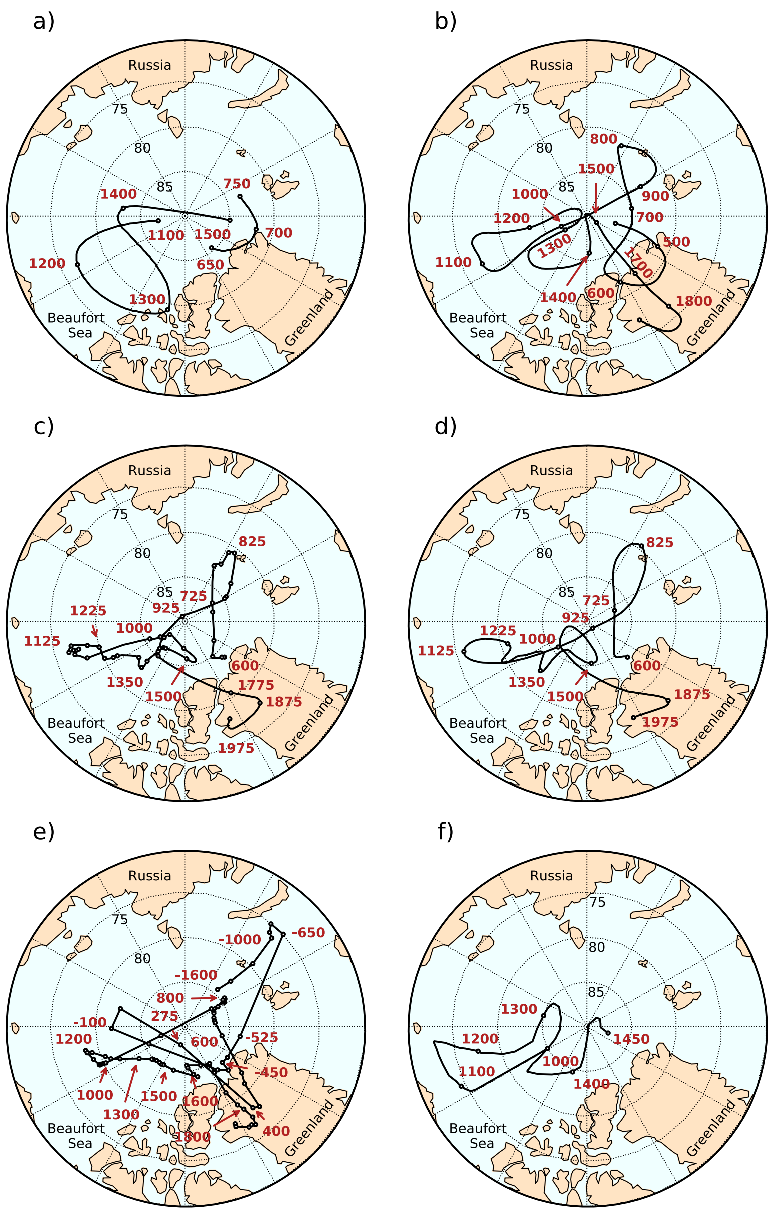
a)
Russia
75
80
85
750
1400
1100
1500
700
1200
650
1300
Beaufort Sea
Greenland
b)
Russia
75
80
800
1500
85
1000
900
1200
700
1300
500
1100
1700
600
1400
1800
Beaufort Sea
Greenland
c)
Russia
75
80
825
85
725
925
1225
1000
1125
600
1350
1775
1500
1875
1975
Beaufort Sea
Greenland
d)
Russia
75
80
825
85
725
925
1225
1000
1125
600
1350
1500
1875
1975
Beaufort Sea
Greenland
e)
Russia
75
-650
-1000
80
-1600
800
275
-100
1200
600
-525
-450
1000
1500
1300
1600
400
1800
Beaufort Sea
Greenland
f)
Russia
75
80
85
1300
1200
1450
1000
1100
1400
Beaufort Sea
Greenland

Figure 3.

Table 1
MagIC Terminology Use in This Paper

Column name	MagIC definition	Geologic example	Archaeodirectional application (this archive)
Location	Geographical location with several different aged sites	Stratigraphic section	Archeological site
Site	Feature whose magnetic properties and age are expected to be uniform	A single lava flow	Archeological feature (e.g., hearth)
Sample	Piece of material collected from a single site	Multi-centimeter drilled cylinder of lava	Plaster cube encasing burned material
Specimen	Piece that was measured	Standard 1-inch paleomagnetic core	Subdivisions of the material[a]
Region (optional)	Larger geographic area encompassing multiple locations	Maui Island, Hawaii	Mesa Verde National Park

[a]In this study, no original plaster cubes (samples) were subdivided into specimens; as such, the MagIC sample and specimen names are equivalent. For simplicity, in this study, the MagIC sample table reports the interpreted vector direction in geographic coordinates, transformed using the field azimuth and dip. The MagIC specimen table reports the interpreted vector direction in the same coordinate system as the measurements.

the sampling custom used in archaeomagnetism in the United States is to collect material from multiple points on the heated surface of the feature. The samples discussed in this study were collected as material encased within individually oriented plaster cubes. In a spatial sense, each archaeomagnetic cube is synonymous with the MagIC definition of a sample. Any subdivisions of these sample cubes would be defined as multiple MagIC specimens. However, subdividing samples into specimens was not the common practice of United States-based archaeomagnetists. Therefore, each collected sample is equivalent to the measured specimen. As such, the legacy data recovered in this project and compiled into MagIC compatible data files use a cube's identification number for both the MagIC sample name and the MagIC specimen name.

All archeological sites (MagIC locations) are recorded in the MagIC compatible table with a country identifier and, where possible, state/province information. Some of this information was clearly defined within the recovered data set's metadata, but not always. Where the political boundary information was not defined in the legacy records, it was identified (often by latitude and longitude) and added by the authors of this study. These political boundary identifiers are useful for the sorting and analysis of these data by geographic region. The authors of this study advocate for the inclusion of this information in future archaeomagnetic contributions to MagIC.

All the geographical metadata included in this data set are with respect to the archaeologists' concept of a sample's provenience (the point of recovery in the archeological record) (Blinman, 1988:97). In this project, the site provenance (the geographic point of origin) (Blinman, 1988:97) and the provenience of a sample are equivalent, since the thermal remanent magnetization (TRM) vector under investigation was imparted in the same location and orientation that it was recovered (a requirement of directional paleomagnetic studies). This equivalence may not hold true for pottery-based archaeointensity studies, since pottery can be transported great distances between the location of magnetic acquisition (provanance) and the point of archeological recovery (provenience).

Figure 3. Past virtual geomagnetic pole (VGP) reference curves from the Four Corners region: Over the decades, several VGP reference curves have been developed for the Four Corners region of the United States Southwest (not all presented here). (a) Kawai et al. (1965), the first published VGP curve for the region, was never used for archaeomagnetic dating. (b) DuBois (1989), the first VGP reference curve used for archaeomagnetic dating in the region is hand-drawn. (c) SWCV 595 (LaBelle & Eighmy, 1995) and (d) SWCV2000 (Lengyel & Eighmy, 2002) are computer-calculated moving-windows average derived reference curves. Both have been used by the Eighmy laboratory for archaeomagnetic dating, SWCV2000 replaced SWCV 595 and continues to be applied to dating applications. (e) The VGP curve based on the declination-inclination curves published in Hagstrum and Blinman (2010), computer-calculated using a moving-windows averaging technique, never used for archaeomagnetic dating. (f) The unpublished, hand-drawn curve, employed by Wolfman for archaeomagnetic dating. All ages are CE.

4. Context and Chronology

The locational and chronological metadata for the DuBois data set were derived from DuBois (2008), a catalog compiled by DuBois but published after his death. The data were included "as is" and were not verified for accuracy. In the decades since its publication, a few inaccuracies have been noted. For the sake of consistency, any edits were not included unless the inaccuracy was an egregious error in the latitude and longitude reported. These few locational errors were generally longitudinal hemisphere errors, since the convention used in DuBois (2008) was −180° to 180°. Occasionally, a similar hemispherical error was discovered in the latitudinal data and corrected. In a few cases, typos in the longitudinal value resulted in sites from the continental United States plotting in the wrong location (i.e., in the ocean or in an incorrect state), these were also corrected. All corrections were easily made because in most cases multiple sets of specimen cubes were collected from the same archeological sites (i.e., multiple features from one archeological site), so the correct latitude and longitude were borrowed from those data.

Chronological metadata of the DuBois data set presented here are derived from DuBois (2008). For the most part, the ages reported are age estimations provided by the field archeologist and recorded by DuBois at the time of sample collection. These dates were rarely updated when the official archeological reports were published, or as additional information was acquired during subsequent excavation. The exception to this norm is the chronology data compiled by archeologist Tom Windes for the specimens collected from the Chaco Canyon National Historical Park (U.S. National Park Service). Windes compiled detailed chronologies and reviewed the metadata for each heated feature that DuBois sampled for archaeomagnetism. These detailed and cited information are included in the description column of the MagIC formatted file.

Due to DuBois' convention of asking for an age estimate at the time of collection and recording that age on his field records, nearly all the data from the DuBois estate are associated with an age estimate. In general, these age estimates are usually quite accurate because the chronology of the United States Southwest is well understood. The quantity and quality of archeology conducted over the last century in this region, paired with the precision and reliability of independent dating techniques (dendrochronology, radiocarbon, pottery seriation, and calibrated architectural change) allow for accurate in-field age estimations within a few dozen years. This is a unique attribute of the United States' Southwest archeology. Although a detailed reassessment of the chronology is planned as part of the long-term aims of this project, that reassessment is likely to improve the precision of the original estimates, rather than significantly change the age attributions.

In contrast to DuBois' nearly complete age record, Wolfman and Eighmy have a significantly lower percentage of archaeomagnetic samples with associated ages. But in general, their reported chronologies are based on post-fieldwork analyses, are more precise than DuBois', and are usually associated with citable archeological reports.

The Wolfman metadata were compiled from paper documents into a Microsoft Access database (by a volunteer in the early 2010s) with referencing to project names, archeological site names, archaeologists, and cited reports. Each archeological feature sampled for archaeomagnetism had varying levels of completeness in their metadata, ranging from very detailed to almost no information.

The chronological data for the Eighmy data set was accessed from the Colorado State University Archaeometric Lab Technical Series (CSU Technical Series) (Eighmy et al., 1987; Eighmy & McGuire, 1989; Eighmy & Klein, 1988, 1990; LaBelle & Eighmy, 1995; Premo & Eighmy, 1997). These volumes include the age for each sampled archeological feature that Eighmy, Lengyel, Sternberg, and associates used in their regional paleosecular VGP models (e.g., Eighmy, 1991; LaBelle & Eighmy, 1997; Lengyel & Eighmy, 2002; Lengyel, 2010), but do not always cite the archeological report that qualifies those chronologies.

5. Formatting Challenges, Creating Master File, Merging the Data Sets

Following the digitization, the three data sets were independently reformatted into MagIC compatible files to ensure that the idiosyncrasies of each data set could be addressed completely. Since the DuBois data set was completely hand-digitized, the formatting idiosyncrasies were limited but still numerous. The DuBois data sets had several unique data formats, 9 of the 12 formats worked within this project. In many cases, there was ambiguity in the units of the measured moments as well as the order of magnitude of the

Table 2
Acceptance Criteria: All the Data Digitized as a Result of This Project Were Reinterpreted Using Modern Statistical Conventions and Subject to a Set of Acceptance Criteria Threshold to Determine the Highest Quality Sample Vectors and Site Averages

Criteria group	Statistic	Threshold
Specimen/sample criteria	[illegible]	≥3
	DANG	≤5°
	MAD	≤5°
Site criteria	[illegible]	≥3
	κ	≥100
	α_{95}	≤5°

Note. Criteria described in Paterson et al. (2014).

measured magnetic moment. As such, all the DuBois moments have been classified as "uncalibrated moments," which is consistent with the MagIC column conventions. Future, detailed and time-consuming work may be able to reconcile the unit ambiguity for a few of the nine formats, but it is unlikely that a complete reconciliation will be possible.

The Wolfman database was stored in two formats. About half the accessible data were stored in a 1990s era digital format with two files for each archaeomagnetic site: a file with the basic locational metadata and a second file with the measured magnetizations. The other half of the data were stored in printouts; these were hand-digitized. Similar to the DuBois data set, there was ambiguity in the units of the measured moments and order of magnitude. These ambiguous moments are also classified as "uncalibrated moments." Future work will be required to address this challenge. Additionally, there were significant difficulties with referencing the magnetic data to the chronological and locational metadata. These metadata were stored within a Microsoft Access database in a format that was not easily exportable into a single column delimited file (like a Microsoft Excel file). The result was multiple exported files that were inconsistently referenceable, limiting the ability to easily merge the metadata together and then merge it with the magnetic data.

The Eighmy database had far more idiosyncrasies than the DuBois and Wolfman data sets. The data were preserved in a Microsoft Word document, and magnetic data and basic locational information included typographical errors and were inconsistently delimited. Transferring the data from the Word document to a delimited format that could be converted into a MagIC compatible file required the development of a short python script to search line-by-line for specific string patterns and characters. This python script worked remarkably well but not completely. Accuracy verification was done visually and was corrected by hand. The most common challenges were related to demagnetization steps. Character number constraints in the original program that stored the specimen name and demagnetization steps truncated demagnetization steps of 50, 100, 150, 175 Oe, to 50, 10, 15, and 17, respectively. It also led to demagnetization steps 100 and 1,000 Oe both being recorded as 10. These corrections were easily edited by hand because the data were organized by increasing demagnetization level and the sequence of demagnetization steps was regular. All demagnetization steps have been converted to tesla, for compatibility with the MagIC database. Another common challenge was typos in the specimen or site name that made referencing for principal component analysis and Fisher mean site-level averaging difficult. These typos were also corrected by hand. Where appropriate, all edits were noted in the description column of MagIC compatible file. For consistency with Dubois and Wolfman data sets, the reported magnetic moments are labeled as "uncalibrated moments." It is likely that the units for these moments can be verified with moderate ease in the future.

The biggest challenge with the Eighmy data set was merging the chronology data from the CSU Technical Series publications with the magnetic data. The chronological data presented in the CSU Technical Series publications are associated with an archaeomagnetic sample's DVPG number rather than the laboratory specimen number. In most cases, an association between the two numbers could be established, but not always. Where the association was possible, the DVGP number is recorded in the "alternative sample name" column of the MagIC compatible file.

6. Data Processing

After the three data sets were compiled into their respective MagIC compatible files, the data sets were filtered for quality (Table 2) and visualized independently using the plotting scripts within the PmagPy software package (Tauxe et al., 2016). After plotting the sample data that passed the acceptance criteria (Figure 4), it was noted that each data set had idiosyncrasies resulting in sample vector directions that were improbable, as every site sampled is less than a few thousand years old (i.e., during the current normal polarity field state). For example, the Dubois and Wolfman data sets (Figures 4a and 4c) showed clusters of data, not only in the direction of the expected field (green dots) but also to the east (blue), south (magenta), and west

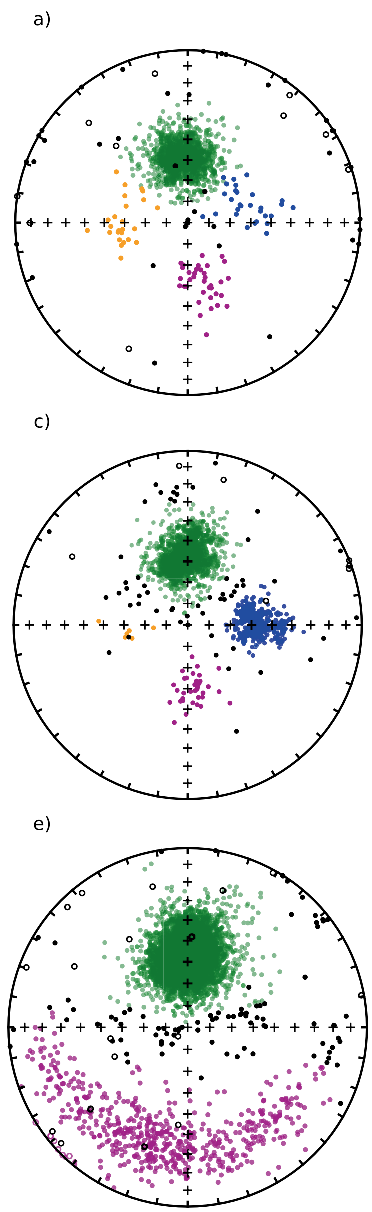

Figure 4.

(yellow). As no excursions have been reported for the last few thousand years, the unexpected directions are likely the result of field or laboratory errors in the orientations of the sample cubes.

To adjust for the evident idiosyncrasies within the data sets, the data from each collector's data sets were analyzed independently and by region. The regions were very broadly defined as data from the United States, from Mexico and Central America, and from South America. These divisions were required to limit the latitudinal dependence of inclination within the data sets that would add ambiguity to the cluster analyses used in classifying the data that required adjustment. Any data from regions not defined above, were not evaluated for adjustment, due to the low number of records. Mathematical clustering using functions within the OPTICS function in the sklearn.cluster python module (Pedregosa et al., 2011) were used to identify the data that required systematic adjustment. These functions helped eliminate the subjectivity of human bias, while allowing for the expected variability in magnetic direction due to the paleosecular variation over the last several thousand years. A discussion of parameters used is included in Supporting Information S1 and a sample python Jupyter Notebook is provided (see Acknowledgments for the link).

The DuBois and Wolfman data sets required very similar adjustments of 90°, 180°, or 270° in the measured field azimuth. The prevalence of this inaccuracy is likely the result of the collection protocol used by both these contributors. Their convention was to collect heated anthropogenic material encased in plaster cubes, level the top surface of the cube (i.e., a dip of 0°), and then measure the azimuth with respect to a reference corner marked on the top of the cube. The clustering analysis indicates that there are a non-negligible number of sample cubes with azimuth directions measured along an incorrect side of the cube, resulting in the prevalence of magnetic vector directions that are 90°, 180°, of 270° off the expected northerly direction for this recent time period (Figures 4a and 4c).

The cluster analysis was used to classify each of the sample directions into five clusters (expected northerly direction, 90° east of north, 180° from north, 90° west of north, and unable to cluster). For the Dubois and Wolfman USA data, this clustering was completed in two steps, due to the overwhelming prevalence of northerly directions. The first clustering code isolated out the northerly directions, while the second code clustered the remaining non-north data into their respective clusters. Then the data were merged back together and the required 90°, 180°, or 270° azimuth adjustment was applied (Figures 4b and 4d).

The Eighmy data set required a different adjustment, the data set does not exhibit the same prevalence of 90°, 180°, and 270° clusters. It is unclear if this distinct lack of 90° inaccuracies is a result of corrections applied before the data set's submission to this project or if the field collection procedure used by the Eighmy laboratory lessened this type of error. Eighmy also collected archaeomagnetic material using the plaster cube convention, but instead of measuring the field azimuth with respect to a reference corner like DuBois and Wolfman, his convention was to measure the azimuth with respect to an arrow inscribed parallel to the side of the cube chosen for measurements.

The pre-adjustment Eighmy sample data exhibit a southern hemisphere spread of positive directions, with shallower inclinations than predicted by the geocentric axial dipole (GAD) equation (Figure 4e). This practice is not consistent with an inaccuracy in the field azimuth reading, as was seen in the Wolfman and DuBois data sets. But the shallowed inclination is consistent with an inaccuracy in the dip reading (recording 0° instead of 90°, or vice versa) in addition to a non-90° inaccuracy in the field azimuth.

Visual interpretation of the specimen data (i.e., the vector data in specimen coordinates—not transformed into geographic coordinates) yielded a cluster of data with the expected inclination and northerly declination. Through comparing the specimen data and the geographically transformed sample data, it was noted that the cube identification numbers were the same between the southern hemisphere spread with shallow positive inclination in the sample data and the northerly cluster in the specimen data. This suggests that

Figure 4. Stereonets of accepted samples, by contributor, pre-adjustment and post-adjustment: Inconsistencies in data collection and management through time resulted in idiosyncrasies within each of the three archives (shown here the US-based data). (a) DuBois directions original. (b) Dubois after adjustment. (c) Wolfman original. (d) Wolfman after adjustment. (e) Eighmy original. (f) Eighmy after adjustment. The clusters of data-oriented East, South, and West in the DuBois and Wolfman data sets (a, c) are attributed to reading the field azimuth along the incorrect side of the sample cube. Applying an adjustment of either 90°, 180°, or 270° to the originally noted field azimuth yields adjusted directions for Dubois and Wolfman (b, d). The swath of south and down directions in the Eighmy data set (e) is attributed to that subset of data already transformed into geographic coordinates, when provided to these authors. Ensuring those data are not doubly transformed into geographic coordinates, results the adjusted Eighmy data set (f).

Table 3
Number of Samples, Sites, and Locations—By Contributor

Category	Contributor	Number
Samples	DuBois	15,312 (1,903 accepted)
Total = 51,166 (16,079 accepted)	Wolfman	29,662 (10,673 accepted)
	Eighmy	6,192 (3,503 accepted)
Sites (e.g., archeological features)	DuBois	1,991 (67 accepted)
Total = 5,377 (1,183 accepted)	Wolfman	778 (331 accepted)
	Eighmy	2,608 (785 accepted)
Locations (e.g., archeological sites)	DuBois	497
Total = 1,185	Wolfman	157
	Eighmy	531

the measurement data received for these cubes were provided in geographic coordinates rather than the expected specimen coordinates. To correct for this inconsistency, mathematical clustering was used to identify and isolate the cubes that required adjustment (those in the southern spread). In the MagIC compatible specimen table, those cubes were identified to be in geographic coordinates, and the vector direction was copied into the MagIC compatible sample table (Figure 4f).

7. Site-Level Results

After the required sample-level adjustments, Fisher means (Fisher, 1953) were calculated for each site using the pmag.fisher_mean function within the PmagPy package. Only samples that satisfied the acceptance criteria were included in the site-level average (Table 2). These site-level averages were filtered for quality using the acceptance criteria in Table 2 then by regional location.

The application of the selection criteria filtered the data significantly (Table 3), especially the number of acceptable sites from the DuBois' data set. The percentage of DuBois' sites that passed this study's selection criteria is extremely low (3.3%). This low percentage is attributed to the laboratory methodologies used by DuBois through the decades, which were customary at the time. DuBois' convention was to measure a "pilot group" of specimen cubes from a site through a multi-step demagnetization protocol, this pilot group usually consisted of only one to three cubes. The remaining cubes collected from the site were usually only measured at NRM and the "optimum" demagnetization step, identified from the pilot group study, typically 150 Oe (15 mT). A side effect of this laboratory convention is that the vast majority of DuBois' specimen cubes have only two demagnetization steps, which results in a significant number of them failing the specimen acceptance criteria. Additionally, due to the low number of cubes measured as part of the pilot group, many sites failed to meet the site-level criteria which require at least three samples. Later in life, DuBois changed his laboratory conventions slightly to increase the number of cubes within his pilot group, this change results in a higher percentage of DuBois' later studies passing our acceptance criteria. Fortunately, nearly all of DuBois' original specimen cubes still exist in storage at OAS, so additional steps could be measured and the percentage of sites that pass this study's acceptance criteria may increase.

8. Results From the Four Corners Region

One of the motivations for initiating this project, in addition to archiving these valuable data sets into FAIR compliant database, was to use the composite data set to develop a model that reconciles the differences between the commonly used models of the Four Corners region of the United States Southwest. Historically, the different scientists used primarily their own laboratory's data in the production of their VGP curves, separate from the data of the other contributors. Because the data, up to now, were not pub-

10.1029/2021JB022874

Table 4
Summary of the Number of Archaeomagnetic Sites Within the Data Sets by Contributor and Region

Region	Contributor	Sites	Sites with ages	Accepted sites with ages
Four Corners	DuBois	1,050	71	22
	Wolfman	486	229	114
	Eighmy	2,384	122	87
Lower Mississippi River	DuBois	287	17	3
	Wolfman	33	5	4
	Eighmy	63	0	0
Mesoamerica	DuBois	251	18	10
	Wolfman	117	29	14
	Eighmy	8	0	0
Northern Mexico	DuBois	3	1	0
	Wolfman	14	7	7
	Eighmy	7	0	0
South America	DuBois	56	9	4
	Wolfman	37	5	2
	Eighmy	0	0	0

licly available, it has not been possible to develop a regional model of paleosecular variation, using the composite data sets of DuBois, Wolfman, and Eighmy.

The aim of producing a composite regional model requires the chronology information to be reported with the magnetic vector information collected by the contributors. Filtering for sites that have reported chronology eliminates a significant number of sites from all three contributor's data sets. The quality of the ages reported was not used as a filter, and the chronology reported was not updated (as described in Section 4).

In the Four Corners region, a combined 3,920 archeological features were sampled for archaeomagnetism. Of these, 422 have reported ages and 223 passed the selection criteria (Table 4). Plotted against age, these data show a clear trend in declination and inclination over the last 1,500 years (Figures 5a and 5b). The data are plotted by contributor, with the accepted archaeomagnetic sites noted as solid symbols and all the data with ages noted as open symbols. Superimposed on these data is a degree-10 polynomial fit calculated using functions within the python Seaborn module. The uncertainty bounds are defined through a Monte Carlo style resampling with 1,000 iterations.

The declination and inclination data modeled by the polynomial fit and its respective uncertainty bounds are based on the sub-portion of the data set that satisfies the filter of α_{95} ≤4°, paired with 11 predictions from the GUFM paleosecular variation model equally spaced between 1700 and 1950 CE (Jackson et al., 2000). The latter are denoted as black plus-signs. The addition of the GUFM predictions constrains the polynomial fit model in the historic time period, during which there is a low density of archaeomagnetic records. We chose 1700 CE as the minimum extent of the GUFM predictions used in these models because in the land-locked Four Corners region of the United States few historical records before 1700 CE were included in the development of GUFM, limiting the precision of the predictions for the region during the 17th century.

In addition to modeling the data with a polynomial fit based on the subset of data that satisfy α_{95} ≤4°, three other fits were explored (all the data with age constraints, the data that passed this study's acceptance criteria, and α_{95} ≤3°). Analysis of the four polynomial fit models resulted in the decision to select the curve derived from the subset of data that meet the α_{95} ≤4° A discussion is included in Supporting Information S1.

Using the python function get_children, one hundred declination and inclination pairs of data were retrieved from the polynomial fit derived from the subset of data with α_{95} ≤4°. These data pairs were evenly distributed between the ages 550 and 1950 CE. A central latitude and longitude defined as 36°N, 108°W was used in the conversion of the modeled fit to VGP coordinates (Figure 6). Before plotting, the modeled curve was truncated to between 600 and 1840 CE to limit the any potential inaccuracies at the margins of the polynomial fit model caused by a lack of data.

The model shown in Figure 6 is the first VGP curve developed from a composite data set with significant contributions from DuBois, Wolfman, and Eighmy. To first order, this new polynomial-derived curve corroborates the pattern of VGP motion depicted in the regional curves presented by the three individual data sets (Figures 3b–3d and 3f). The characteristic clockwise loop at roughly 800 CE, followed by a rapid movement toward Alaska and the Pacific Ocean between 900 and 1100 CE, is seen in all curves, including ours. Additionally, the clockwise loop at roughly 1200 CE is consistent with the previously presented curves, as is the trend toward Greenland post-1600 CE.

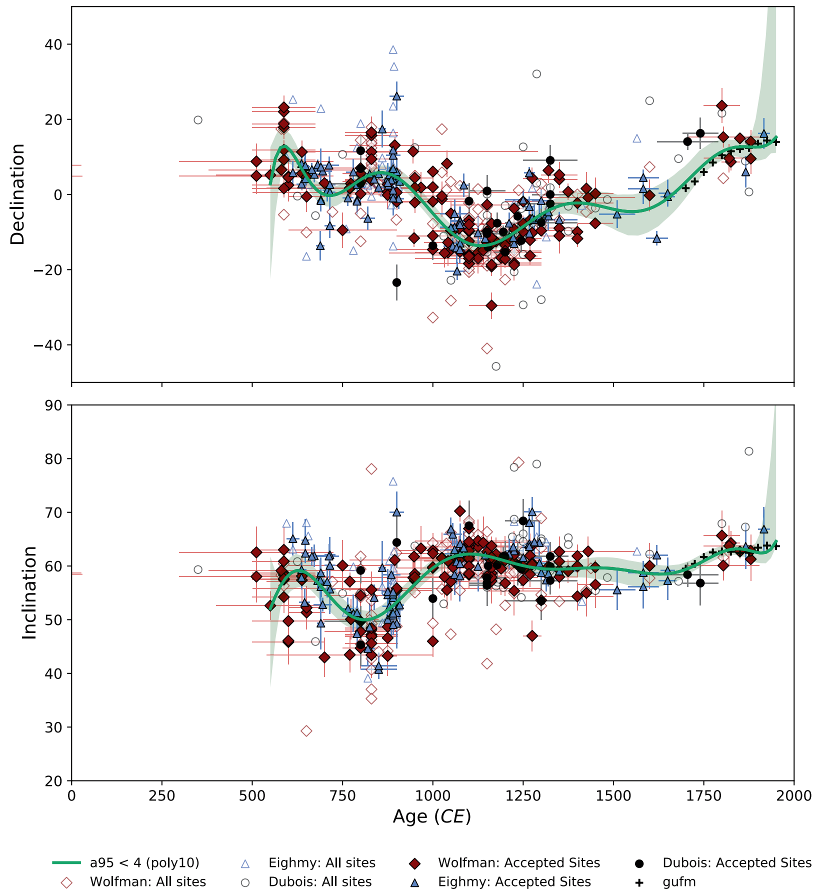

Figure 5. Magnetic declination and inclination of sites from the Four Corners region with respect to time: The data are plotted by contributor. Sites that do not meet our acceptance criteria but have ages are represented as open symbols. The accepted archaeomagnetic sites are denoted as solid symbols. Superimposed on the data is a degree-10 polynomial model fit based on the subset of data that satisfy a filter of $\alpha_{95} \leq 4°$. The uncertainty bounds of the fit are defined by a Monte Carlo style bootstrapping of 1,000 iterations. The black plus-signs are field values predicted by GUFM (Jackson et al., 2000) to constrain the polynomial fit during the most recent centuries that have limited data density.

However, there are stark differences between this new polynomial-derived VGP curve and the previous curves. Most notably, the amplitude of the loops is significantly decreased in this new model compared to past curves. Additionally, the paleosecular variation seen between 1200 and 1600 CE is inconsistent among all curves. We attribute these differences to variations in the methods used in curve construction. Reconciliation is important, as the various curves have been and continue to be used as reference VGP curves for enterprise archaeomagnetic dating (Blinman & Cox, 2018). A statistically more robust model with uncertainty bounds is required to further this aim; this work is ongoing.

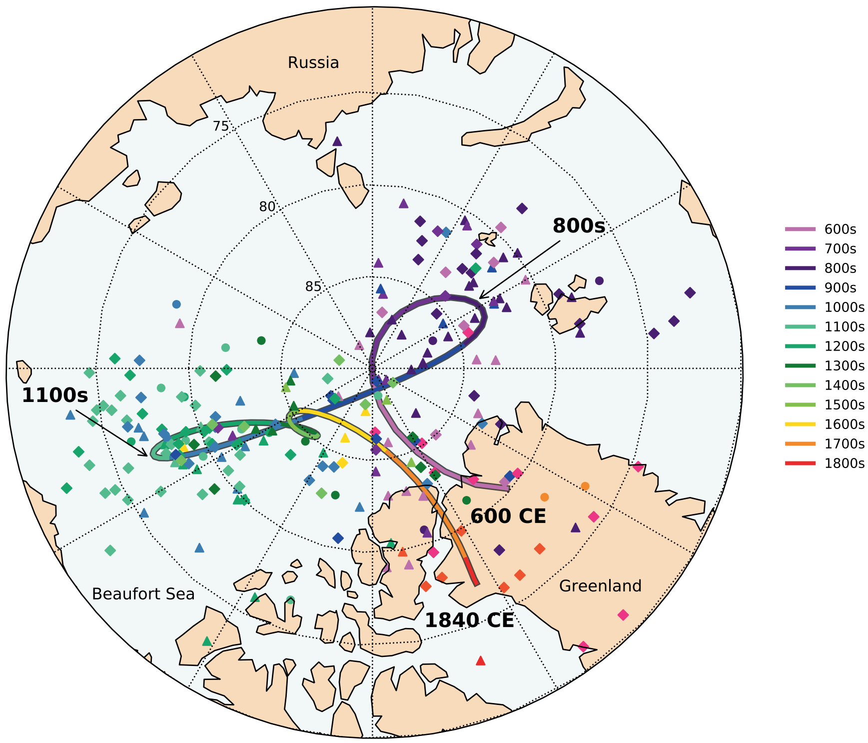

Figure 6. Newly interpreted Four Corners regional virtual geomagnetic pole (VGP) curve, superimposed on the accepted sites by contributor and colored by age: The overlaid VGP curve is based on the accepted sites from the composite data set that have age chronology recorded in the metadata. The curve is transformed from a degree-10 polynomial fit model of regional declination and inclination. The data and curve are colored by century between 600 and 1900 CE. Circle symbols represent data derived from the DuBois estate. Diamond symbols represent Wolfman data and triangle symbols represent Eighmy data.

9. Results From the Regions of Mesoamerica, South America, and the Lower Mississippi River

In addition to the significant volume of work conducted in the Four Corners region of the United States Southwest, a large amount of work was also conducted by DuBois and Wolfman in other regions of the Western Hemisphere. Specifically, their work targeted Mesoamerica, and, to a slightly lesser degree, the Lower Mississippi River region of the United States. There are also data in the archives from the greater Peruvian region of South America and northern Mexico in the archives.

The Lower Mississippi River region, formally replacing Wolfman's use "Southeast" or "Arkansas and the border areas," is defined by the roughly 650-km radius centered on Memphis, Tennessee and extending to New Orleans, Louisiana. This newly defined Lower Mississippi River region includes the states of Louisiana, Mississippi, Alabama, Tennessee, Kentucky, Missouri, and Arkansas, and portions of southern Indiana, southern Illinois, and eastern Texas (to roughly the city of Dallas). Within this region, DuBois sampled material from 287 burned features, Wolfman sampled 33 features, and Eighmy sampled 63. Of these only 22 have independent age chronology, and 7 passed this study's acceptance criteria (Table 4).

Analysis of the data from Mexico and Central America required an additional division between northern Mexico and Mesoamerica. A latitude of 25°N was chosen as a threshold, which is consistent with the climatic variation that influenced the cultural trends of the indigenous populations. This division is important for analysis because of the latitudinal dependence of inclination. The few archaeomagnetic sites sampled in northern Mexico (24 sites) are culturally similar to the indigenous populations of southern New Mexico and Arizona and may be in close enough proximity they could be included in the Four Corners regional data set for future modeling purposes. In total, samples were collected from 400 archaeomagnetic sites in Mexico and Central America; of those only 55 have reported ages, of which 31 satisfied the acceptance criteria (Table 4).

The fewest number of sites were collected from South America, with a total of 96 archaeomagnetic sites. Of these, DuBois collected the majority of the data (56 sites), and Wolfman in partnership with Dodson sampled 37 archaeomagnetic sites. Only 14 sites have independently dated age constraints and of those only 6 passed the acceptance criteria (Table 4).

The low quantities of accepted archaeomagnetic sites from these regions, complete with independent chronology, limit our ability to corroborate the previously developed models from these areas (Lower Mississippi River region—Wolfman, 1982, reproduced in Wolfman, 1990a:250–251; Mesoamerica—Wolfman, 1973:179, 238, 244, 247, and Wolfman, 1990b:287; Peruvian—Dodson & Wolfman, 1983, Wolfman & Dodson 1986, 1998). Reproductions of these previously published curves are available upon request. The recovered magnetic vector data for each region are plotted against age and available in Supporting Information S1.

10. Discussion

This project reflects the challenges, opportunities, and urgencies of preserving legacy data. Before his death, some of the DuBois' data were archived with the Oklahoma Geological Survey (OGS), but archaeomagnetism was not within their curation or research mission. The remainder of DuBois' data and samples were in extremely poor storage conditions and were scheduled for disposal after his death. Just before their disposal date, and with the cooperation of OGS, the DuBois archaeomagnetic estate was physically recovered by OAS staff and volunteers, and approximately 6,000 kg of materials and records were transported to New Mexico.

The Wolfman data are part of an ongoing archaeomagnetic dating laboratory at OAS, but Wolfman's laboratory had been moved three times in 20 years with no opportunity for systematic organization after each move. The Eighmy data set has been entrusted to and maintained by Lengyel in her archaeomagnetism laboratory. But her first laboratory at the Illinois State Museum was abruptly closed forcing her relocation to Eastern Tennessee State University in 2017.

The DuBois and Wolfman archives are now maintained by OAS at the Center for New Mexico Archeology. These archives are nearly complete repositories of the respective research legacies, including nearly all samples, field notes, measurement data, metadata, and some equipment. The need for, and value of, designated repositories for legacy data, meta-data, and samples is clear.

11. Conclusions and Future Goals

The data sets compiled by this multi-year recovery and digitization project contribute previously unpublished measurement data for 51,166 archaeomagnetic specimens from 5,377 heated archeological features. Of these, 1183 reinterpreted archaeomagnetic sites have been accepted by our selection criteria. At present, only 283 archaeomagnetic sites are recorded with independent age constraints, and 239 of the dated sites come from the Four Corners region of the United States Southwest.

Future work on these data sets aims to increase the proportion of data that satisfy this study's selection criteria, while also improving the accuracy and precision of the independent chronologies. These improvements are possible through continued demagnetization of the archived specimens, further analysis of existing

Table 5
Number of Sites Targeted for Further Study—By Contributor

Category	Contributor	Number
Have independent chronology and at least eight sample cubes	DuBois	890
Total = 1,138	Wolfman	169
	Eighmy	79
Accepted quality of magnetism but requires an independent chronology	DuBois	22
Total = 878	Wolfman	159
	Eighmy	697

demagnetization data, and recovering additional metadata for the archeological features that currently have limited archeological details.

The value of verification and refinement of the archeological chronologies is highlighted in Figure 6, where occasional VGP pole positions are incongruent with the expected positions based on its assigned ages. Although the vast majority of independent ages appear to be accurate, ages were assigned beginning in the early 1960s. Archeological dating tools and models have improved over the decades, and reassessment can correct errors and improve the accuracy and precision of the age assignments, while maintaining the independence and integrity of the geomagnetic data. Verifying and refining the chronology of these archeological features that have incongruent VGP pole positions is an ongoing project.

Additionally, just over 2,000 archeological features (MagIC sites) from the data set have been targeted for continued research (Table 5). These archeological features have been targeted because they either passed this study's acceptance criteria but were not paired with an independent age date (878 features), or they have an independent age date and at least eight cubes were collected from the feature but did not pass this study's selection criteria (1,138 features). The majority of the latter group features within the DuBois archive, nearly 890, and their failure to pass this study's selection criteria is usually the result of DuBois' use of a "pilot group" protocol for demagnetization. Fortunately, the sample cubes for these archeological features are accessible for further demagnetization and measurement. With effort, the inclusion of these additional data will greatly enhance the spatial diversity of accepted data and has the potential to aid in the development of additional regional VGP reference curves (Figure 7).

And finally, over the years, there have been a number of additional scientists, primarily archaeologists, that have contributed to and are contributing to the archaeomagnetic record of the United States. Identifying all the collaborators and finding their data has proved to be a challenge. Their contributions are not presented in this study, as that work is ongoing.

The effort directed at documenting these existing records is critically important because one of the unique aspects of this archive is that nearly all of the samples were collected from archeological features that either no longer exist or are no longer accessible. Most United States-based archeology today occurs when features are set to be destroyed by construction development projects and archeology tends to be inherently destructive. In either case, the data and physical specimens within these archives are often the only surviving components of the archeological and archaeomagnetic record.

These data represent the legacy of nearly 130 person-years of collective archaeomagnetic sampling and measurement by DuBois, Wolfman, and Eighmy. This archive will serve as the foundation for continued archaeomagnetic research in North America and will enhance global magnetic field modeling efforts for decades to come. The data, specifically from the Four Corners region, in particular, span a temporal and spatial completeness that is unprecedented in North America. Such high quality, temporally diverse, and globally distributed data are required for accurate time-varying global magnetic field models.

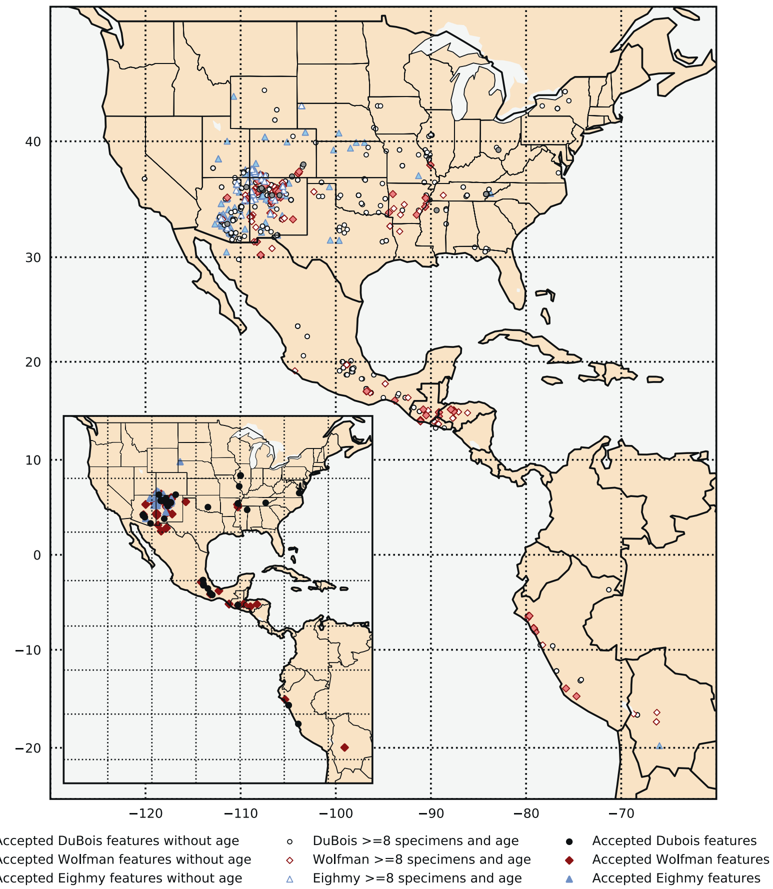

Figure 7. Provenance location map for sites targeted for future study, by contributor: The solid symbols on the inset map depict the 283 site locations that do satisfy this study's criteria (Table 4). The 878 faded-solid symbols do not satisfy this study's criteria because an independent chronology is not paired with the accepted magnetic data (Table 5). The 1,138 white-filled symbols do not currently meet this study's acceptance criteria but have at least eight sample cubes available for reanalysis or continued measurement (Table 5). The circle symbols represent data derived from the DuBois estate. Diamond symbols represent Wolfman data and the triangle symbols represent Eighmy data.

Acknowledgments
This study was supported in part by NSF grants EAR1547263 and EAR1827263 to LT, a private donation from Robert Rex for the support of undergraduate help, and private donations to the Museum of New Mexico Foundation's Friends of Archaeology, a non-profit that funded the physical collection of the DuBois scientific estate. Recovery of the DuBois and Wolfman data sets would not have been possible without the incredible assistance from Tom Windes, Gary Hein, and Arielle Thibeault. Their efforts were instrumental to the acquisition and digitization of the data sets. The authors gratefully acknowledge helpful conversations with Catherine Constable, Nicholas Jarboe, Jeffrey Gee, Maxwell Brown, and many more. The authors wish to acknowledge the reviewers (Catherine Batt and one anonymous) and the Associate Editor (Adrian Muxworthy) for their helpful comments, which improved the manuscript.

Data Availability Statement

The data presented in this study will be available at https://earthref.org/Magic/17115 upon publication of this article. An example Python code used in the clustering and adjustment of the systemic field azimuths is available here: https://earthref.org/ERDA/2478/.

References

Aitken, M. J. (1961). Measurement of the magnetic anomaly. *Archaeometry*, *4*, 28–30. https://doi.org/10.1111/j.1475-4754.1961.tb00528.x
Blinman, E. (1988). *The interpretation of ceramic variability: A case study from the Dolores Anasazi (Unpublished doctoral dissertation)*. Washington State University.

Blinman, E., & Cox, J. R. (2018). Theory, technique, and circularity: Time for renewal in southwestern archaeomagnetic dating. *Paper presented at Southwest Symposium, Denver Museum of Nature and Science*.

Brown, M. C., Donadini, F., Korte, M., Nilsson, A., Korhonen, K., Lodge, A., et al. (2015). GEOMAGIA50.v3: 1. General structure and modifications to the archeological and volcanic database. *Earth, Planets and Space*, *67*(1), 1–31. https://doi.org/10.1186/s40623-015-0232-0

Burlatskaya, S., & Petrova, G. (1961). First results of a study of the geomagnetic field in the past by the "archaeomagnetic" method. *Geomagnetism and Aeronomy*, *1*, 233–236.

Cook, R., & Belshé, J. (1958). Archaeomagnetism: A preliminary report from Britain. *Antiquity*, *32*, 167–178. https://doi.org/10.1017/s0003598x00038709

Deaver, W. L. (1998). Chronological issues of the LVAP. In S. M. Whittlesey, R. Ciolek-Torrello, & J. H. Altschul (Eds.), *Vanishing river: Landscapes and lives of the lower Verde valley, the lower Verde archaeological project* (pp. 447–490). SRI Press.

Dodson, R. E., & Wolfman, D. (1983). *Los resultados arqueomagneticos de las muestras recogidas en el Peru en 1982 (Tech. Rep.)*. Instituto Nacional de Cultura.

DuBois, R. (1989). Archaeomagnetic results from southwest United States and Mesoamerica, and comparison with some other areas. *Physics of the Earth and Planetary Interiors*, *56*, 18–33. https://doi.org/10.1016/0031-9201(89)90033-2

DuBois, R. (2008). *Geomagnetic results, secular variation, and archaeomagnetic chronology, United States and Mesoamerica, including archaeomagnetic data and time assignments (Special Publication 2008-2)*. Oklahoma Geological Survey.

DuBois, R., & Watanabe, N. (1965). Preliminary results of investigations made to study the use of Indian pottery to determine the paleointensity of the geomagnetic field for the United States A.D. 600-1400. *Journal of Geomagnetism and Geoelectricity*, *17*, 417–423. https://doi.org/10.5636/jgg.17.417

Eighmy, J. (1991). Archaeomagnetism: New data on the US southwest master curve. *Archaeometry*, *33*, 201–214. https://doi.org/10.1111/j.1475-4754.1991.tb00698.x

Eighmy, J. (2000). Thirty years of archaeomagnetic dating. In S. E. Nash (Ed.), *It's about time: A history of archaeological dating in North America* (pp. 105–123). University of Utah Press.

Eighmy, J., Hathaway, J., & Counce, S. (1987). *Independently dated virtual geomagnetic poles: The Colorado State University archaeometric data base (Technical Series No. 1)*. Colorado State University Archaeometric Laboratory.

Eighmy, J., & Klein, P. Y. (1988). *1988 additions to the list of independently dated virtual geomagnetic poles and the south-west master curve (Technical Series No. 4)*. Colorado State University Archaeometric Laboratory.

Eighmy, J., & Klein, P. Y. (1990). *1990 additions to the list of independently dated virtual geomagnetic poles and the south-west master curve (Technical Series No. 6)*. Colorado State University Archaeometric Laboratory.

Eighmy, J., & McGuire, R. H. (1989). *Archaeomagnetic dates and the Hohokam phase sequence (Technical Series No. 3)*. Colorado State University Archaeometric Laboratory.

Fisher, R. A. (1953). Dispersion on a sphere. *Proceedings of the Royal Society of London, Series A*, *217*, 295–305. https://doi.org/10.1098/rspa.1953.0064

Hagstrum, J., & Blinman, E. (2010). Archaeomagnetic dating in western North America. *Geochemistry, Geophysics, Geosystems*, *11*(6), Q06009. https://doi.org/10.1029/2009GC002979

Haury, E. (1976). *The Hohokam: Desert farmers and craftsmen*. University of Arizona Press.

Jackson, A., Jonkers, A. R. T., & Walker, M. R. (2000). Four centuries of geomagnetic secular variation from historical records. *Philosophical Transactions of the Royal Society of London*, *358*, 957–990. https://doi.org/10.1098/rsta.2000.0569

Jones, S., Tauxe, L., Blinman, E., & Genevey, A. (2020). Archeointensity of the four corners region of the American southwest. *Geochemistry, Geophysics, Geosystems*, *21*, e2018GC007509. https://doi.org/10.1029/2018GC007509

Kawai, N., Hirooka, H., & Sasajima, S. (1965). Counterclockwise rotation of the geomagnetic dipole axis revealed in the world-wide archaeo-secular variations. *Proceedings of the Japan Academy*, *41*, 398–403. https://doi.org/10.2183/pjab1945.41.398

LaBelle, J., & Eighmy, J. (1995). *1995 additions to the list of independently dated virtual geomagnetic poles and the south-west master curve (Technical Series No. 7)*. Colorado State University Archaeometric Laboratory.

LaBelle, J., & Eighmy, J. (1997). Additional archaeomagnetic data on the south-west USA master geomagnetic pole curve. *Archaeometry*, *39*, 431–439. https://doi.org/10.1111/j.1475-4754.1997.tb00818.x

Lengyel, S. N. (2010). The pre-ad 585 extension of the US southwest archaeomagnetic reference curve. *Journal of Archaeological Science*, *37*(12), 3081–3090. https://doi.org/10.1016/j.jas.2010.07.008

Lengyel, S. N., & Eighmy, J. (2002). A revision to the U.S. southwest archaeomagnetic master curve. *Journal of Archaeological Science*, *29*, 1423–1433. https://doi.org/10.1006/jasc.2001.0807

Paterson, G., Tauxe, L., Biggin, A., Shaar, R., & Jonestrask, L. (2014). On improving the selection of thellier-type paleointensity data. *Geochemistry, Geophysics, Geosystems*, *15*(4), 1180–1192. https://doi.org/10.1002/2013GC005135

Pedregosa, F., Varoquaux, G., Gramfort, A., Michel, V., Thirion, B., Grisel, O., & Duchesnay, E. (2011). Scikit-learn: Machine learning in python. *Journal of Machine Learning Research*, *12*, 2825–2830.

Premo, L. S., & Eighmy, J. (1997). *A reanalysis of archaeomagnetic samples collected for the Mimbres foundation project (Technical Series No. 10)*. Colorado State University Archaeometric Laboratory.

Schiffer, M. B. (1982). Hohokam chronology: An essay on history and method. In R. H. McGuire, & M. B. Schiffer (Eds.), *Hohokam and patayan: Prehistory of southwestern Arizona* (pp. 299–344). Academic Press.

Tauxe, L., Shaar, R., Jonestrask, L., Minnett, R., Koppers, A. A. P., Constable, C. G., et al. (2016). PmagPy: Software package for paleomagnetic data analysis and a bridge to the Magnetics Information Consortium (MagIC) Database. *Geochemistry, Geophysics, Geosystems*, *17*(6), 2450–2463. https://doi.org/10.1002/2016GC006307

Thellier, E., & Thellier, O. (1951). Magnétisme terrestre: Sur la directioni du champ magnétique terrestre, retrouvée sur des parois de fours des époques panique et romaine, à carthage. *Comptes Redus des Seances de l'Academie des Sciences*, *233*, 1476–1479.

Watanabe, N. (1959). The direction of remnant magnetization of baked earths and its application to chronology for anthropology and archaeology in Japan. *Journal of the Faculty of Science, University of Tokyo*, *2*, 1–188.

Watanabe, N., & DuBois, R. (1965). Some results of an archaeomagnetic study of the secular variation in the southwest of North America. *Journal of Geomagnetism and Geoelectricity*, *17*, 395–397. https://doi.org/10.5636/jgg.17.395

Weaver, K. F. (1967). *Magnetic clues help date the past*. (pp. 696–701). National Geographic.

Wilkinson, M. D., Dumontier, M., Aalbersberg, I. J., Appleton, G., Axton, M., Baak, A., et al. (2016). The fair guiding principles for scientific data management and stewardship. *Scientific Data*, *3*, 160018. https://doi.org/10.1038/sdata.2016.18

Wolfman, D. (1973). *A re-evaluation of Mesoamerican chronology: A.D. 1-1200 (Unpublished doctoral dissertation)*. University of Colorado.

Wolfman, D. (1982). Archeomagnetic dating in Arkansas and the border areas of adjacent states. In N. Trubowitz, & M. Jeter (Eds.), *Arkansas archeology in review* (pp. 277–300).
Wolfman, D. (1990a). Archaeomagnetic dating in Arkansas and the border areas of adjacent states – II. In J. Eighmy, & R. Sternberg (Eds.), *Archaeomagnetic dating* (pp. 237–260). University of Arizona Press.
Wolfman, D. (1990b). Mesoamerican chronology and archaeomagnetic dating, A.D. 1-1200. In J. Eighmy, & R. Sternberg (Eds.), *Archaeomagnetic dating* (pp. 261–308). University of Arizona Press.
Wolfman, D., & Dodson, R. E. (1986). *Los resultados arqueomagneticos de las muestras recogidas en el Peru en 1983 (Tech. Rep.)*. Instituto Nacional de Cultura.
Wolfman, D., & Dodson, R. E. (1998). Archaeomagnetic results from Peru: A.D. 700–1500. *Andean Past*, *5*(20). digitalcommons.library.umaine.edu/andean_past/vol5/iss1/20

Supporting Information for MagIC as a FAIR repository for America's directional archaeomagnetic legacy data

Shelby A. Jones [1,2], Eric Blinman [2], Lisa Tauxe [1], J. Royce Cox [2], Stacey Lengyel [3], Robert Sternberg [4], Jeffrey Eighmy [5], Daniel Wolfman [6], Robert DuBois [6]

[1]Scripps Institution of Oceanography, University of California, San Diego, La Jolla, CA 92093

[2]New Mexico Department of Cultural Affairs, Office of Archaeological Studies, Santa Fe, NM, 87507

[3]East Tennessee State University, Johnson City, TN, 37614

[4]Franklin and Marshall College, Lancaster, PA, 17604

[5]Unaffiliated

[6]*Posthumously

:

Contents of this file

Introduction

Four subsets of data from the Four Corners region were explored in the development of the polynomial fit model of paleosecular variation. Only the selected model based on the subset of data that satisfy $\alpha_{95} \leq 4$ was included in the main text and transformed into to a VGP projection. The other three (all the data, $\alpha_{95} \leq 5$ or $\kappa \geq 100$, and $\alpha_{95} \leq 3$) are presented here in Figure S1.

Due to the low density of accepted data from the Lower Mississippi River region, northern Mexico, Mesoamerica, and South America, those data were not graphically depicted in the text. The magnetic declination and inclination of the sites from these regions, with respect to time, are presented here in Figures S2, S3, S4 and S5, respectively.

Digital reproductions of previously published but difficult to access VGP models for the other regions are available by contacting the corresponding author (saj012@ucsd.edu).

:

A brief history of archaeomagnetism in the US

By the early 1970s, as a professor at University of Oklahoma, DuBois supported many students, most notably Daniel Wolfman and Jeffrey Eighmy, who later became trailblazers in archaeomagnetism in the United States. Wolfman, an archaeologist by training, helped expand DuBois' range to include Mesoamerica, and the Andean region of South America (specifically Peru). Post-graduation in 1973, Wolfman went on to develop his own archaeomagnetic research program in Arkansas, where he held positions until 1988. With the support of the National Science Foundation, Wolfman partnered with Dodson at the Rock Magnetism Laboratory at UC Santa Barbara (UCSB) in 1982-83. This collaboration resulted in the publishing of their reference work on Peruvian archaeomagnetism (Wolfman & Dodson, 1998). It was during this partnership that contacts were developed between Wolfman and Jeffrey Royce Cox, who later became Wolfman's primary laboratory technician.

In 1988, Wolfman moved from Arkansas to the Office of Archaeological Studies (OAS) in New Mexico where he founded the Archaeomagnetic Dating Laboratory. While Wolfman set up the OAS laboratory, Cox continued to make measurements at UCSB until 1993 when he joined Wolfman in New Mexico. Following Wolfman's sudden death in late 1994, Cox continued Wolfman's legacy under the supervision of Eric Blinman (then deputy director of OAS). Since then, Cox and Blinman have continued to collect and measure additional archaeomagnetic samples primarily from New Mexico for the purpose of enterprise archaeomagnetic dating. They also worked to increase the precision of field sampling methods and refine their archaeomagnetic dating procedures. For more detailed

:

descriptions of Wolfman's work and legacy, see Schaafsma & Schaafsma, 1996; Sternberg, 1996, and Eighmy, 2000:105-123).

The other notable student of DuBois is Jeffrey Eighmy, also an archaeologist. Eighmy worked as an undergraduate field technician for DuBois in the early 1970s, collecting samples from archaeological sites across the United States Midwest and the Southwest (Eighmy, 2000:107). Following the completion of his dissertation in 1977, he formed a collaboration with Robert Butler and Robert Sternberg at the University of Arizona. This multi-decade collaboration with Sternberg led to the development of several VGP models of paleosecular variation used primarily for enterprise archaeomagnetic dating aims, the later models are derived from a moving-windows statistical program (e.g. Eighmy et al., 1980, Sternberg, 1982, Hathaway et al., 1983, Sternberg, 1989, Eighmy & Sternberg, 1990, Eighmy, 1991, LaBelle & Eighmy, 1997, Lengyel & Eighmy, 2002, and Lengyel, 2010). These models confirm the large-scale field movements depicted in DuBois' original VGP models (DuBois & Watanabe, 1965, Watanabe & DuBois, 1965, and DuBois, 1989) but also show small-scale discrepancies that have still not been reconciled. That is one of the aims and application of this data recovery project.

In his professorial role, Jeffrey Eighmy trained and worked extensively with Stacey Lengyel, now a faculty member at East Tennessee State University (ETSU). Together they expanded the datasets from Arizona and brought new paleomagnetic perspectives to the conventional archaeomagnetic approach founded by DuBois. After Eighmy's retirement, Lengyel continued to work in the discipline and founded an archaeomagnetism laboratory at the Illinois State Museum, before moving to ETSU. Of all the dedicated archaeomagnetists in the United States, Lengyel and Eighmy are best known for pub-

:

lishing their data in accessible journals. The majority of the archaeomagnetic data in GeoMAGIA (Brown et al., 2015) from the United States is a result of their efforts, often in partnership with Sternberg.

:

Figure S1: Other polynomial fit models explored

Blue (top-left): The model derived from all the data (402 data points in the last 2000 years) does not reliably fit the declination predictions from gufm, black plus-sign symbols.

Yellow (top-right): The model derived from the subset of data that passed this paper's selection criteria (239 data points in the last 2000 years) has a phase offset in the declination during the 8^{th} – 14^{th} centuries that does not fit the data adequately.

Red (bottom-right): An α_{95} threshold of 3 degrees, decreased the subset of data available for modeling to 130 data points in the last 2000 years and was deemed to be an overly strict interpretation for the data.

Green (bottom-left): A balance of precision and quantity of data was favored, resulting in the preference to select this model based on the subset of data with an α_{95} threshold of 4 degrees (152 data points during the last 2000 years) for conversion into VGP coordinates.

:

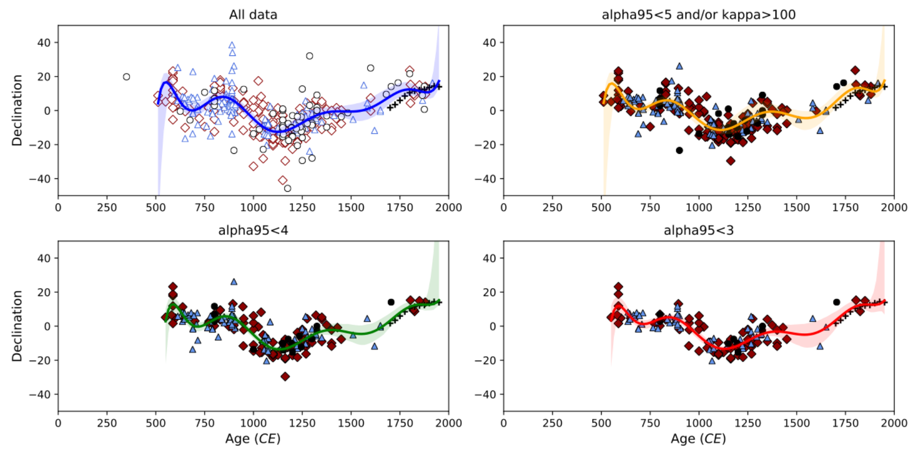
All data
alpha95<5 and/or kappa>100
alpha95<4
alpha95<3
Declination
Age (CE)

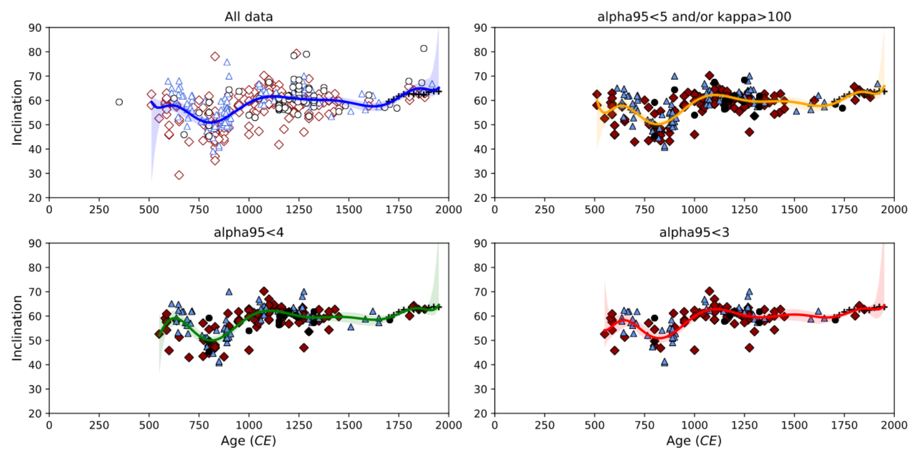
All data
alpha95<5 and/or kappa>100
alpha95<4
alpha95<3
Inclination
Age (CE)

:

Figure S2: Lower Mississippi River region

Within the Lower Mississippi River region, DuBois sampled material from 287 burned features, Wolfman sampled 33 features, and Eighmy sampled 63. Of these only twenty-two have independent age chronology (ten of which are older than 2000 years before present), and seven passed this paper's acceptance criteria (Table 4 in the main text). Those data are presented here, with respect to age. There are too few data to confirm or refute the previously published models for the region that were compiled by Wolfman.

:

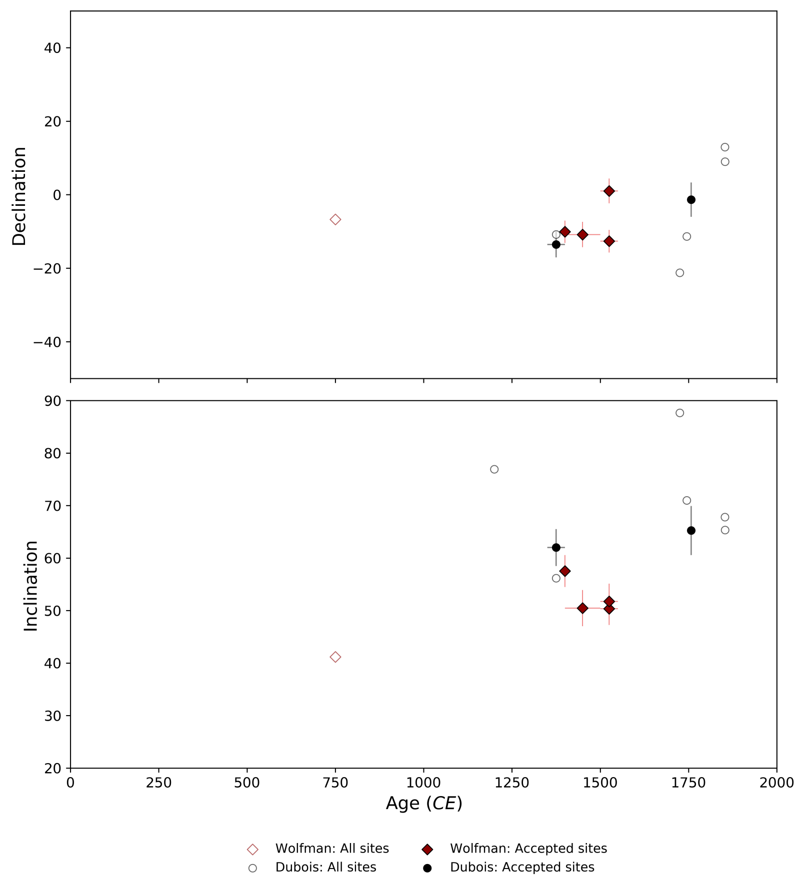

Declination
40
20
0
−20
−40
Inclination
90
80
70
60
50
40
30
20
0
250
500
750
1000
1250
1500
1750
2000
Age (*CE*)
Wolfman: All sites
Dubois: All sites
Wolfman: Accepted sites
Dubois: Accepted sites

:

Figure S3: Northern Mesoamerica

Due to the latitudinal dependence of inclination, the data from Mexico and Central America were interpreted in two divisions - northern Mexico and Mesoamerica. The few sites in the northern region (24 archaeological features), are culturally similar to the indigenous populations of the southern Four Corners region and are in close enough proximity that they could potentially be included in regional modeling efforts in the future. Those data are presented here, with respect to age. The eight sites are overlaid on top of the new polynomial fit model for the Four Corners region. The inconsistency noted between the inclination data and the model could be the result of a latitudinal dependence but could also be an artifact in the model, due to low data density in the Four Corners region, during the same time interval.

:

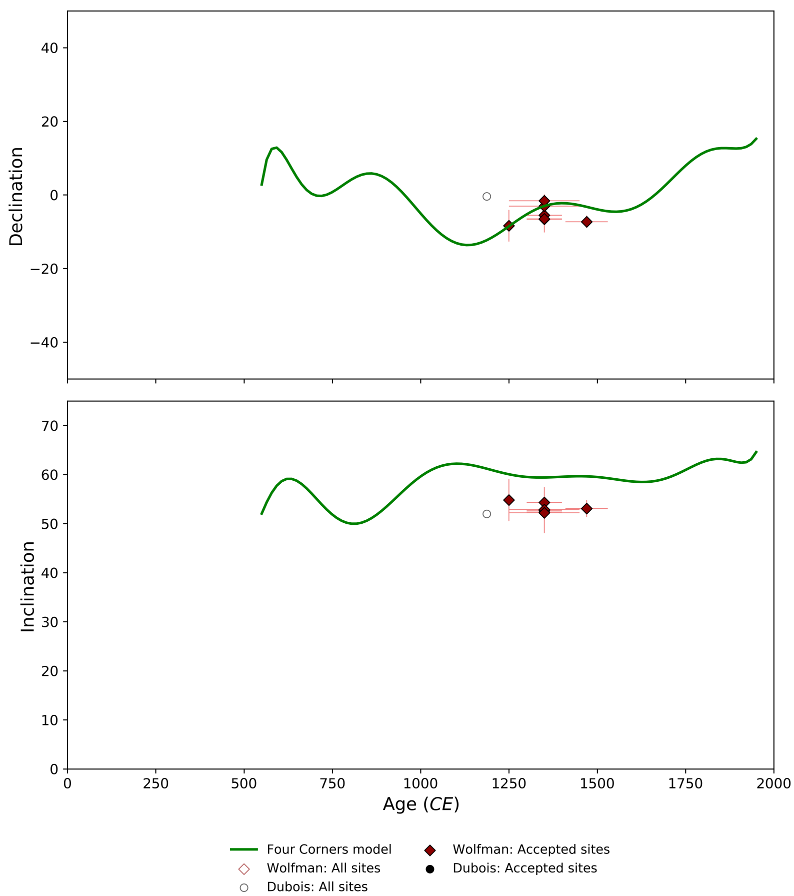
Declination
Inclination
Age (CE)
Four Corners model
Wolfman: All sites
Dubois: All sites
Wolfman: Accepted sites
Dubois: Accepted sites

:

Figure S4: Mesoamerica

Of the 376 archaeomagnetic sites sampled in Mesoamerica, forty-seven have independent age constraints and only twenty-four passed this paper's acceptance criteria (Table 4 in the main text). Those data are presented here, with respect to age. The data are too dispersed to confirm or refute the previously published models for the region that were compiled by Wolfman.

:

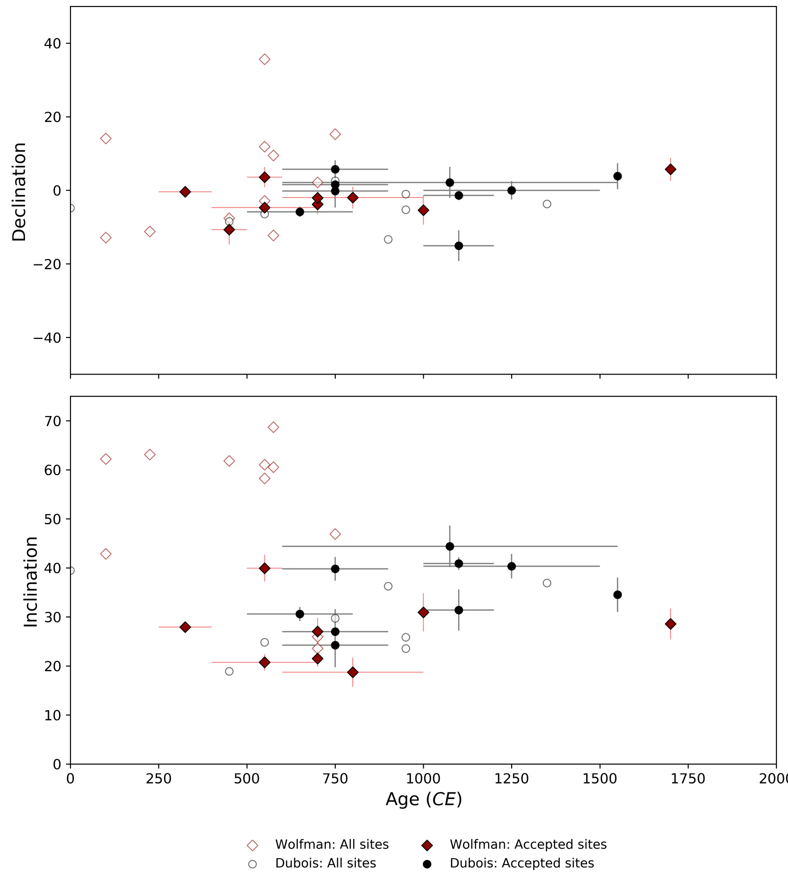

40
20
0
−20
−40
Declination
70
60
50
40
30
20
10
0
Inclination
0
250
500
750
1000
1250
1500
1750
2000
Age (CE)
Wolfman: All sites
Dubois: All sites
Wolfman: Accepted sites
Dubois: Accepted sites

:

Figure S5: South America

South America is the least sampled region in the archive and of those, only fourteen archaeomagnetic sites passed our acceptance criteria. Those data are presented here, with respect to age. There are too few data to confirm or refute the previously published models for the region that were compiled by Wolfman and Dodson.

:

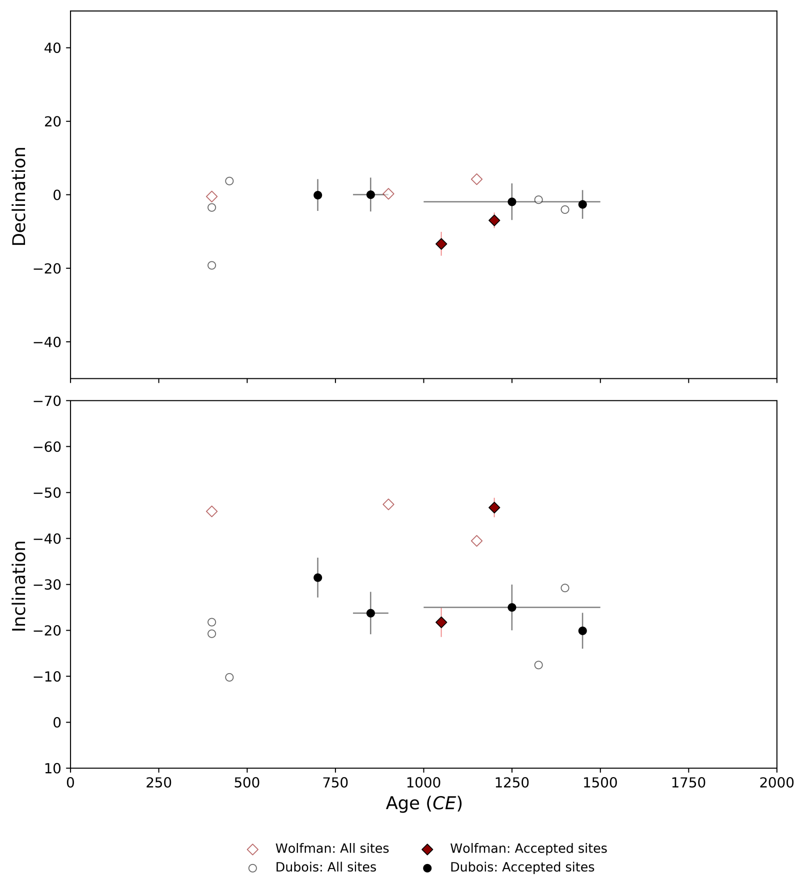
Declination
Inclination
Age (CE)
Wolfman: All sites
Wolfman: Accepted sites
Dubois: All sites
Dubois: Accepted sites

:

Table S1: Parameters used in data clustering

To eliminate subjectivity of human bias and ensure that the scatter caused by paleosecular variation was maintained, the azimuth adjustments required to correct the archived data were completed using the OPTICS clustering functions within the sklearn.cluster python module. The parameters used are presented in Table S1 and an example python Jupyter Notebook, associated with this paper, is available on ERDA (https://earthref.org/ERDA/2478/). The notebook presents the code used to cluster and adjust the DuBois data from the United States.

In some cases, a filter was used in addition to the OPTICS clustering to ensure that directions that fell between clusters (i.e. Declination = 45 or 135°) were not included in a cluster. Instead those data were filtered out and assigned to no cluster, to avoid misidentifying the cluster they belong to.

:

Contributor	Step 1	Step 2
DuBois		
- USA	Epsilon = 11	Epsilon = 19
- Mexico and Central Am.	*Not Corrected*	
- South America	*Not Corrected*	
Wolfman		
- USA	Epsilon = 10	Epsilon = 18
- Mexico and Central Am.	Epsilon = 21	Filter = Decs 330-20°, 60-110°, 150-220°, and 240-290°
- South America	Filter = Decs 60-130°	
Eighmy		
- USA	Epsilon = 18	
- Mexico and Central Am.	*Not Corrected*	
- South America	*Not Corrected*	

:

References

Brown, M. C., Donadini, F., Korte, M., Nilsson, A., Korhonen, K., Lodge, A., ... Constable, C. G. (2015). GEOMAGIA50.v3: 1. general structure and modifications to the archeological and volcanic database. *Earth, Planets and Space*, *67*(1), 1-31. doi: doi.org/10.1186/s40623-015-0232-0

DuBois, R. (1989). Archaeomagnetic results from southwest united states and mesoamerica, and comparison with some other areas. *Physics of the Earth and Planetary Interiors*, *56*, 18-33.

DuBois, R., & Watanabe, N. (1965). Preliminary results of investigations made to study the use of indian pottery to determine the paleointensity of the geomagnetic field for the united states a.d. 600-1400. *Journal of Geomagnetism and Geoelectricity*, *17*, 417-423.

Eighmy, J. (1991). Archaeomagnetism: new data on the us southwest master curve. *Archaeometry*, *33*, 201-214.

Eighmy, J. (2000). Thirty years of archaeomagnetic dating. In S. E. Nash (Ed.), *It's about time: A history of archaeological dating in north america* (p. 105-123). Salt Lake City, Utah: University of Utah Press.

Eighmy, J., & Sternberg, R. (1990). *Archaeomagnetic dating.* Tucson, Arizona: University of Arizona Press.

Eighmy, J., Sternberg, R., & Butler, R. F. (1980). Archaeomagnetic dating in the american southwest. *American Antiquity*, *45*, 507-51.

Hathaway, J., Eighmy, J., & Kane, A. (1983). Preliminary modification of the southwest virtual geomagnetic pole path ad 700 and ad 900: Dolores archaeological program results. *Journal of Archaeological Science*, *10*, 51-59.

:

LaBelle, J., & Eighmy, J. (1997). Additional archaeomagnetic data on the south-west usa master geomagnetic pole curve. *Archaeometry*, *39*, 431-439.

Lengyel, S. N. (2010). The pre-ad 585 extension of the us southwest archaeomagnetic reference curve. *Journal of Archaeological Science*, *37*(12), 3081-3090.

Lengyel, S. N., & Eighmy, J. (2002). A revision to the u.s. southwest archaeomagnetic master curve. *Journal of Archaeological Science*, *29*, 1423-1433.

Schaafsma, P., & Schaafsma, C. (1996). Daniel wolfman 1939-1994. *American Antiquity*, *61*(2), 291-294. doi: doi.org/10.1017/S0002731600051921

Sternberg, R. (1982). *Archaeomagnetic secular variation of direction and paleointensity in the american southwest* (Unpublished doctoral dissertation). University of Arizona, Tucson, Arizona.

Sternberg, R. (1989). Secular variation of archaeomagnetic directions in the american southwest, a.d. 750-1425. *Journal of Geophysical Research*, *94*, 527-546.

Sternberg, R. (1996). Daniel wolfman: 1939-1994. *Society for Archaeological Science Bulletin*, *19*(3/4), 5-6.

Watanabe, N., & DuBois, R. (1965). Some results of an archaeomagnetic study of the secular variation in the southwest of north america. *Journal of Geomagnetism and Geoelectricity*, *17*, 395-397.

Wolfman, D., & Dodson, R. E. (1998). Archaeomagnetic results from peru: A.d. 700-1500. *Andean Past*, *5*(20). Retrieved from `digitalcommons.library.umaine.edu/andean_past/vol5/iss1/20`

Acknowledgements

Chapter 3, in full, is a reprint of material as it appears in *Journal of Geophysical Research - Solid Earth*. Jones, Shelby A.; Blinman, Eric; Tauxe, Lisa; Cox, J. Royce; Lengyel, Stacey; Sternberg, Robert; Eighmy, Jeffrey; Wolfman, Daniel; Dubois, Robert, 2021. The dissertation author was the primary investigator and author of this paper.

Chapter 4: Archaeomagnetic directional studies as a tool for understanding feature form and function: A case study of two burned rock features in a multi-component site in east Texas, USA

Abstract

Directional archaeomagnetic techniques were used to propose use-history models for two burned rock features at archaeological site 41AN162, in Anderson County (Texas, USA). Rock clusters were located with magnetic survey and showed visual evidence of heating upon excavation. While common in the region, such burned rock features are rarely associated with cultural artifacts that indicate their function. Archaeologists have debated how these features are related to human behavior in their creation, use, and abandonment. Archaeomagnetic studies can be employed to shed light on these questions. Thirteen oriented rocks were collected from two features for analysis. Where possible, oriented archaeomagnetic specimens were prepared from the tops, interiors, and bottoms of each rock. The rocks of Feature 5 were thoroughly heated and the vector results of the rock surfaces and interiors show a north and down direction nearly parallel to the expected field for the locality, implying that the individual rock components of the feature have remained substantially in-situ since the feature's last significant heat exposure. Preserved magnetic remanences of the Feature 16 rocks, were severely overprinted and have within-rock magnetic qualities that suggest reuse and lower temperature of use. The magnetic inclination data and archaeological context suggest that the rocks may have been heated as part of a covering layer rather than as a pit lining. The magnetic declination orientations of the studied rocks within Feature 16 are suggestive of an unloading or dismantling pattern in which the covering layer was removed and set aside to expose the target of the heating event.

4.1 Introduction

Burned rock features and rock clusters are commonly found at archaeological sites around the world in sites with ages dating to at least 30,000 years (Black and Thoms, 2014: 206). But often the rock features have few artifacts that yield insight into their form and function. Most research and publications are related to the ethnobotanicals that are found in association with the rocks in the cluster and most features have been interpreted to be various forms of cooking technology (e.g. Blinman et al. 2017). But despite this growing body of ethnobotanical literature, there is no standardized terminology to objectively describe rock features in archaeological sites, hindering objective interpretations of feature form that are critical to the feature's use, site use, spatial and temporal comparisons, and discussions human behavioral adaptation (Black and Thoms, 2014). One explanation for this limited knowledge is that archaeologists rarely have the opportunity to utilize direct and measurable evidence (aside from ethnobotanicals) to understand these rock features. Archaeomagnetic studies offer a variety of techniques that can inform on outstanding research questions related to feature form and function including directional archaeomagnetic studies that can yield insight into feature geometry. This paper presents data and interpretation from two features at an archaeological site in Anderson County (east Texas). The directional data provide information about the two feature's use and form and the behavior practices of the past residents. This work builds on the applications explored by Wulf Gose, specifically the archaeodirectional research design (Gose, 2000).

4.1.1 Study area: Archaeological background

In 2020, Terracon Consultants, Inc. conducted eligibility testing and data recovery-level investigations at site 41AN162 on behalf of Texas Department of Transportation (TxDOT) in advance of a road expansion project. A total of ~56m^3 of site sediments was excavated, in addition to 64 shovel tests that were utilized to help determine boundaries for different site elements and deposits. Excavation efforts and volumes of sediment removed are summarized in Lohse et al. (2020). Based on the nature of artifacts recovered and features exposed, the site contains three primary components. The earliest component dates to Woodland period (Late Archaic); the next component dates to the Caddo period, primarily an early Middle Caddo (1250-1440 CE) component but with a single feature dating to a later in the Middle Caddo period; and the youngest is a circa 1920s-1930s tenant farmstead. One feature was dated to the Middle Archaic period; this feature along with a few diagnostic stone tools indicates that the site's overall occupation history is more extensive than indicated by the three primary components.

During eligibility testing, multiple rock features were identified by magnetic survey (gradiometer) that defined anomalies for further investigation by test unit excavations. Test units encountered two burned rock features that were sufficiently large and complex that they were selected for detailed excavation and archaeomagnetic study, as part of the subsequent data recovery investigations.

For site security reasons, a precise location more detailed than Anderson County Texas is not provided, nor is a site location map.

4.1.1.1 Excavation of Feature 5

During testing, four 1-by-1 meter excavation units confirmed the presence of a tight cluster of heat affected rock that was initially identified in preliminary magnetic survey anomaly data and was designated Feature 5. Early in data recovery and excavation, three rocks were selected for archaeomagnetic field sampling (Figure 4.1, dashed borders) and preliminary laboratory analysis to ensure the potential for archaeomagnetic study. Additional field excavation enlarged the exposure to encompass the roughly 3-meter diameter burned rock concentration of Feature 5. The rocks of the feature were left undisturbed (in situ) until archaeomagnetic field sampling was completed on six additional rocks from across the cluster (Figure 4.1, solid borders). Following the completion of the archaeomagnetic field sampling protocol, all the remaining rocks were removed to confirm that the rock cluster was a single layer and to collect artifacts and environmental samples from between and below the rocks. The excavations confirmed the apparent single layer organization of the rocks, and there was no evidence of an encompassing or of an internal pit. The morphological characterization of the burned rock feature is that it appeared to be a platform, or a surface within a slight depression, with no stratigraphic evidence of significant post-use disarticulation of the rock elements. The morphology of the feature is consistent with Black and Thoms' (2014) definition of an earth oven.

Flotation samples collected from between and beneath the rocks yielded potential radiocarbon dating materials. Three different specimens of carbonized nutshells were selected for dating. All are assumed to have been processed as part of, or contemporary with, the use of the thermal feature. Accelerated mass spectroscopy (AMS) dates of 2,326 ± 29 radiocarbon years (rcy) BP (SUERC-98387; GU57777) and 2,309 ± 29 rcy BP (SUERC-98388;

GU57778) were produced on a *Carya sp*. and a Juglandaceae specimen, respectively. Four additional AMS dates were derived from CO_2 produced by low energy plasma oxidation of a third nutshell (*Fagus sp*.) at the Office of Archaeological Studies (OAS) Radiocarbon Sampling Laboratory (210215C-1, 210215C-2, 210215C-3, 210215C-4). The AMS dates are 2,430 ± 60 rcy BP, 2,310 ± 60 rcy BP, 2,630 ± 70 rcy BP, and 2,290 ± 70 (ETH 114251.1, ETH 114252.1, ETH 114940.1, and ETH 114941.1, respectively). Since the four CO_2 samples were produced from a single specimen, averaging is appropriate, and the average of the OAS dates is 2,410 ± 30 rcy BP. These dates are consistent with a late Archaic use of the feature.

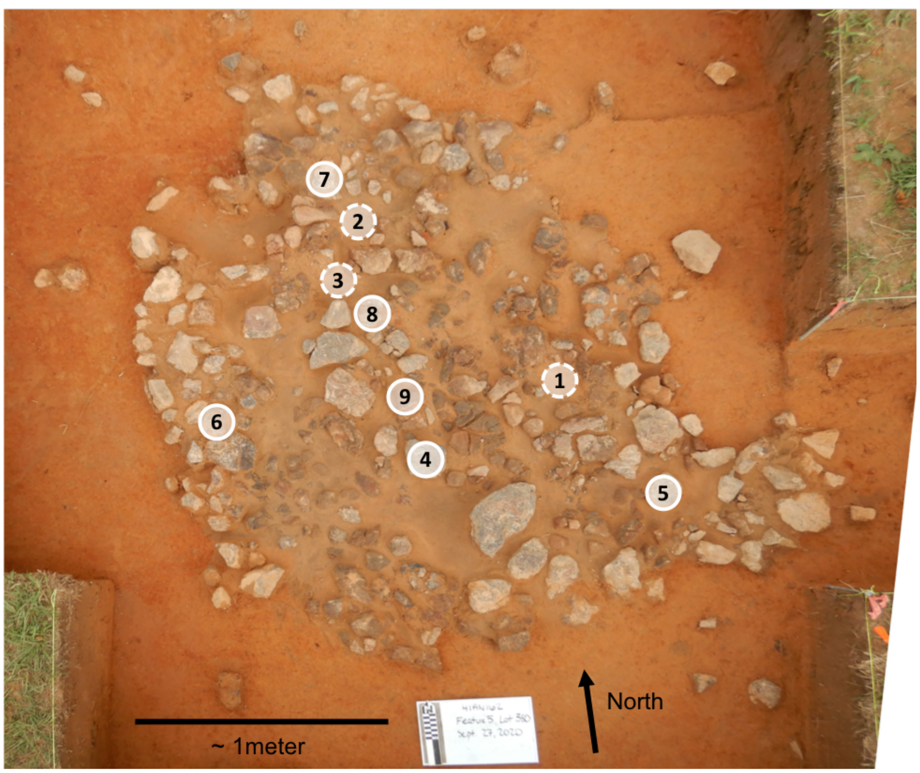

Figure 4.1: Feature 5, partially rectified, labeled showing the locations of all nine rocks sampled for archaeomagnetism. Rocks 1-3 (dashed borders) were removed prior to photography. Rocks 5-9 (solid borders).

4.1.1.2 Excavation of Feature 16

Feature 16 was defined as a scatter of fire-affected rocks that occurred in discontinuous discrete clusters, within a 2-meter dispersion. Four rocks, one within each cluster, were selected for field sampling analysis after data recovery exposure. Clusters and rocks with specimen cubes attached are indicated in Figure 4.2. No pit features were defined, but the rocks were within, and rested upon, darker organic-rich sediments (dispersed charcoal).

A fragment of *Juglans negra* shell collected from a flotation sample and in association with rock cluster 1 (the cluster just northwest of archaeomagnetic rock 1) yielded an AMS date of 641 ± 29 rcy BP (SUERC-98401, GU57788). Due to the nature of the radiocarbon calibration curve for this time period, this radiocarbon age falls within the broader range of the very late thirteenth through the fourteenth centuries CE, well within the Caddo period of regional culture history.

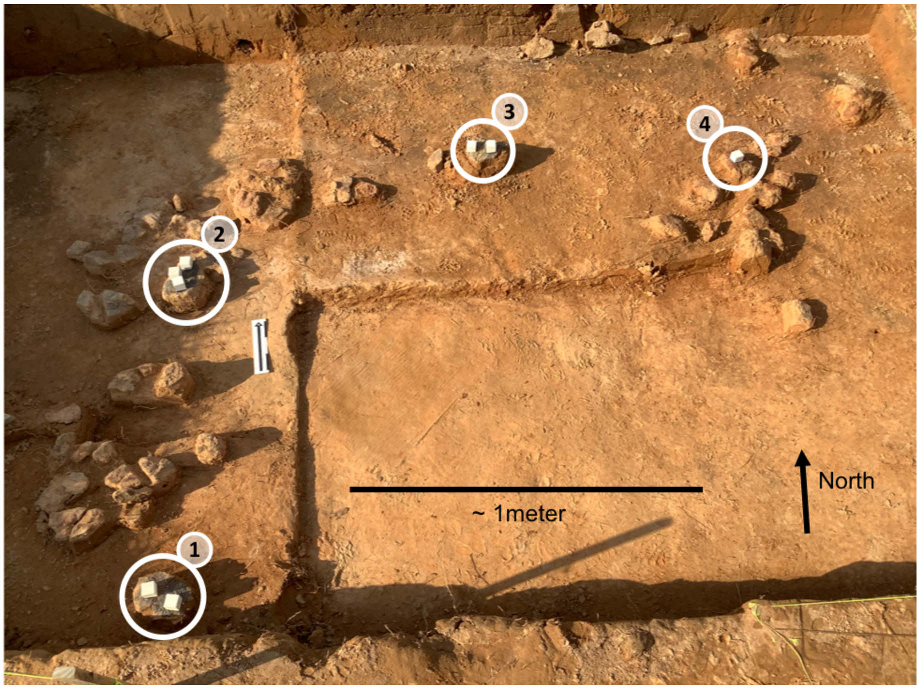

Figure 4.2: Feature 16 with archaeomagnetic rocks selected and specimen cubes attached for Rocks 1-4.

4.1.2 Study area: Geologic Context

No field surveys of rock resource availability could be conducted on the private property adjacent to the highway construction zone in the vicinity of 41AN162, and the exact geologic locality(ies) harvested by the past humans cannot be identified with confidence; however, the previously mapped local geologic units are known to have facies consistent with the rocks submitted for archaeomagnetic study. The Sparta Sand Formation, Weches Formation, and Queen City Sand are the only three mapped geologic formations in the area (Groat, 1975), implying that the feature rocks likely were harvested from one of these three formations. Research into resource threshold distances related to raw material collection for pottery production indicates that distances vary but are usually on the order of a few kilometers, depending on the sedentary nature of the population and their access to navigable water sources and animal labor (Arnold, 1985: 35). While, not perfectly analogous it is reasonable to expect that the resource threshold distance for the collection of rocks for heated rock features is similar to that of pottery resource collection. All of three formations within a few kilometers of site 41AN162 are Eocene in age, and primarily ferruginous sandstones with interbedded silt and mudstones (Groat, 1975).

Of the three formations, the description of the Sparta Sand Formation is the only one that mentions rare coal layers, and the Weches Formation is the only one described to have a presence of limonite and siderite iron bearing minerals. We believe that outcrops of either the Sparta Sand Formation or the Weches Formation are the source of the mudstone rocks that were harvested by the past humans. Another option is that these rocks were retrieved from the local Holocene alluvium; however, the angular shapes of the rocks and lack of stream rolling evidence makes this origin less likely. If indeed the rocks were harvested from the alluvial rather than an outcrop, the tabular and angular shaping of the rocks imply the rocks did not travel great distances in the fluvial system from their natural outcrop.

Ferruginous sands are common to all three of the local geologic formations, so without a known harvesting source, it is uncertain which formation the sandstones from Features 5 and 16 derive. The sandstone rocks were less angular and less tabular than the mudstone rocks, and suggesting they are more likely than the mudstones to have been derived from alluvium deposits.

The lithologies present, in both the initial and the final rock selections for the archaeomagnetic studies were from sedimentary systems, range from carbonaceous mudstones to weak iron-cemented sandstones. All rocks taken from the archaeological contest and submitted to the Office of Archaeological Studies Archaeomagnetic Dating Laboratory (OAS ADL) are considered “anthropogenically influenced” because their presence at the site resulted from the human selection and transport behaviors. Of the thirteen Feature rocks submitted for archaeomagnetic study, nine are carbonaceous mudstones and four are iron-cemented sandstones.

4.2 Materials and Methods

4.2.1 Lithology of the Feature Rocks: Mudstones

The majority of the mass of the carbonaceous mudstones is composed of silty-mud grains in circa 2mm thick layers (Figure 4.3). Thinner layers between the mud layers are <1mm thick irregular laminar voids that appear to have once been layers of dense organics, often associated with fine sands. The rocks preferentially crack along these voids. The patterning of the layers is fairly regular, but there is some variation. In some regions of the rock, the organic and fine sand layers are nearly non-existent, and the mud layers are in direct contact with each other. In these more homogeneous regions, the rock is much more stable and less likely to fracture. No identifiable fossils or impressions were observed in association with the mud-void surfaces. The organic layers appear to be heat and pressure affected, becoming what appears to be thin coal-like or carbonaceous layers. The rocks have a dark reddish-brown appearance (Feature 5, Rock 2, Munsell: 5YR 4/3d; observed on a cut and rinsed face), yet the mud resulting from the diamond saw cuts is a burnt-red color (Munsell: 10R 3/6d). The density, color, and material properties of the rocks suggest these rocks were heated completely through after their initial formation, and this interpretation is supported by the preliminary magnetic data. Our interpretation of the rocks is that they are derived from a sediment-rich “clinker-like” deposit, a coal shale or mudstone protolith that was subject to a significant later heating event, probably a naturally occurring coal fire. The original shale was likely deposited in a low energy shallow basin (lake or sea) environment that had alternating contributions of mineral and organic sediment. Consultation with regional USGS geologic maps further support this interpretation of a shallow basin.

Figure 4.3: Two pieces of one of the mudstone rocks from Feature 5, post-cutting. Note the orange-brown hue to the rocks. This color is seen in all the mudstones but reverts to a bright red-brown hue upon laboratory heating in air. The silty-mud layers vary in thickness from roughly 2-3mm (left image) but in some areas are completely conjoined (right image). The rock preferentially breaks along the voids between the silty-mud layers and is most stable in areas were the layers have conjoined.

4.2.2 Lithology of the Feature Rocks: Sandstones

The four sandstone rocks received are all slightly different from each other, indicating that they may have been harvested from a variety of sources or that the parent formation is internally variable. All of the rocks are composed of fine to medium grain sands held in a silty-mud matrix (Figure 4.4). The rocks exhibit some small-scale grading and morphological variation resulting from their individual depositional environments. All the rocks have significant red staining, indicating the presence of iron as either a primary element of the rocks or as a secondary deposition, likely the result of ground water percolation. Upon sectioning, as part of the archaeomagnetic specimen preparation, one rock (Feature 16, rock

4) showed internal variability that suggests the mudstone and sandstone feature rocks could represent facies from a single locality that fluctuated in depositional environment through time. Although some rocks were internally cracked, all the rocks were well lithified and maintained their structural integrity during cutting. This allowed for the creation of oriented columns of the rock substrates, from which multiple archaeomagnetic specimens could be cut.

Figure 4.4: Sectioned example of a sandstone (Feature 5, Rock 9). Variation in texture and iron cement characteristic reflects variation in depositional conditions.

4.2.3 Preparation of specimen cubes

The archaeomagnetic field sampling approach used in this study for the rocks from Features 5 and 16 was to adhere one to three leveled and carefully oriented pre-cast 1-inch cubes of plaster of Paris to the exposed (upper) surface of each rock. Prior to adhering to the rock, the bottom face of each pre-cast cube was rough sculpted to conform to the rock's surface, so that the top face of the cube remained level. Any small gaps in the rough sculpting were bridged by a moderately thick layer of gel epoxy. The top face of the cube was intentionally untouched during sculpting so it could support a high precision bullseye level. The bullseye level remained in place as the epoxy cured, ensuring the cube remained level and creating a consistent reference plane. During sculpting and adhering, a side cube face was kept accessible and as pristine as possible to serve as a reference side for later field orientation measurement (Figure 4.5). After the epoxy fully cured, the details essential to magnetic study were recorded (specimen identification number, compass field azimuth orientation, location within feature, and description). The rocks were then removed from the feature and carefully packed for transit to the OAS ADL at the Center for New Mexico Archaeology (CNMA) in Santa Fe.

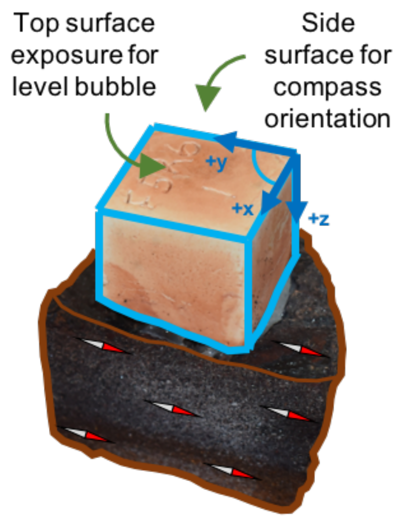

Figure 4.5: Annotated example of a shaped plaster cube adhered to a burned rock using epoxy. Note that it is critical for the side surface to be accessible for compass orientation. The order of cube placement and the identified reference corner is a tactical consideration when placing multiple cubes on a single rock.

The thirteen rocks were collected over multiple field sessions in 2020 by the Terracon Consulting, Inc. field crews. Those crews were provided with a written documentation of sampling protocol, phone consultations, and a full field sampling kit on loan from the OAS ADL. This remote sampling strategy was an adaptation to the travel limitations resulting from the COVID-19 pandemic. During the first test unit exposures (August 2020), an initial group of three rocks was selected for oriented archaeomagnetic field sampling (Figure 4.6) from Feature 5. The rocks were judiciously selected to represent the apparent spatial and lithological diversity of the feature elements. The initial three rocks were transmitted to the OAS ADL for laboratory analysis and confirmation of the suitability of the rock types and the feature's proposed thermal history for further archaeomagnetic study. The magnitude of the preserved magnetic moments of the initial samples were sufficient to measure and indicative of a thermally acquired remanent magnetization, suggesting that there was potential for archaeomagnetic study (NRM $\gtrapprox 1.0e^{-07}$ Am^2; congruent with Butler 1992: 14), and an investment in the field sampling of additional rocks from Feature 5 and other 41AN162 features was recommended.

Subsequent field sampling was conducted by the Terracon field crews with additional recommendations from the OAS ADL staff during the September 2020 excavations. This sampling yielded an additional group of six rocks from Feature 5 (Figure 4.7) and four rocks collected from Feature 16 (see Figure 4.2).

Figure 4.6: Feature 5 at the initiation of data recovery excavations. The three initially sampled rocks are indicated.

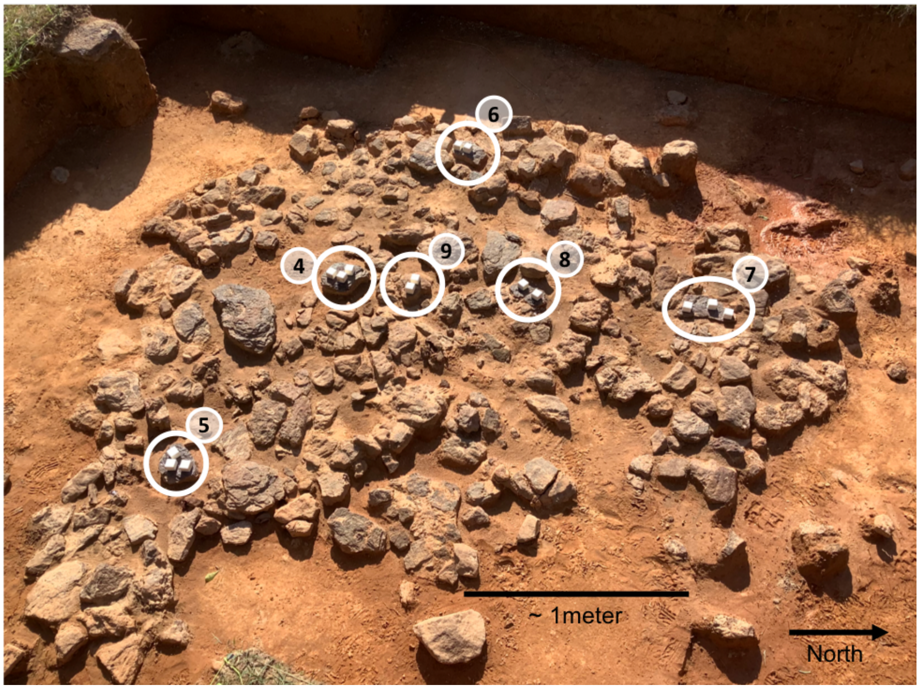

Figure 4.7: Feature 5 after more complete exposure showing archaeomagnetic sampling locations. Orientation specimens were attached to Rocks 4-9.

In the laboratory, each rock was carefully placed on a sand bed oriented within their sand beds such that the original cubes were level and their azimuths were in close agreement with those on the field notes. To achieve a statistically valid analytic database, additional cubes were adhered to each of the rocks while on the sand bed. The orientations of the newly attached cubes were recorded within the reference frame of the original field-adhered cubes. Once the epoxy adhesive was cured, rocks were cut first into columns supported on one end by the blank plaster cube, and where possible, the columns were then subdivided into specimens for archaeomagnetic laboratory measurement. Cutting was done using a water-cooled circular tile saw with a smooth diamond blade. The water, as a coolant, ensures no weak magnetic signatures were imparted on the rocks during this step as a result the frictional heat of the saw.

Taking advantage of the cohesiveness of the rocks' lithology, the columns of substrate allowed the preparation of multiple oriented specimens. The adhered material ranged in thickness from about 5mm to ~8cm (the total thickness of the thickest rock). The shortest columns (generally less than 1.5cm in height) were prepared for magnetic study as individual specimens (Figure 4.8). The longer columns of substrate (i.e. greater than about 1.5cm) were subsampled into additional specimens. Standard OAS ADL 1-inch archaeomagnetic molds were placed over the columns of substrate in alignment with the original rough-cut and adhered cube. Plaster was then poured into the molds, encasing the columns of substrate in plaster. The encased columns were cut into specimens of at least 4mm in thickness (~1cm was preferred). Each of the new specimens was recast in the standard OAS ADL 1-inch cubic mold to form a complete jacket of plaster around the substrate. They were then labeled and prepared for magnetic study.

The specimens encasing the material from the top rock surfaces were all labelled as specimen “A” of the original cube number, and subsequent deeper specimens within each column were identified with incremented letters. The incremental letter sequence was carried out to the bottom of the column for the rocks of Feature 5, but for the rocks from Feature 16, the bottom specimen of each column was labeled “Z” for ease of data analysis. Specimens without an alphanumeric specimen number represent specimens that span the entire depth of the rock from top to bottom.

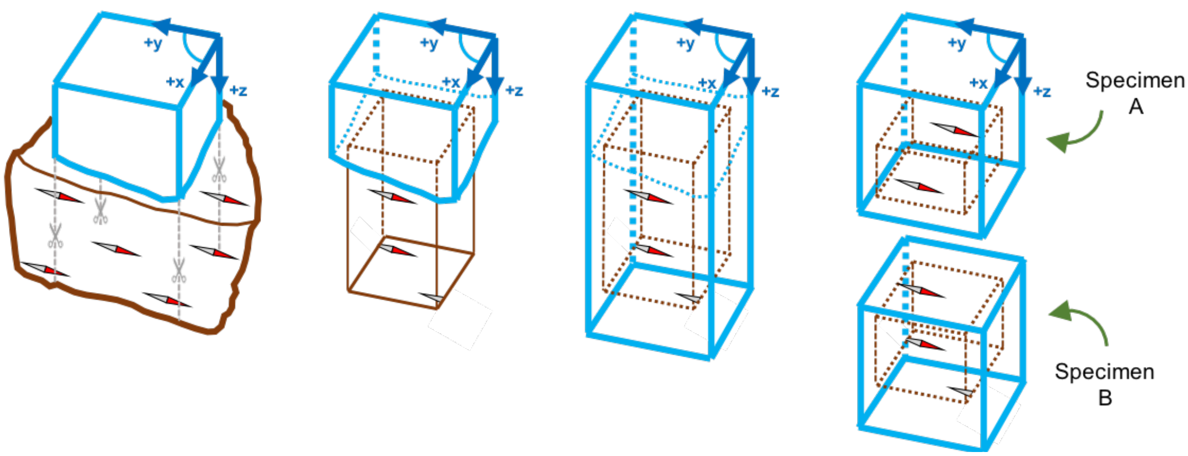

Figure 4.8: Process of sampling a rock from a burned rock feature for archaeomagnetic study, using a plaster cube. Once all plaster cubes were fully adhered to the rock and their essential data for magnetic study were recorded. The rocks were carefully cut to isolate each cube and its adhered column of substrate. Those columns were then further trimmed, with the intent of making multi-centimeter tall columns that would fit within the standard OAS ADL molds. Preservation and sampling of full columns was not always possible, due to weaknesses within the rocks, but it was preferred so the within-rock magnetic properties could be studied.

4.2.4 Laboratory measurement and analysis

Initial measurements were made on every specimen determine if the magnetic minerals and heating history of the substrates were sufficient for the creation of a Thermal Remanent Magnetization (TRM; or partial TRM (pTRM)) that could be measured reliably. A few specimens were eliminated from further measurement at this step because their magnetic moment was too weak to reliably measure on the OAS laboratory Molspin (NRM ⪋ 3.0e^{-08} Am^2; most of the weak magnetic moments could be attributed to small volumes of substrate within the plaster cubes). After initial measurement, those specimens that passed the initial selection were progressively demagnetized, using an alternating field demagnetization protocol to precisely quantify the preserved pTRM or TRM of interest within the heated substrate. The demagnetization increments and maximum step were determined for each specimen independently, based on the specimen's individual behavior.

Analysis of the measurement data for each specimen was completed using Demag_gui, an analysis software within the open source PmagPy package (Tauxe et al. 2016). Each specimen was analyzed using one of three statistical methods to quantify the preserved magnetic vector of the specimen (Figure 4.9). If the measurement data for the specimen formed a linear trend, then principal component analysis (not including the origin) was the preferred method (Figure 4.9a; e.g. Kirschvink, 1980). If the progressive demagnetization measurement data formed a cluster of roughly equivalent moments and vector directions, then the data were interpreted using a 3D statistical angular mean, known as a Fisher mean (Figure 4.9b; Fisher, 1953). In some cases, the progressive demagnetization data form a trend along a great circle, which is indicative of mixed vector direction between a weak pTRM that is overprinting a stronger pTRM or TRM. In these cases, the measurement data were interpreted with great circle analysis (Figure 4.9c).

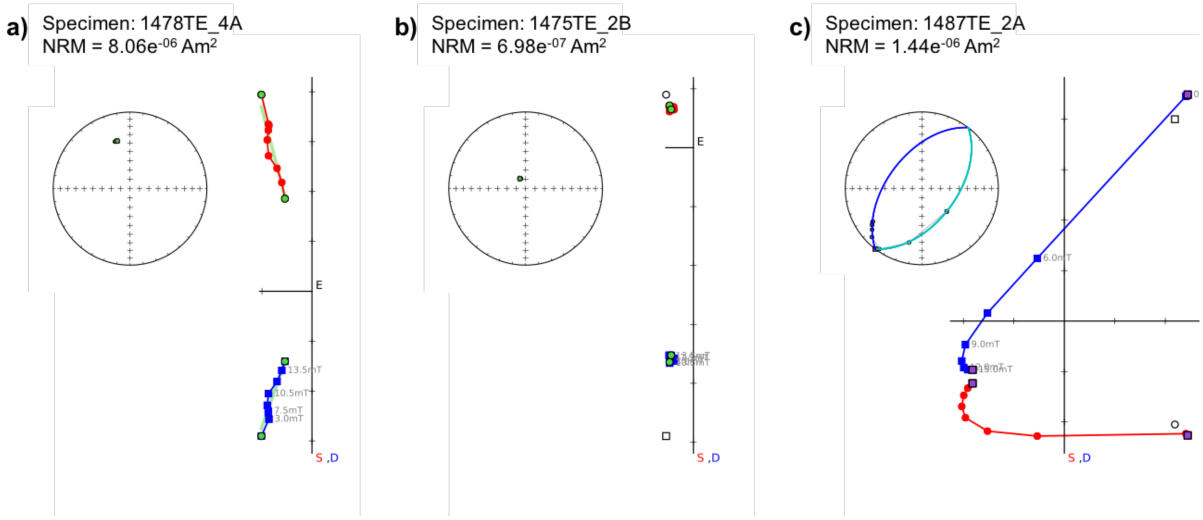

Figure 4.9: Different techniques used in analysis of the archaeomagnetic specimen data. a) Feature 5, Rock 5, Specimen 4a. Analyzed using principal component analysis. b) Feature 5, Rock 1, Specimen 2b. Analyzed as a Fisher mean. c) Feature 16, Rock 4, Specimen 2A. Analyzed using great circle analysis.

The surface, interior, and bottom specimens were all analyzed independently for each rock. This ensured that each of the potential magnetic vectors that might imply reuse of the rock were closely examined. Following specimen interpretation, a characteristic mean magnetic vector for each rock was calculated from the specimen vectors. In some cases, not all specimens were used in the determination of the characteristic vector for each rock. Those that were eliminated have been noted (i.e. inaccuracies in the reading of the field azimuth or the epoxy failed causing a loose specimen). After each rock was evaluated independently, the rocks of each feature were analyzed together, yielding interpretations of feature form and use and reuse.

4.2.5 Comparative hand sample

Preliminary archaeomagnetic data and observations early in sampling and measuring of specimens prepared from Feature 5 rocks highlighted questions that could not be addressed satisfactorily by only considering the feature rocks, all of which have a suspected anthropogenic influence on heating.

1) The mechanical properties of the mudstones were reminiscent of ceramic, suggesting that the rocks experienced significant heating. But was the heating solely anthropogenic in nature or could the rocks have experienced a geologic or wildfire heating event as well?
2) The ceramic-like mudstone rocks are mechanically quite stable, which is atypical of fine-grained carbon-rich mudstones that usually are friable. Were these rocks collected and included in the feature as friable mudstones or as the ceramic-like mudstones observed during excavation? If they were collected as friable mudstones, why would such friable rocks be selected, was there human preference or advantage?

For comparison, a sample of mudstone from a geologic outcrop was requested by OAS ADL staff and was provided by Terracon Consulting, Inc. Unfortunately, due to private land access restrictions in the vicinity of site 41AN162, no field survey of rock resource availability was conducted. Instead, an unoriented comparative hand sample was collected from an outcrop from a farm near Palestine, Texas (Figure 4.10; 31.7°N, 95.6°W). The formations accessible at the farm are the same three formations that are accessible at site 41AN162 – Sparta Sand Formation, Weches Formation, and Queen City Sand (Fisher, 1993). The hand sample reflects the same lithologic and ceramic-like mechanical characteristics as the carbonaceous mudstone rocks excavated from site 41AN162. The only difference between the comparative outcrop rock and anthropogenically influenced rocks is their color. The comparative rock sample has a slightly more yellow-brown hue (Munsell: 7.5YR 4/4d; color observed on a cut and rinsed face) as compared to mudstones from 41AN162 that all exhibit a dark-reddish brown hue (e.g., Feature 5, Rock 2, Munsell: 5YR 4/3d; also observed on a cut and rinsed face). The observable physical properties of the comparative outcrop rock (including the ceramic-like nature of the rock) suggest that it too experienced a robust heating event, but due to its collection from an outcrop, the heating event was likely geologic rather than anthropogenic.

Figure 4.10: Hand sample of a mudstone from a farm near Palestine, Texas. There is no suggestion of anthropogenic alteration or use of the specimen.

Two columns of specimens (three specimens per column, six total) were produced from the comparative rock for alternating field demagnetization. Although, stratigraphic up was not noted at the time of field collection, characteristics on the planar surfaces of the rock suggest an up direction. Both columns of sampled material were collected assuming the assigned stratigraphic up direction and a level orientation as closely parallel with the bedding planes as possible. This sampling strategy was intentional, as it provides a reference frame for inclinations that could have meaningful value, even though the rock and sampled columns were unoriented. The geologic history and mapping of the area (Fisher, 1993), show that there are no geologic features (tilting or folding) in the region, so a sampling protocol that uses the bedding planes of the rock to indicate stratigraphic positioning is likely sufficient to answer the comparative research question posed.

4.3. Theory

Magnetic studies of heated archaeological features require substrates with magnetic minerals whose magnetic moments are realigned under conditions of heating and cooling. The magnetic mineralogy and grain size, and prevailing grain orientation influence the fidelity with which the material preserves the ancient magnetic field characteristics. Usually a material with smaller mineral sizes (clay-based matrix) and fully randomized mineral orientations, preserves a more reliable magnetization upon heating and cooling than a material with a sand-based matrix and a grain anisotropy. Anisotropy describes non-random mineral orientations within rock types, usually due to physical mineral alignments that result from constraints of crystal growth or flow regimes during rock formation.

Archaeomagnetism has the potential to contribute to studies of thermal features through relative calendric chronology, reconstructions of feature form and history, and perspectives on feature function. Contributions of archaeomagnetic analyses to larger culture historical interpretive goals are dependent on whether the sampled material supported the acquisition of a preserved remanent magnetization under the conditions of its ancient use.

The archaeological materials most often studied are those that are anthropogenically heated (hearths, burned floors, pottery, etc.) because the heating and subsequent cooling of the material generally preserves a stable and measurable magnetization. When heated in the presence of a magnetic field, a subset of the atomic-scale magnetic moments (vectors) within the magnetic mineral crystals enter a state of magnetic instability, with no memory of their former alignment. Upon subsequent cooling the atomic magnetic moments re-enter a state of magnetic stability with a statistical preference for the Earth's prevailing magnetic field, effectively documenting the direction and in some cases the intensity of Earth's magnetic field at the time of cooling. If the temperature reached is sufficiently high (580º and 675ºC for magnetite [Dunlop and Özdemir, 1997] and hematite [O'Reilly, 1984], respectively), all the material's magnetic moments enter the state of magnetic instability at temperature and all the moments re-align upon cooling, preserving a thermal remanent magnetization (TRM). This temperature is known as the Curie temperature. If the temperature reached does not exceed the Curie temperature of the magnetic mineral crystals in the material, then the subset of magnetic moments that did enter a state of instability (at their magnetic unblocking temperature) and re-aligned upon cooling (through their magnetic blocking temperature) preserve a partial thermal remanent magnetization (pTRM). Often, this pTRM is still detectable during laboratory measurement and is common in anthropogenically heated materials, since most heating events do not reach as high as the Curie temperatures.

The total net magnetization of the material is formally referred to as the natural remanent magnetization (NRM) and represents the integrated effect of the substrate's magnetic history. In archaeomagnetism, the NRM is commonly complex because archaeological materials often experience multiple heating (re-magnetizing) events. In these cases, the complex history may be detailed through laboratory study, but not always, especially if the durations of the multiple heating events are short lived. Since (re)heating can re-initiate magnetic instability, additional heating events effectively erase the vector alignments that were previously acquired at the new temperature and below. In instances where a subsequent heating event of a higher temperature occurs, there will be no preserved magnetic signature of the earlier heating event. But in cases where subsequent heating event(s) occur at lower temperatures than an earlier heating, there is a potential that measurement and data analysis maybe able to differentiate the magnetic signatures of the original vectors (TRMs and high temperature pTRMs) and overprinting vectors (low temperature pTRMs).

Successful directional archaeomagnetic studies require appropriate substrates with sufficiently well-behaved magnetic minerals, heating events (i.e. fires) sufficiently hot to induce a magnetic realignment, recovery of a carefully aligned set of specimens from an archaeological feature, and laboratory measurement of the specimens. In most US-based archaeomagnetic studies, the research and data collection have been in support of archaeomagnetic dating (Blinman and Cox, 2022). Archaeomagnetic dating focuses on the subtle variations of Earth's magnetic field that occur through time and space, known as paleosecular variation (PSV). Since the Earth's magnetic field is constantly changing, the preserved TRMs (and pTRMs) in archaeological substrates are effective tools in tracing the location of the past apparent north pole or virtual geomagnetic pole (VGP) at the time of the heating/cooling event. With enough well-dated discreet data, regional models of PSV that trace the location of the VGP through time can be developed and used for archaeomagnetic dating. These PSV traces are known as VGP reference curves or calibration curves.

Presently, only three regions in the United States have proposed VGP calibration curves:

1) The Four Corners region of the United States Southwest has by far the most data, and multiple generations of reference curves have been proposed (summarized in

Jones et al. 2021 and reviewed in Blinman and Cox, 2022). The curves proposed for this region have and continue to be used for archaeomagnetic dating.

2) A curve encompassing the Lower Mississippi River region of the Southeastern U.S. (Arkansas focus) was proposed by Dan Wolfman (1982; 1990).
3) A mid-continent curve covering the latitudes north of the Lower Mississippi River curve (but also including much of Wolfman's data) was proposed by Stacey Lengyel (Lengyel 2004; Lengyel et al. 1999).

Much of the rest of the US does not yet have VGP reference curves, largely due to a low density of data. This includes Texas, part of the little studied region between the Four Corners region and the Lower Mississippi River region. However, the PSV of the eastern seaboard from 1600 CE to present has been modeled from historical records of magnetic direction in sea captains' log books (Jackson et al. 2000). This model, known as gufm, can be utilized in much the same way as a VGP calibration curve for applications of archaeomagnetic dating along the east coast of the US. Further, recent work by Jones et al. (2021) has combined data from the three largest archaeomagnetic laboratories and collections in the United States (DuBois, Wolfman, and Eighmy/Lengyel). This large (and growing) data set will provide new opportunities for curve development and refinement in the US and the greater Americas.

Archaeomagnetic dating relies on the successful preservation, collection of specimens, measurement, and interpretation of TRMs and pTRMs vectors in an archaeological feature. If successful, a feature-level magnetic vector can be determined and converted to its respective VGP position. This position can be compared with the regional calibration curves of VGP movement through time. Any overlap of uncertainty of the measured VGP position and proposed calibration curve, can be interpreted as a date range with an associated uncertainty bound.

In addition to dating individual features, the contemporaneity of multiple features within a site can be evaluated by measuring and comparing the TRM (or pTRM) of each, whether or not a regional reference curve exists for the area. If different features have non-parallel vector directions, this can be interpreted as evidence that the features are not contemporaneous or were moved since they were last fired. Conversely, if different features have parallel vector directions, those features have the potential to be contemporaneous; however, there is a chance for an erroneous conclusion. PSV variation is not unidirectional, and at times the VGP reference curves cross over themselves. This overlap can result in a single pole position that is achieved at different times in the past, resulting in parallel but not contemporary vectors. In these cases, and if a full TRM is present in the material, specialized measurements that estimate the strength of Earth's past magnetic field can be used to distinguish the timing of some points of overlap.

Beyond dating and contemporaneity assessments, archaeomagnetic analyses have the potential to contribute to the understanding of the use and taphonomy of burned rock features. Wulf Gose from the University of Texas at Austin applied paleomagnetic methods that were originally developed to address tectonic questions to archaeological burned rock features (Nickels et al. 1998; Gose 2000). The approach evaluates whether the magnetization vectors of the individual rocks within a thermal feature are coherent or dispersed (non-parallel) in their preserved directions. If the rocks are coherent in their vector directions, it can be inferred that the thermal feature is intact or in-situ. If the vector directions from the rocks are dispersed, it can be inferred that the rocks moved since their magnetic acquisition. Minor movements in the vector directions of in-situ rocks are expected as a result of normal post-abandonment taphonomic processes (bioturbation). But radical realignments of the vector directions may support interpretations of human behavior at or after the time of heating and use.

4.4. Results and Discussion

The lithologic properties of the rocks from Features 5 and 16 of site 41AN162 permitted a detailed study of the features. The cohesion of the mudstones and sandstones allowed the preparation of several columns of material that were then subdivided into specimens that spanned the entire depth of the rocks. In total, 175 specimen cubes were prepared from the fourteen rocks subjected to laboratory analysis (nine from Feature 5, four from Feature 16, and the comparative mudstone from the farm). The characteristic directions for each rock are presented in Tables 1, 2 and 3, and are superimposed the Feature 5 and 16 feature plans in Figures 4.11 and 4.12, respectively.

4.4.1 Comparative hand sample: Archaeomagnetism

The six specimens from the arbitrarily oriented two columns of material, span the depth of the comparative rock. Alternating field demagnetization of all six specimens confirm that a preserved magnetization is present throughout the entire rock. The precision within each column (Table 1) and relative strength of the measured magnetization suggest the magnetic acquisition is thermal in nature (a TRM; Butler 1992: 14), confirming the inference of significant heat exposure based on observable physical characteristics.

The magnetic results, in combination with the congruent lithologic and mechanical properties of the comparative outcrop rock and the feature rocks, imply that the ceramic-like feature rocks were not collected as friable mudstones that were then anthropogenically heated to ceramic, but were rather collected as ceramic-like mudstones that had already been heated. The harvesting of already ceramic-like and cohesive material explains why no small well-burned flakes of ceramic-like mudstone debitage were found in the interstitial spaces between the rocks of the features.

Table 4.1: Characteristic archaeomagnetic vector results, for the comparative rock (ADLN = 1488TE).

Column	**Substrate**	**dec**	**Inc**	**α_{95}**	**κ**	**$N/N_m/N_T$**	**Specimens included in mean**
Column 1 (Unoriented)	Mudstone	80.2	75.6	7.4	277	3/3/3 L=3, P=0	1A, *1B,* 1C*
Column 2 (Unoriented)	Mudstone	222.7	71.3	4.4	800	3/3/3 L=3, P=0	2A, *2B,* 2C*
Average of inclinations:		**--**	**73.3**	**--**	**--**	**6**	**Calculated as an arithmetic mean**

ADLN = Archaeomagnetic Dating Laboratory identification number. Collectively the declination (dec) and inclination (inc) define the vector direction of the preserved magnetization. α_{95} refers to the angular confidence bounds of the mean direction; it is the 3-dimensional angular equivalent to a 2-sigma confidence bound. **κ** is a statistical measure of the concentration of the distribution about the mean, independent of number (N); a larger number reflects more concentrated data. N refers to the number of specimen directions (L=lines and P=planes) that are included in the mean. N_m denotes number of specimens measured. N_T denotes the total number of specimens collected. Specimens noted with an A are surface specimens, * denotes bottom specimens, and italicized denotes interior specimens.

4.4.2 Comparative hand sample: Radiocarbon extraction

Two radiocarbon samples were prepared from the comparative rock in the OAS Radiocarbon laboratory. One was collected from darkened material that was interpreted to be infused carbon into the surface of the rock but had the opportunity for the inclusion of contaminating carbon due to natural weathering and exposure. The other was sampled from the black surface within the voids between two layers of mud, interpreted to be the remnants of the interbedded carbonaceous layers within the mudstone rock with lower risk contamination by younger carbon through time. The sampled void was exposed in the process of the cutting the rock into archaeomagnetic specimens, through the use of a water-cooled tile saw.

Radiocarbon extraction of both samples yielded minute amounts of carbon. While it is not unexpected that the surface infused carbon would yield low quantities of carbon, it is unexpected that such a tiny amount of carbon was extracted from the proposed carbonaceous rich void spaces. Samples containing dead carbon (as expected in this case) still release larger quantities of carbon during extraction, but with ratio of radiocarbon isotopes skewed towards ^{12}C rather than ^{14}C. That was not seen in the sampling of black material from the voids, which in conjunction with the robustness of the magnetization and the physical properties, suggests that the geologic fire was intense enough to completely burn away any organic material. One potential explanation is a nearby coal seam fire. If this hypothesis is correct, the ceramic-like mudstones would be more accurately classified as “clinker-like”.

4.4.3 Feature 5

Feature 5 is characterized as a rock platform roughly 3-meters in diameter, composed of rocks of two distinct lithologies. The dominant rock lithology is the laminated carbonaceous mudstones, which describes seven of nine rocks collected for archaeomagnetic study. The less common lithology is sandstone, which describes two of the nine rocks sampled. The nine rocks vary in thickness from roughly 2.5cm to 12cm, with the tabular mudstones typically the thinnest and the sandstones typically thicker. Where possible, columns of oriented material were cut from each of the rocks to assess magnetic qualities throughout the thickness. With the exception of Rock 2, all of the specimens collected from all of the rocks exhibit a moderately-strong single component magnetization that is uniform throughout the individual rocks, from top to bottom. This suggests that the conditions which imparted the magnetization were robust in either (or both) heat and heating duration.

This robust heating episode is interpreted to be anthropogenic in origin since all nine rocks from Feature 5 preserve northerly directions that are loosely parallel to each other ($\boldsymbol{\kappa}$ = 23.4). Additionally, the mean of all nine rocks (declination = 353.4°, inclination = 57.8°) is consistent with the expected direction for Anderson County, Texas in the recent past (Table 2). Had these rocks been harvested and arranged by the past humans without an anthropogenic heating, the preserved direction induced by geologic heating would have been dispersed and it is very likely that roughly half of the rocks would have had negative inclinations and the declinations would be random. This is because the act of harvesting and transporting the rocks to site 41AN162 for inclusion in Feature 5, would have randomized the any preserved geologic vector directions. The tabular shape of the rocks, roughly parallel to the bedding planes, would have encouraged the installation of the rocks into Feature 5 in either an up or down orientation, thus randomizing the declinations but causing roughly half the rocks to maintain a positive inclination while the other half preserved a negative inclination. This is not observed; all the rocks have a northerly declination and a positive inclination that is expected for recent (last millennium) magnetic fields.

The moderate degree of inconsistency in the north and down direction (α_{95} = 10.9°) is likely the result of the individual rocks settling independently through time, augmented by bioturbation (animals roaming the surface and compressing the soil inconsistently, and burrowing animals that cause inconsistent instability under parts of the rocks).

Table 4.2: Characteristic archaeomagnetic vector results, for Feature 5.

Rock (ADLN)	Substrate	dec	inc	α_{95}	κ	$N/N_m/N_T$	Specimens included in mean
Rock 1 (1475TE)	Mudstone	331.6	76.5	2.5	474	8/11/20 L=8, P=0	6A, *2B, 4B, 6B, 5C, 5D,* 4E*, 6E*
Rock 2 (1476TE)	Mudstone	342.3	50.1	7.6	34	12/12/12 L=11, P=1	No Bottoms: 1A, 2A, 3A, 4A, 5A, 6A, *3B, 4B, 6B, 3C, 6C, 6D*
Rock 2* (1476TE)	Mudstone	295.2	-41.3	38	45	2/2/2 L=2, P=0	Bottoms only: 3D*, 6E*
Rock 3 (1477TE)	Mudstone	13.2	65.4	2.8	1940	3/4/8 L=3, P=0	3A, 4A, 5A
Rock 4 (1479TE)	Mudstone	33.6	71.6	2.6	171	19/21/22 L=19, P=0	1A, 4A, 6A, *1B, 2B, 3B, 7B, 9B, 10B, 1C, 2C, 3C, 8C, 9C, 11C, 1D,* 1E*, 8E*, 11*
Rock 5 (1478TE)	Mudstone	2.5	45.3	11.6	28	7/9/10 L=7, P=0	1A, 2A, 4A, 6A, *1B, 2B, 5B*
Rock 6 (1480TE)	Sandstone	331.4	57.0	10.3	81	4/12/12 L=4, P=0	2A, 5A, *2B, 4B*
Rock 7 (1481TE)	Mudstone	332.8	55.3	5.1	80	11/12/14 L=11, P=0	2A, 3A, 5A, 9A, *1, 4, 7, 8,* 2E*, 5E*, 6E*, 9E*
Rock 8 (1482TE)	Mudstone	355.2	32.6	12.1	17	10/10/12 L=10, P=0	1A, 2A, 3A, 4A, 5A, 6A, 7A, 2E*, 3E*, 4E*
Rock 9 (1483TE)	Sandstone	6.7	55.3	4.1	216	7/12/17 L=7, P=0	1A, 3A, 4A, 6A, 1E*, 3E*, 4E*
Feature 5: Fisher mean		**353.4**	**57.8**	**10.9**	**23.4**	**9**	**Does not include the bottom direction of Rock 2; csd = 16.75**
41AN162 IGRF in 2020		**2.3**	**60.7**	**--**	**--**	**--**	**At 31.8°N, 95.4°W**
GAD approximation for 41AN162			**51.4**	**--**	**--**	**--**	**At 31.8°N**

Same caption as Table 1. The International Geomagnetic Reference Field (IGRF) is an internationally agreed upon model of the current magnetic field and can be used to predict characteristics of the magnetic field at given locations on Earth. The Geoaxial Dipole model of Earth's magnetic field can be used to predict the characteristics of the magnetic field at given latitudes, assuming the field is completely dipolar and centered on Earth's geographical North Pole. This assumption is accurate averaged over tens of thousands of years.

4.4.3.1 Feature 5, Rock 2

Contrary to the consistent northerly direction all the rocks of Feature 5, the two bottom specimens analyzed from Rock 2 suggest an incomplete re-magnetization event. The preserved vectors of the two bottom specimens are coherent with each other and yield a mean declination of 295.2° (roughly WNW) with a negative inclination, which is atypical of the recent regional direction (Table 2). This negative inclination implies that either:

1) The rock was incompletely heated during the anthropogenic episode and the bottom vectors record a geologic heating event that occurred prior to the rock's inclusion in the feature, or
2) The rock was moved after an initial anthropogenic heating and reinstalled into the feature upside-down prior to the final anthropogenic heating.

The second option is our preferred interpretation, on the basis that the remaining rocks including the thickest rocks (Rocks 1 and 4) and the most adjacent rocks (Rocks 3 and 7, Figure 4.13) preserve a single magnetization throughout their entire thickness. Additionally, due to Rock 2's proximity to the border of the feature (Figure 4.11) the likelihood of human influenced movement is higher.

The two preserved vector directions in Rock 2, in conjunction with the single northerly direction preserved in the remaining rocks of Feature 5, suggest that this feature may have been used in its current configuration at least twice. The time between uses was likely short because the other preserved northerly vectors are univectorial and any significant time lapse would have increased the likelihood of producing a slightly different overprinting northerly direction, due to paleosecular variation (mapped as a VGP movement). But multi-component northerly vectors were not seen in single specimens or throughout the thickness of the rocks. However, these observations do not preclude the possibility of additional heating episodes because the VGP curves can loop back over themselves and additional heating episodes could have completely overprinted the signature of the first episode of heating. This is an unlikely interpretation because it does not explain why Rock 2 is the only rock with two preserved magnetizations, including a direction with a negative inclination direction, which is unexplainable by just paleosecular variation over the last few thousand years.

A single period of heating and use (probably including at least two heating events, over a short window of time) is consistent with the results of radiocarbon dating. Radiocarbon dating of three carbonized *Fagus sp*. nutshells fragments found in the interstitial spaces of the rocks yield an average date of the feature of 2354 ± 37 rcy BP, calibrated to the 30-year window of 410-380 BCE.

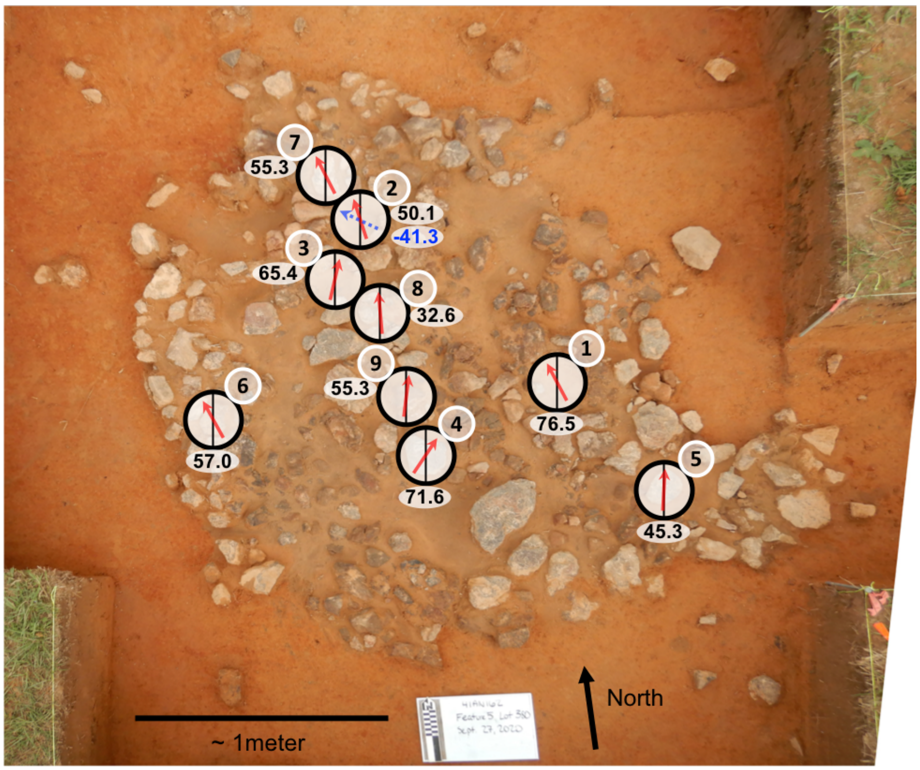

Figure 4.11: Feature 5 after the removal of nine rocks for archaeomagnetic study with the declination and inclination superimposed on the voids, which depict the rocks' locations across the feature. Rock 2 has two preserved magnetizations. The magnetization averaged from the surface and interior specimens is depicted as a red arrow with the inclination in black text, congruent with the other eight rocks. The magnetization preserved in the bottom two specimens is depicted as a blue arrow and blue text.

4.4.4 Feature 16

Feature 16 is defined by four small clusters of rocks across a roughly 2-meter diameter surface. The field excavators did not identify any associated pit or depression. The rocks are of the same two distinct lithologies as Feature 5. The dominant lithology is the laminated carbonaceous mudstone, comprising three of four rocks collected for archaeomagnetic study. Similar to Feature 5, these mudstones are quite angular and tabular, but were in general thinner than the mudstones of Feature 5. The fourth rock sampled (Rock 4) is a sandstone and has a slightly less angular and tabular form, in comparison with the mudstones.

Where possible, columns of oriented material were prepared from each of the rocks to assess magnetic qualities throughout the thickness. However, due to the thinness of the mudstones (Rocks 1, 2, and 3 were only about 3cm thick) no interior specimens could be prepared. If rocks were thick enough (>1.5cm), each column of material was cut into top and bottom specimens, otherwise the entire column was processed into a single specimen, to ensure enough material was encased for reliable measurement using the OAS ADL Molspin magnetometer.

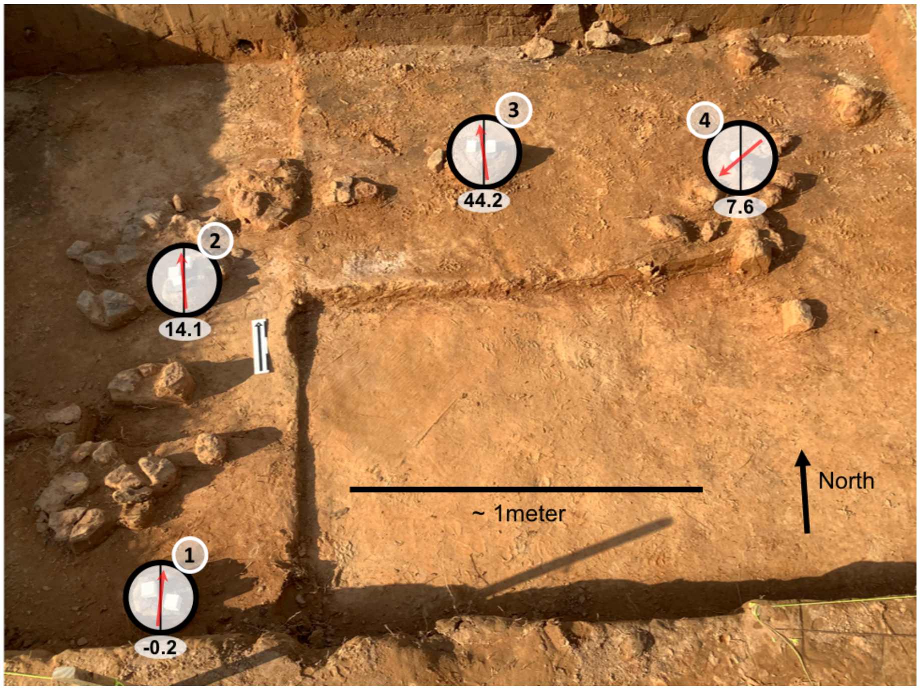

Figure 4.12: Feature 16 and the four rocks sampled for archaeomagnetic study with the declination and inclination superimposed on the rocks. Rocks 1, 2, and 3 have a magnetization that is incongruent with the expected direction for the site through time, primarily in inclination. Rock 4 has preserved a direction that is completely incongruent with the expected direction.

All of the specimens collected from the rocks of Feature 16 exhibit weaker magnetizations than was typical of the rocks from Feature 5, but all are coherent within each independent rock (Figure 4.12). While, there are many possible explanations for the change in magnetic behavior resulting in a weaker magnetization (including but not limited to degree of heating, duration of heating, magnetic mineralogy, magnetic grain size, etc.), we assert that the robustness of the Feature 16 heating episode was less intense than that of Feature 5, given the lithologies of the rocks appear to be identical. Further rock magnetic experimentation could assist in understanding the difference in the firing robustness between Features 5 and 16.

Even still, the preserved magnetizations of Feature 16 are interpreted to be anthropogenic in origin because three of the four rocks preserve a northerly declination (Fisher mean declination = 358.4°; Table 3). Similar to Feature 5, had these rocks been harvested and arranged by the past humans without an anthropogenic heating, the preserved geological induced directions would have been scattered in declination and the inclinations would have been closer to the expected inclination for the area through time (Table 3), due to the tabular shape of the rocks. This randomized distribution is not observed, so an anthropogenic origin for the magnetizations is interpreted.

Table 4.3: Characteristic archaeomagnetic vector results, for Feature 16.

Rock (ADLN)	**Substrate**	**dec**	**inc**	**α_{95}**	**κ**	**$N/N_m/N_T$**	**Specimens included in mean**
Rock 1 (1484TE)	Mudstone	5.9	-0.2	7.2	61	8/8/8 L=8, P=0	4A, *1, 2, 3, 5, 6, 7,* 4Z*
Rock 2 (1485TE)	Mudstone	355.2	14.1	9.2	23	12/12/12 L=12, P=0	1A, 2A, 3A, 5A, 6A, *4, 7,* 1Z*, 2Z*, 3Z*, 5Z*, 6Z*
Rock 3 (1486TE)	Mudstone	352.3	44.2	11.4	21	9/9/9 L=9, P=0	1A, 2A, 3A, 5A, *4,* 1Z*, 2Z*, 3Z*, 5Z*
Rock 4 (1487TE)	Sandstone	229.8	7.6	15.1	11	10/10/11 L=8, P=2	1A, 2A, 3A, 4A, 5A, 1Z*, 2Z*, 3Z*, 4Z*, 5Z*
41AN162 IGRF in 2020		**2.3**	**60.7**	**--**	**--**	**--**	**At 31.8°N, 95.4°W**
GAD approximation for 41AN162			**51.4**	**--**	**--**	**--**	**At 31.8°N**

Same caption as Table 4.2.

4.4.4.1 Feature 16, Rock 3

Rock 3 is the most conforming to expectations of the sampled rocks from Feature 16. Assuming a Geocentric Axial Dipole (GAD) model of Earth's magnetic field, which models the field as solely a dipole, the expected inclination for the location of site 41AN162 is 51.4°. But, a GAD field does not consider the non-dipole fields that contribute to PSV through time.

As such, the inclination for the region through time is expected to deviate somewhat from 51.4°. As an example, the modern (2020) field in the region has an inclination of 60.7° or +9.3° from the GAD predicted inclination.

Applying this concept to the rocks of Feature 16, there is a likelihood that Rock 3, with a northerly declination (352.3°) and an inclination of 44.2° (-7.2° from the GAD predicted inclination), could be more or less in situ since its last use (specifically its last cooling event). Some post-cooling movement due to settling and natural taphonomic bioturbation, will fall within the -7.2° factor. But intentional movement by past humans (incidental dislodging or conscious rearrangement) is unlikely.

4.4.4.2 Feature 16, Rocks 1 and 2

The variations in the inclinations of Rocks 1 and 2 from the GAD predicted inclination or from Rock 3 (assuming it is in situ) are too great to be explained by just post-depositional settling and bioturbation. Both Rocks 1 and 2 preserve northerly declinations, but their inclinations vary from GAD by -51° and -44°, respectively, which is far too great to be a result of PSV or bioturbation. The large change in inclinations from the GAD prediction and from Rock 3 (-44° and -37°, respectively) suggest that the past humans influenced the rocks' post-cooling positions.

The somewhat consistent northerly declinations are not incompatible with this hypothesis. Anecdotal observations from experimental pottery firings include the systematic movement of rocks while the kiln is being unloaded (i.e. rocks or bricks that support the vessels within the firing pit). Repetitive motions from a single kneeling position adjacent to the cooled fire can result in the stones being lifted out and placed in roughly the same orientation (i.e. the declination) outside of feature. This method of unloading the feature could explain both the northerly declinations and the large deviation in inclination from expected (Figure 4.13). These two rocks were likely heated and cooled in an orientation (i.e. the declination) roughly equivalent to how they were found, but with a change in tilt of roughly 40-60° (as compared with the range of expected values defined by both Rock 3 and the modern field).

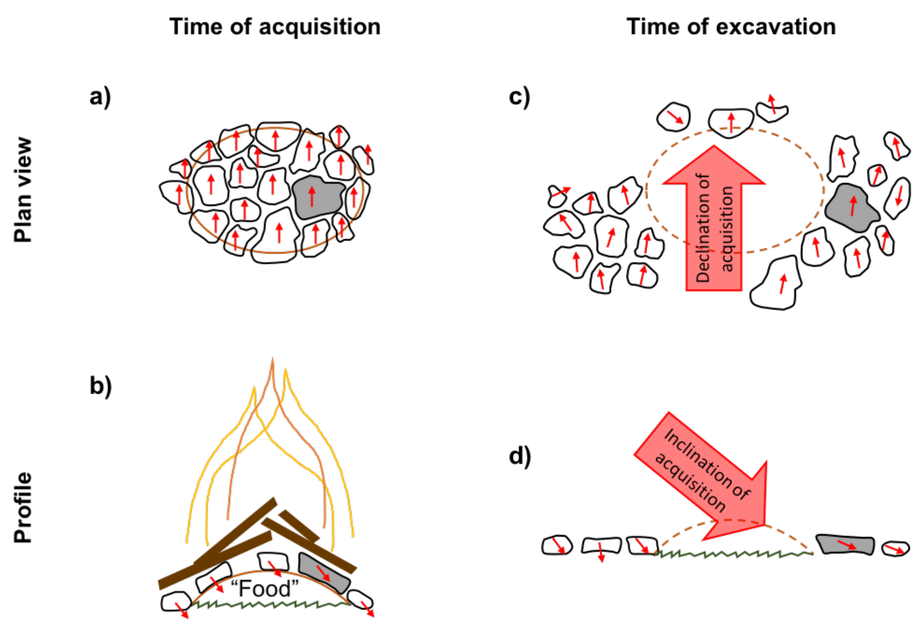

Figure 4.13: Depiction of a heating scenario congruent with the data and interpretations of Feature 16. Since no archaeological evidence of a pit was detected, the feature is modeled as a surface feature. Shaded in grey is a modeled rock that could represent Rocks 1 and 2 from Feature 16. a) The modelled heating feature in plan view, at the time of TRM acquisition. The dashed oval represents the baking target. Notice that all rocks have a magnetic declination parallel to each other and to the prevailing magnetic field. b) The same modelled heating feature in profile depicting the magnetic inclination of the rocks as they cooled over the domed baking target. Before unloading the feature, the modelled inclinations are 51.4° down, the expected inclination for Anderson County Texas according to GAD predictions for the location. c) The same heating feature in plan view at time of excavation. Note the variation in the preserved magnetic declinations from the direction of acquisition. Rocks can vary little or considerably, determined by how they are moved from their cooled positions during feature unloading. Some rocks may be flipped upside down during unloading, but most are simply slightly rotated, preserving a declination similar to that acquired at cooling. d) The

rock feature at time of excavation in profile, depicting the variation in preserved inclinations. The tabular nature of the rocks of this study preserve a record of their tilted position on the domed baking target as the difference between their archaeological inclination and the GAD predicted inclination.

4.4.4.3 Feature 16, Rock 4:

Rock 4, the only sampled sandstone of Feature 16, preserved a magnetization that was weaker and far more difficult to interpret than the three sampled mudstones (Rocks 1, 2, and 3). All the specimens prepared from Rock 4 preserved multiple magnetic vectors, some more robust than others. The interpreted composite magnetic direction for Rock 4 shows a rock that has had significant movement since its last heating event (declination = 229.8°, inclination = 7.6°). Like Rocks 1 and 2, Rock 4 preserved an inclination that is so shallow, that its deviation from the GAD (51.4°) predicted inclination or from Rock 3 -44.2° (assuming it is in situ) is too great to be explained by solely post-depositional settling and bioturbation.

The interpretation is that, similar to Rocks 1 and 2, Rock 4 was unloaded from a heated feature and placed into the orientation found during excavation. It is likely that the rock was heated and cooled with a tilt of roughly 35-50° (range defined by Rock 3 and the modern field). It was also likely heated in an orientation that is 130° clockwise from how it was found during excavation.

4.4.4.4 Archaeomagnetic dating potential

A single piece of carbonized nutshell (*Juglans negra*) collected from the interstitial spaces in Rock Cluster 1 (the SW cluster). The piece was dated at SUERC and the single date was shared with OAS ADL by Terracon Consulting, Inc. The nutshell piece dated to 641 ± 29 rcy BP, calibrated to either 1285 – 1329 CE or 1339 – 1396 CE.

The radiocarbon age dates the heating event to within the time range of calibrated reference curves of PSV in the adjacent Four Corners region of the United States Southwest. We recognize that the reference curves for the Four Corners region may not be applicable to eastern Texas, due to their distance apart; however, currently no reference curves have been produced that compasses the Anderson County area. The archaeomagnetic direction preserved in Rock 3 has a large uncertainty term (α_{95} of 10.9°), considered too large for precise archaeomagnetic dating by the OAS ADL. But, the direction of Rock 3 (converted into VGP coordinates) does overlap with curves designed for archaeomagnetic dating for the Four Corners region (Jones et al. 2021), during time periods in the late thirteenth and early fourteenth centuries. By itself the archaeomagnetic record of Feature 16 would not support date interpretations but the consistency between the radiocarbon date and the archaeomagnetically derived date does affirm the potential of heated archaeological rock features to support the development of regional PSV curves and eventual archaeomagnetic dating.

4.5. Conclusions

This study builds on the vision of Wulf Gose – that the techniques of archaeomagnetism can be used to inform on archaeological site and feature use. The archaeomagnetic staff at OAS used alternating field demagnetization to show that all the rocks sampled by Terracon Consulting, Inc. field crews from Features 5 and 16 and the comparative natural outcrop did retain stable magnetizations. The retained magnetizations were internally consistent within each rock, with the exception of Rock 2 from Feature 5.

Rock 2 preserved a different magnetic direction in the specimens prepared from its bottom surface than those prepared from its top surface and interior.

Study of the comparative outcrop mudstone yielded insights into the thermal history of the rocks within Feature 5 and 16. The congruency in the physical characteristics between the geologic hand sample and the anthropogenically influenced feature rocks, further supported by the USGS maps and the magnetic properties, show that the feature rocks have a complex history. We suggest that the feature rocks and comparative rock were likely sourced from the Sparta Sand or Weches Formations. These formations were deposited during the Eocene and subsequently experienced only limited tilting and folding. At some point in the geologic past, the rocks of the formations experienced a robust fire (coal fire) that converted the likely friable mudstone into a ceramic-like rock or "clinker-like" rock with almost no traces of carbon remaining

At some more recent time (~2410 rcy BP for Feature 5 and ~640 rcy BP for Feature 16) the rocks were harvested for use in the heating features. While these secondary heating episodes could be robust, as indicated by the complete heating through the entire thickness of some of the feature rocks (Feature 5), other feature rocks show that the heating episodes did not fully overprint the geologically induced magnetization (Feature 16).

The magnetizations of the nine rocks from Feature 5, are all roughly parallel with northerly declinations and inclinations that are consistent with the expected direction for Anderson County, Texas, through time. The roughly parallel results suggest that the sampled rocks of Feature 5 were heated post-emplacement, implying an anthropogenic design of the feature, an anthropogenic origin to the heating episode, and that the rocks have remained in situ since their last use. The non-conforming magnetization preserved in the two bottom specimens of Rock 2, suggest the rock experienced multiple heating events, at least one before and one after the rock was flipped in its orientation. The origin of the heating event that resulted in the non-conforming direction cannot be ascertained with certainty; however, it is possible that the magnetizations preserved in the rock imply the feature was used anthropogenically at least twice with Rock 2 displaced between uses. Since PSV is subtle over a few decades, it is unlikely that directional archaeomagnetic study will be able to reveal multiple heating events during a short-lived heating episode, unless (as in this case) the rock is displaced significantly.

The four rocks of Feature 16 tell a different story of use. The magnetization of three of the four rocks exhibit inclination shallowing that requires post-heating movement prior to their arrangement within the excavated feature. These rocks (1, 2, and 4) suggest that the configuration of the rocks was modified after the heating event from a tilted orientation during heating and cooling to the near horizontal orientation that the rocks were found in during excavation. This reconfiguration to the horizontal would have had to occur before feature or site abandonment because post-abandonment taphonomic processes cannot explain the degree of post-heating tiling that the rocks experienced, which supports an anthropogenic organization of the rocks into the clusters that were excavated. Further, two of the rocks with shallowed inclinations (Rocks 1 and 2) also preserve a northerly declination, which in unlikely to occur at random, further suggesting an anthropogenic influence. Rock 4's non-northerly declination with a positive inclination does not contradict this hypothesis of an anthropogenic influence placement of the rocks post-heating. One explanation for these preserved directions is a feature where the use pattern involved "unloading" the rocks from a heating facility after cooling. Rock 3 is different from the other three rocks. Its northerly declination and a slightly shallowed inclination, as compared to the GAD field or modern inclination, could imply that it is in situ, but also does not preclude it from having been reconfigured to its archaeological position post-heating. Features like Feature 16 would benefit from a larger number of studied rocks within each cluster.

This archaeomagnetic analysis project was successful in contributing to a richer understanding of archaeological feature use. This success was in part because the lithologic characteristics of the mudstones proved to be remarkable carriers of stable magnetizations. The fine-grained nature of the mudstone increased the likelihood that the preserved magnetization would be stable, strong, and measurable. Conversely, while the sandstones did record a magnetization, the quality of the preserved vector was less than ideal, likely a result of larger magnetic grain sizes and differing magnetic mineralogy characteristics. Further the tabular nature of the mudstones, permitted interpretations (especially on Feature 16) that would otherwise not have been possible if the shape of the rock was more rounded which would have resulted in more randomized post-abandonment movement.

Acknowledgements

Chapter 4, in full, has been submitted to the *Journal of Archaeological Sciences: Reports* for publication of the material. Jones, Shelby A.; Blinman, Eric; Lohse, Jon C.; Cox, J. Royce; Nichols, Melanie; Kimbell, Jenni, 2022. The dissertation author was the primary investigator and author of this paper.

References

Arnold, D.E. (1985) Ceramic Theory and Cultural Process. Cambridge University Press. New York, New York.

Black, S.L., and A.V. Thoms. (2014) Hunter-Gatherer Earth Ovens in the Archaeological Record: Fundamental Concepts. *American Atinquity*. 79(2), 204-226. https://10.7183/0002-7316.79.2.204

Blinman, E., and J.R. Cox. (2022) Theory, technique, and performance: Time for renewal in southwestern archaeomagnetic dating. In S.E. Nash and E.L. Baxter (eds.), *Pushing boundaries: Proceedings of the 16th biennial southwest symposium (Chapter 8)*. University Press of Colorado. Boulder, Colorado.

Blinman, E., J.M. Heidke, and M.R. Miller (2017) Cooking Technologies. In B.J. Mills and S. Fowles (eds.), *Oxford Handbook of Southwest Archaeology (Chapter 31)*. Oxford University Press, New York.

Butler, R.F. (1992) *Paleomagnetism: Magnetic Domains to Geologic Terranes*. Blackwell Scientific Publications. Boston, Massachusetts. Available digitally: https://www.geo.arizona.edu/Paleomag/

Dunlop, D.J. and Ö Özdemir (1997) *Rock Magnetism Fundamentals and Frontiers*. Cambridge University Press. Cambridge.

Fisher, R.A. (1953) Dispersion on a sphere. *Proceedings of the Royal Society of London, Series A*. 217, 295-305. https://doi.org/10.1098/rspa.1953.0064

Fisher, W.L. (1993) Geologic Atlas of Texas, Palestine Sheet. 1:250,000. The University of Texas at Austin, Bureau of Economic Geology.

Gose, W.A. (2000) Palaeomagnetic Studies of Burned Rocks. *Journal of Archaeological Science*. 27, 409-421. https://doi.org/10.1006/jasc.1999.0465

Groat, C.G. (1975) Geologic Atlas of Texas, Tyler Sheet. 1:250,000. The University of Texas at Austin, Bureau of Economic Geology.

Jackson, A., A.R.T. Jonkers, and M.R. Walker (2000) Four centuries of geomagnetic secular variation from historical records. *Philosophical Transactions of the Royal Society of London*. Series A: 358, 957-990. https://doi.org/10.1098/rsta.2000.0569

Jones, S.A., E. Blinman, L. Tauxe, J.R. Cox, S. Lengyel, R. Sternberg, J. Eighmy, D. Wolfman, and R. DuBois. (2021) MagIC as a FAIR repository for America's directional archaeomagnetic legacy data. *Journal of Geophysical Reviews: Solid Earth*. 126. https://doi.org/10.1029/2021JB022874

Kirschvink, J.L. (1980) The least square line and plane and the analysis of paleomagnetic data. *Geophysical Journal International of the Royal Astronomical Society*. 62(3), 699-718. https://doi.org/10.1111/j.1365-246x.1980.tb02601.x

Lengyel, S.N. (2004) *Archaeomagnetic Research in the U.S. Midcontinent*. PhD dissertation. University of Arizona. Tucson, Arizona. https://repository.arizona.edu/bitstream/handle/10150/290039/azu_td_3131615_sip1_m.pdf?sequence=1

Lengyel, S.N., J.L. Eighmy, and L.P. Sullivan (1999) On the Potential of Archaeomagnetic Dating in the Midcontinent Region of North America: Toqua Site Results. *Southeastern archaeology*. 18, 156-171.

Lohse, J.C, M. Nichols, and J. Kimbell (2020) *Interim Report of Archaeological Data Recovery at Site 41AN162*. Submitted to Texas Department of Transportation. Terracon Consultants, Inc.. Houston, Texas.

Nickels, D.L., B.J. Vierra, and Wulf Gose. (1998) Fire-cracked Rock. In B.J. Vierra (ed.), *41MV120: A Stratified Late Archaic Site in Maverick County, Texas (Chapter 10)*. Published by the Center for Archaeological Research, The University of Texas at San Antonio. San Antonio, Texas. https://doi.org/10.21112/ita.1998.1.1

O'Reilly, W. (1984) *Rock and Mineral Magnetism*. Blackie. Glasgow.

Tauxe, L., R. Shaar, L. Jonestrask, R. Minnett, A.A.P. Koppers, C.G. Constable … (2016) PmagPy: Software package for paleomagnetic data analysis and a bridge to the Magnetics Information Consortium (MagIC) Database. *Geochemistry, Geophysics, Geosystems*. 17(6), 2450-2463. https://doi.org/10.1002/2016GC006307

Wolfman, D. (1982) Archeomagnetic dating in Arkansas and the border areas of adjacent states. In N. Trubowitz and M. Jeter (eds.), *Arkansas archeology in review* (p. 277-300). Fayetteville, Arkansas.

Wolfman, D. (1990) Archaeomagnetic dating in Arkansas and the border areas of adjacent states – II. In J. Eighmy and R. Sternberg (eds.), *Archaeomagnetic Dating (Chapter 14)*. University of Arizona Press. Tucson, Arizona.